REPRODUCING PICTURES WITH NON-REPRODUCIBLE COLORS

by

ROBERT ROY BUCKLEY JR.

B.Sc.E.E., University of New Brunswick
(1971)

B.A., University of Oxford
(1974)

SUBMITTED IN PARTIAL FULFILLMENT
OF THE REQUIREMENTS FOR THE
DEGREE OF

MASTER OF SCIENCE and
Electrical Engineer
at the

MASSACHUSETTS INSTITUTE OF TECHNOLOGY

February 1978

Signature of Author.....
Department of Electrical Engineering and Computer Science, January 20, 1978

Certified by.....
Thesis Supervisor

Accepted by.....
Chairman, Department Committee

REPRODUCING PICTURES WITH NON-REPRODUCIBLE COLORS

by

ROBERT ROY BUCKLEY JR.

Submitted to the Department of Electrical Engineering and Computer Science on January 20, 1978, in partial fulfillment of the requirements for the Degree of Master of Science.

ABSTRACT

An important problem in the color printing industry is the optimum reproduction of good quality color pictures on a medium with a compressed dynamic range, where there would be colors in the original unattainable and therefore non-reproducible in the reproduction. The constraints are typically expressed in terms of the objective variables of the physical process, such as density, and consequently, the solution usually takes the same form, compressing the input densities. The evaluation of the results however, is a subjective exercise, so that the compression of the input picture should best be performed in the color space of the human observer. The compression of the input picture into the output color solid was investigated in U*V*W* space, where the lightness W* and chromaticness values (U*,V*) were linearly mapped onto those obtainable with the reproduction process. For a color photographic system, it is shown that the reproducible colors are contained in a solid that can be represented as an irregular polyhedron in U*V*W* space.

U*V*W* compression was compared with density and exposure range compression for reproductions with a lower maximum density than the original copy. For two representative pictures, the results of the U*V*W* compression were either preferred to the output of the other schemes or were judged closer to the original. Further enhancement of the compressed picture was obtained economically by spatially filtering either the luminance or lightness component of the original.

Thesis supervisor: William F. Schreiber
Title: Professor of Electrical Engineering

Acknowledgments

I would first like to thank my thesis supervisor, Professor William F. Schreiber, for his generous support and patient encouragement over the course of this project. Since its start, I have had the benefit of a number of discussions with some people knowledgeable in color reproduction. In this regard, there are two people I must especially mention. Dr. Robert Solomon did some of the previous color picture research in our group and was responsible for my introduction both to the computer system and to this project. He has, in addition, been a constant source of encouragement. Alan Ames of Polaroid Corporation was very helpful in the early stages with the photographic aspects of this study.

I would also like to thank Dr. Michael Brill for his critical suggestions for early drafts of the thesis and Mike Daum of Polaroid, who kindly supplied the spectral sensitivity curves of Polacolor 2 film. I am also indebted to Mrs. Kathy Honecke who typed part of this thesis and especially to Robert Buckley Sr. who drafted most of the figures.

During the course of this research, I have been supported as a Teaching Assistant in the Department of Electrical Engineering and Computer Science at the Massachusetts Institute of Technology.

Table of Contents

Page

List of Figures

List of Tables

Chapter 1

Introduction

1.1 Color Reproduction

Almost since its inception in the Middle Ages, mechanized printing has made use of color. It has only been in the current century though that mechanical, photographic and electronic means of rendering color have become commonplace. As a result, the expectations of a large body of experienced observers as to the performance of color reproduction systems are quite exacting and improved color reproduction is the object of a great deal of continuing research.

One common means of color reproduction is the half-tone process. In its simplest version, three screened images or separations (cyan, magenta and yellow), each consisting of a regular pattern of inked dots at or below the threshold of spatial resolution, are superimposed on a sheet of white paper. Since the area concentration of the ink is constant, the reflectance function of the ink-paper combination is shaped by varying the size of the dots. For example, the most saturated red is obtained by combining the maximum size dots of the blue- and green-absorbing (yellow and magenta) inks with the minimum dot size of the red-absorbing (cyan) ink. Combinations of equal size dots on all three separations yield a neutral tone scale, gradated from white through grey to black, as the dots vary in size from smallest to largest. The maximum reflectance (white) is obtained with the minimum dot size and therefore the largest amount of the white substrate visible; the minimum reflectance (black) is obtained with the maximum dot size. A useful property of the process is its reflectance ρ or density D range, where

$$D = - \log_{10}(\rho) \qquad 1.1\text{-}1$$

The minimum density D_{min} corresponds to white and the maximum density D_{max}, to black. The dynamic range or contrast of the process is the ratio of the maximum to minimum reflectance, or more conveniently, the logarithm of that ratio, $D_{max} - D_{min}$.

The success of a process such as this can be judged on comparing an original picture Q and its reproduction P, where

$$P = \phi(Q) \qquad 1.1\text{-}2$$

ϕ is the transformation on the original picture performed by the reproduction system. In the ideal situation, the reproduction would give the same color sensations as the original,

$$\psi(P) = \psi(Q) \qquad 1.1\text{-}3$$

ψ is the mapping from the domain of physical variables, such as spectral energy distribution, image size and spatial frequency content, to the range of color sensations. When P and Q differ only in spectral energy content, Eqn. 1.1-3 reduces to the special case of a colorimetric match.

The economy of this formulation belies a number of difficulties. For one, the function ψ is only known in a qualitative way, so that the precision of Eqn. 1.1-3 is illusory. Even in the well-defined case of a colorimetric match, the physics of a practical system can only approximate the mathematics of the ideal solution. These difficulties have surprisingly posed little problem since the commercial color industry deals mainly with 'acceptable' color reproduction. That is,

$$\left|\psi(Q) - \psi(P)\right| < \psi_o \qquad 1.1\text{-}4$$

where ψ_o is a threshold of acceptability, a tolerance necessarily

qualitative in the absence of a quantitative color picture metric. It is seldom realistic to assume that P and Q are available for direct comparison. Usually, $\psi(Q)$ exists only in the mind of the observer as a set of memory colors acquired through experience, corresponding to Bartleson's internal 'frame of reference' [1].

The most important features of the reproduction system ϕ are the correct reproduction of hue (or color balance) and tone [2]. In general, correctly reproducing the saturation of the colors in the original is not as important since, as Hunt points out [2], saturation is the most variable attribute of a color sensation, given the color and lightness constancy mechanisms of human color vision.

1.2 The Problem

The choice of a color picture to be reproduced is typically made on the basis of a high quality transparency or reflection print. In reproducing it, however, the quality is usually degraded since the reproduction has a smaller dynamic range than the original picture. This is demonstrated in Table 1-1 where the dynamic ranges ΔD of a number of representative processes are compared. For example, a good quality reflectance print could have a density range of 2, while its half-tone reproduction on newsprint would only have a dynamic range of about 1. In this case, the minimum density of the reproduction is determined by the reflectance of the paper on which the separations are printed and the minimum dot size. The maximum density is a function of the quality of the printing inks used. The range of D_{max} shown by some of the samples in Table 1-1 result from the use of a black printer as a fourth separation in color pictures, but not in the printing of text where the

Table 1-1 Dynamic Ranges of Some Typical Processes

Sample	D_{min}	D_{max}	ΔD
New York Times			
newsprint	0.22	1.11	0.9
Sunday magazine	0.20	1.35-1.65	1.15-1.45
Newsweek magazine	0.17	1.35-1.85	1.2-1.7
National Geographic	0.08	1.60-2.10	1.5-2.0
3M Type 7773 paper	0.11	1.60	1.5
Polaroid Type 108 film	0.15	1.65	1.5
Reflection print			<2.4
Transparency			<3.0
Outdoor Scene			1.5-2.8[1]

[1] This is the $\log_{10}$ of the ratio of maximum to minimum luminance in typical scenes [4].

expense of a fourth printer is not justified.

The restriction of the dynamic range $[D_{min}, D_{max}]$ in the reproduction vis-a-vis the original means that the whitest whites (highlights) and the blackest blacks (shadows) of the original could exceed the reproducible tone range. Similarly, there could be saturated colors in the original that would require a density (or dot size) outside the dynamic range of the reproduction. As a result, these colors would be non-reproducible. This is a familiar problem to the graphic arts and printing industry [3,5]. A reduction in contrast and in the gamut of reproducible colors leads to a lower quality in the reproduction, compared to the original.

The problem then is to design a color reproduction system ϕ that, given this compressed dynamic range, minimizes the degradation in picture quality and yields the optimum reproduction.

1.3 The Solution

The first order solution of this problem requires preserving the information in the original outside the density range of the reproduction. Otherwise, shadow and highlight detail and color discrimination for particularly saturated hues would be lost. Therefore, the non-reproducible colors in the original must be compressed to fit within the tone scale and color gamut of the reproduction. The RCA Color Corrector, one solution to this problem, compresses only those hues with non-reproducible saturations [6]. This will mean the desaturation of some of the colors in the original and not others, with a resulting change in the color balance. One constraint that can be imposed on the compression is the invariance of color balance and hue under the transformation ϕ, given their importance to acceptable color reproduction. Therefore, the transformation ϕ is to

be optimized for the reproduction of tone and saturation.

The compression of the colors of the original picture into the subspace that is physically realizable by the reproduction needn't necessarily mean that the range of reproducible color sensations is similarly limited. This follows from the fact that the mapping ψ of the psychophysical stimulus space to the color sensation space is only 1:1 for the restricted viewing conditions imposed on the Standard Observer by the CIE. In the viewing situations more usually encountered, this mapping can be n:1 or 1:n, that is, n "colors" can appear identical or one "color" can appear as n, depending on the spatial and temporal context in which the stimuli are viewed. This arises, in part, due to simultaneous color contrast and suggests a means of inducing color sensations beyond those that would be expected, given the limitations of the color gamut. By modifying the reproduced colors then, within bounds set by the output gamut, it may be possible to increase simultaneous color contrast effects and make colored areas in the reproduction appear brighter or more saturated than they "really" are (i.e. produce the equivalent of lightnesses outside the tone scale or saturations beyond the color gamut). This enhancement could be had by increasing color differences across the borders between colored areas. It has been pointed out that this "sharpening" of borders tends to increase color and brightness [1,7]. Ditchburn [8] has suggested that the colors we see may be largely determined by edge effects occuring at the boundaries separating colored fields on the retinal image.

The use of a computer in the color reproduction system allows for a great deal of flexibility in the choice of compression and enhancement schemes for investigation. The traditional analogue reproduction methods,

predating the introduction of electronic color scanners, were limited to operations in the density domain. The digital computer, however, is able to calculate and then manipulate psychophysical variables as easily as densities.

Given the qualitative nature of the transformation ψ, the only means of determining the optimum reproduction ϕ is psychological testing, where human observers compare the output of various schemes. With a view to the ultimate application of the results of this study, the best choice for the reproduction medium is colored half-tones on newsprint. Their preparation, however, is an expensive and laborious procedure. Polacolor 2 Type 108 reflectance prints provide a more convenient medium for judging the results, without sacrificing the basic nature of the study.

Chapter 2 of this thesis gives a brief outline of colorimetry, the measurement of color. The mathematics of color reproduction are reviewed in Chapter 3. The processing algorithms are developed in Chapter 4 and the experimental reproduction system described in Chapter 5. The results and conclusions of the study are given in Chapter 6.

Chapter 2

Colorimetry

2.1 Introduction

The obvious goal of color reproduction is duplicating the visual stimulation of a given scene or object. A strictly physical approach would require the equality of the spectral distributions of the original and the reproduction. Though attainable [2], it is an impractical objective due to the infinite dimensionality of a spectral distribution, where the energy content must be analyzed over each infinitesimally narrow wavelength interval of the visible spectrum. That the human observer would perform this analysis was deemed inconceivable by Thomas Young when he postulated three retinal sensitivity functions [9]. This by now well-established result permits the specification of visual stimuli by three variables: the responses they elicit in the three retinal receptors. A color reproduction then need only have three degrees of freedom to replicate the effect of an original on the human visual system. This is the fundamental premise of modern color technology, though its first practical demonstration actually preceded Young by nearly a century. In 1704, LeBlon produced color pictures by combining blue, yellow and red mezzotinted plates [10]. Color image processing then, when it appeals to the operating characteristics of the human visual system, properly begins with colorimetry, the measurement of visual stimuli.

2.2 Colorimetry

The experimental basis of colorimetry is that any set of three colored lights, where no single one can be matched by a mixture of the other two, can be mixed so as to match all possible colors. The Commission

Internationale de l'Eclairage (CIE) in 1931 adopted the results of the classic matching experiments of Guild and Wright [11] and defined a Standard Observer. The color mixture functions for the equal energy spectrum, $\bar{r}$, $\bar{g}$, and $\bar{b}$, using as primaries narrowband monochromatic stimuli (R)=700.0nm, (G)=546.1nm and (B)=435.8nm, are shown in Figure 2-1. By definition, unit amounts of the three primaries mixed together match S_E, the equal energy spectrum. Given a color (P) with a spectral distribution $P(\lambda)$,

$$(P) \equiv R\,(R) + G\,(G) + B\,(B) \qquad 2.2\text{-}1$$

where the equivalence signifies that (P) can be matched by a linear combination of the primaries (R), (G) and (B), taken in the amounts R, G and B, referred to as the tristimulus values.

$$R = \int_{\Lambda} d\lambda\, P(\lambda)\, \bar{r}(\lambda) \qquad 2.2\text{-}2a$$

$$G = \int_{\Lambda} d\lambda\, P(\lambda)\, \bar{g}(\lambda) \qquad 2.2\text{-}2b$$

$$B = \int_{\Lambda} d\lambda\, P(\lambda)\, \bar{b}(\lambda) \qquad 2.2\text{-}2c$$

where Λ is the range of visible wavelengths. Since a color mixture curve (for example, $\bar{r}$) can be negative-valued over part of Λ, the corresponding tristimulus value (in this case, R) can be negative for some $P(\lambda)$. This simply means that - R(R) added to (P) matches G(G) + B(B).

Any color then can be characterized by a triplet (R,G,B) or a point in three-dimensional tristimulus space (Figure 2-2). Two colors, (P_1) and (P_2), can have the same tristimulus values and thus appear indistinguishable to the Standard Observer, though they do not have the same spectral

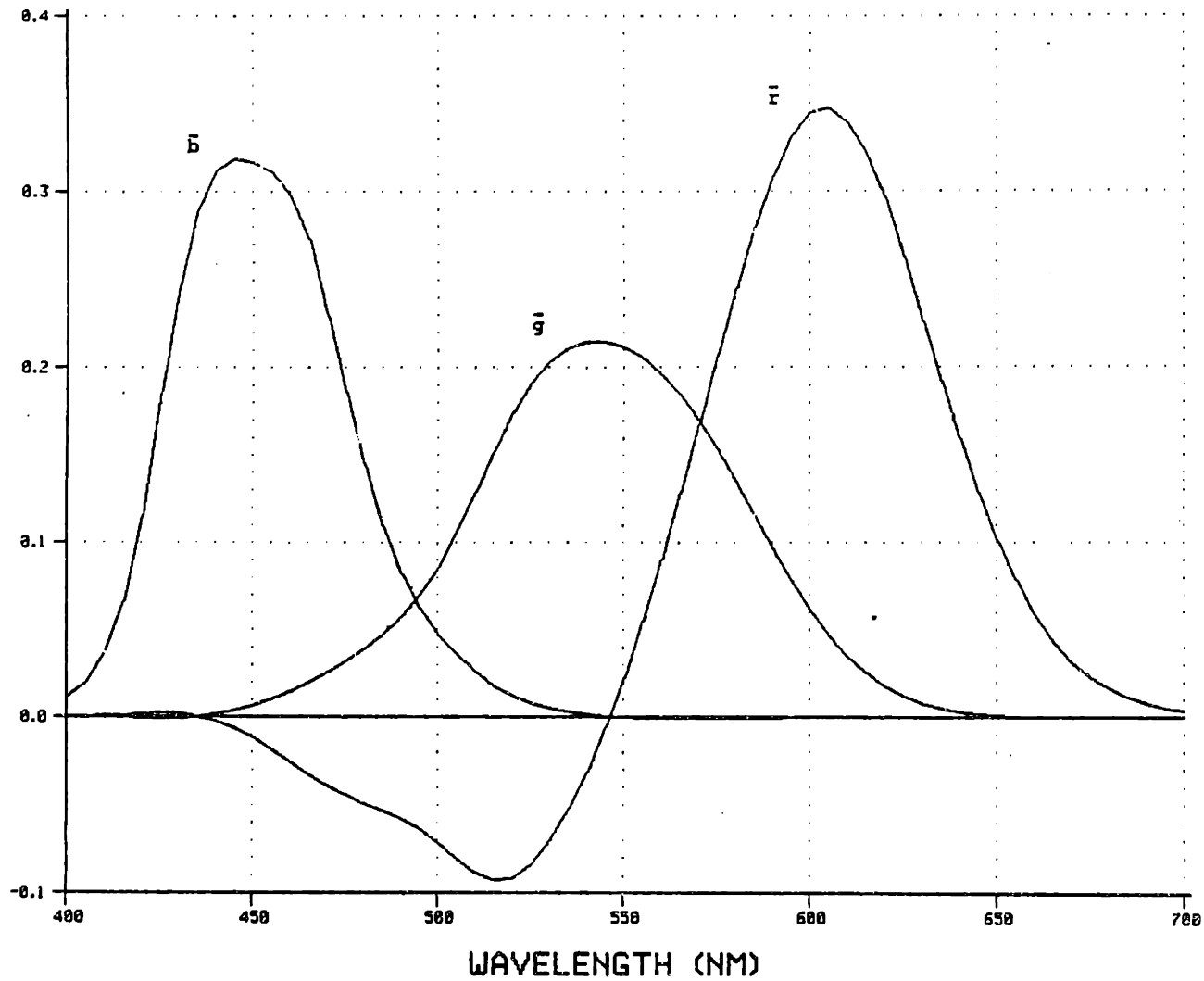

Figure 2-1. $\bar{r}$, $\bar{g}$, $\bar{b}$ Color Mixture Functions.

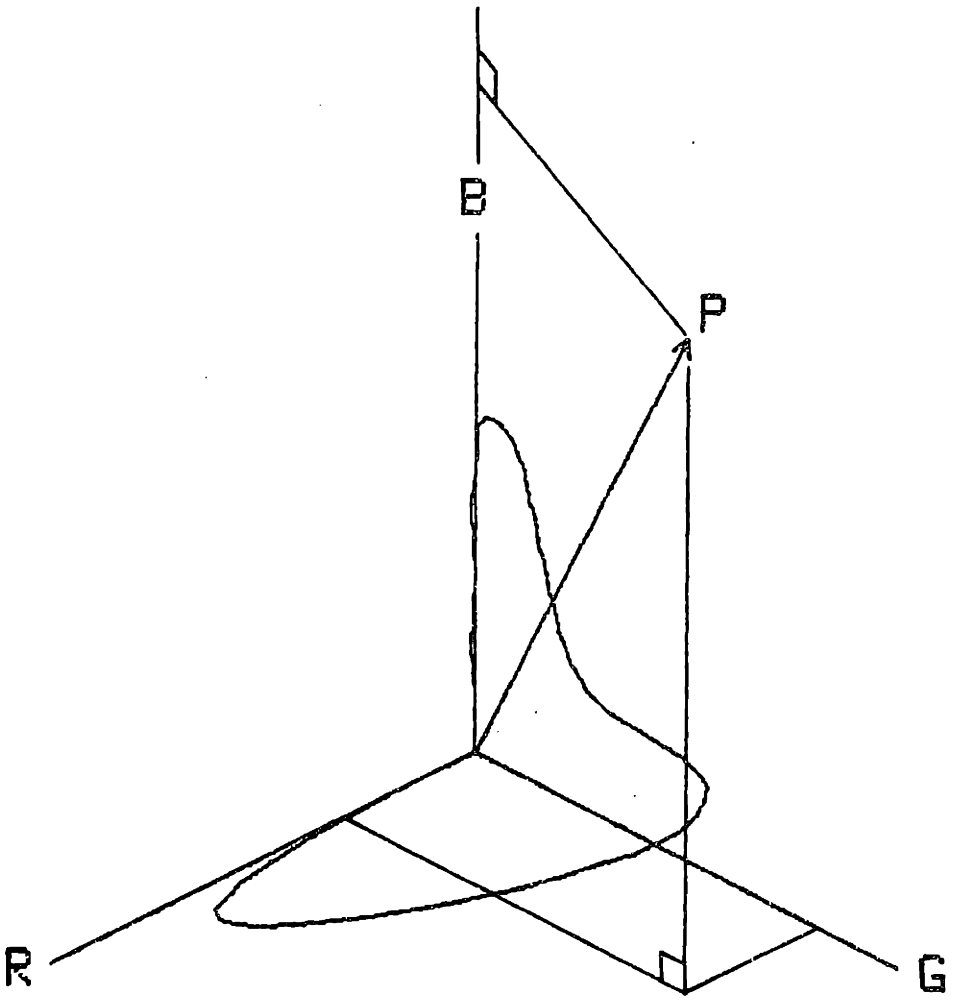

Figure 2-2. RGB Tristimulus Space, the Color Vector P and the Spectral Locus.

distribution, that is, $P_1(\lambda) \neq P_2(\lambda)$. Such stimuli are referred to as metamers. Subjective color reproduction in the narrowest view has the goal of producing metamers of the colors in the original. This was Maxwell's point [9] when he suggested generating metamers by the additive combination of three primaries $P_1(\lambda)$, $P_2(\lambda)$, $P_3(\lambda)$,

$$P(\lambda) = a_1P_1(\lambda) + a_2P_2(\lambda) + a_3P_3(\lambda) \qquad 2.2\text{-}3$$

The analysis of a given color in the original returns coefficients a_1, a_2, a_3 such that the reproduced color, with spectral distribution $P(\lambda)$, is metameric to that color.

Also shown on Figure 2-2 is the spectral locus, obtained by plotting the tristimulus values of $\delta(\lambda)$, the unit energy monochromatic stimulus, as λ is varied. It is the trajectory of $(\bar{r},\bar{g},\bar{b})$ in tristimulus space. The set of all realizable visual stimuli having a non-negative spectral distribution form a convex subset of tristimulus space and lie within the color solid with the spectral locus on its surface.

2.3 Color Space Transformations

The three primaries (R),(G) and (B) are basis vectors spanning the three-dimensional vector space of all realizable colors. Any set of three independent colors, where no one can be obtained as a mixture of the other two, will do as a basis for the color space. Since any color can be written as a linear combination of the primaries (R),(G) and (B), the transformation to a new set of primaries (P_1),(P_2) and (P_3) is given by

$$[(P_1),(P_2),(P_3)]^T \equiv \underline{A}\ [(R),(G),(B)]^T \qquad 2.3\text{-}1$$

where $\underline{A} = [a_{ij}]$ is a non-singular 3x3 matrix of tristimulus values, such

that $(P_i) \equiv a_{i1}(R) + a_{i2}(G) + a_{i3}(B)$. A given color (P) then can be matched by a linear combination of the new primaries

$$(P) \equiv P_1(P_1) + P_2(P_2) + P_3(P_3) \qquad 2.3\text{-}2$$

where P_1, P_2, P_3 are the tristimulus values in the new primary system. Substituting Equation 2.3-1 into 2.3-2 and equating to 2.2-1 gives the transformation of tristimulus values from one primary system to another.

$$[P_1, P_2, P_3]^T = \underline{B}^T [R, G, B]^T \qquad 2.3\text{-}3$$

$$\underline{B} = \underline{A}^{-1}$$

Since the color mixture functions are themselves tristimulus values taken wavelength by wavelength, one can write immediately

$$[\bar{p}_1, \bar{p}_2, \bar{p}_3]^T = \underline{B}^T [\bar{r}, \bar{g}, \bar{b}]^T \qquad 2.3\text{-}4$$

where $\bar{p}_1, \bar{p}_2, \bar{p}_3$ are the color mixture functions corresponding to the primaries $(P_1), (P_2), (P_3)$ respectively.

Since the only restriction on the matrix $\underline{A}$ is that it is non-singular, it is possible that the primaries $(P_1), (P_2), (P_3)$ can be imaginary, that is, non-realizable colors. This presents no difficulty in obtaining the corresponding color mixture functions since they can be had by a formal transformation on those corresponding to a set of realizable primaries, as in Equation 2.3-4.

It is implicit that the color (P) and the matching combination R(R)+G(G)+B(B) have the same brightness or luminance. The notion of matching along this single dimension by flicker photometry or heterochromatic brightness matching yields the visual luminous efficiency function, $V(\lambda)$

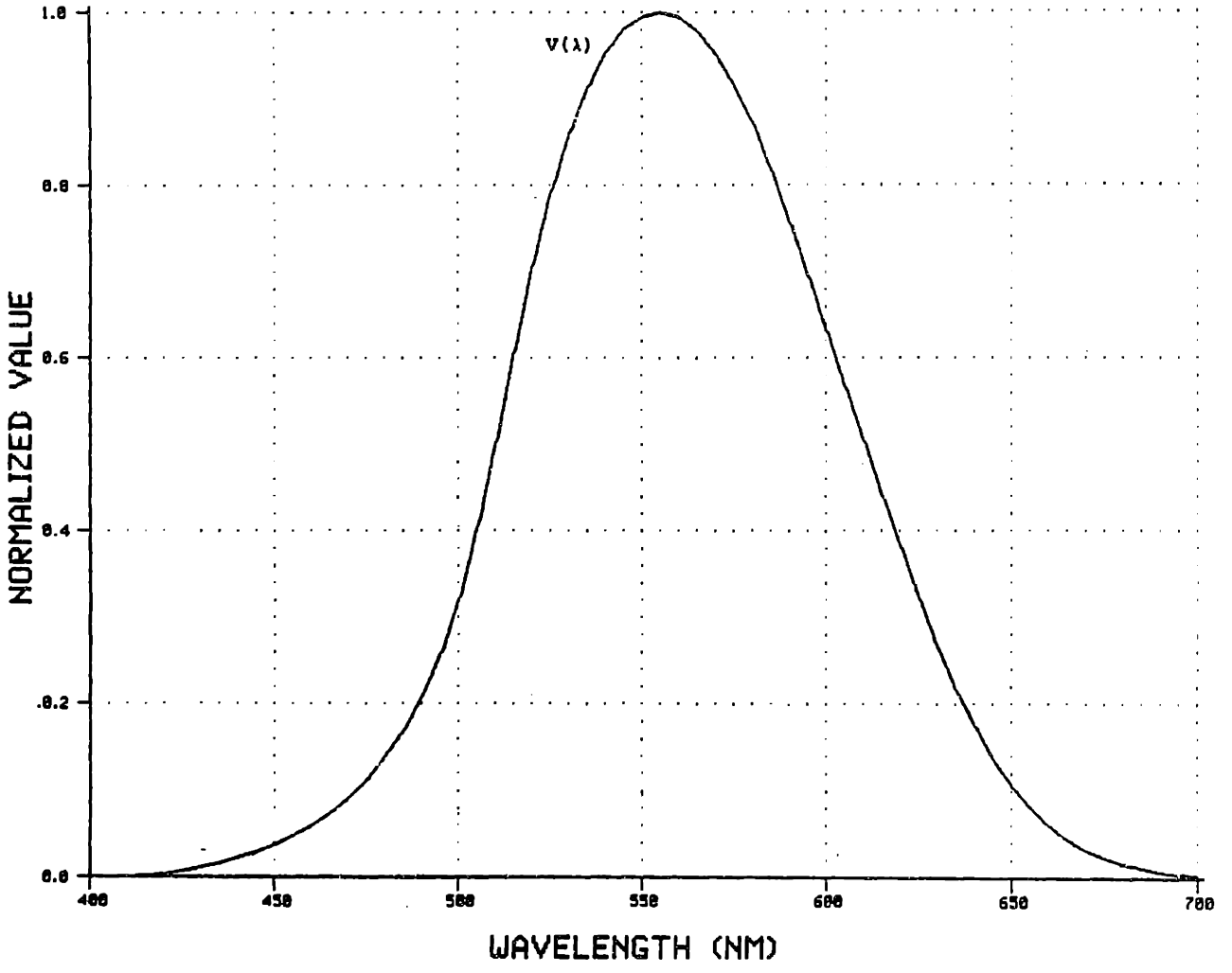

Figure 2-3. Visual Luminous Efficiency Function.

or V_λ, shown in Figure 2-3. To the Standard Observer, $V_\lambda S_E$ and $\delta(\lambda)$ are equally bright. With the assumption that luminance is additive, the luminance V of a color (P) is

$$\begin{aligned} V &= \int_\Lambda d\lambda\ P(\lambda)\ V(\lambda) \\ &= \int_\Lambda d\lambda\ [R(R)+G(G)+B(B)]\ V(\lambda) \\ &= R\int_\Lambda d\lambda(R)V(\lambda) + G\int_\Lambda d\lambda(G)V(\lambda) + B\int_\Lambda d\lambda(B)V(\lambda) \\ &= 0.17697\ R + 0.8124\ G + 0.01063\ B \end{aligned} \qquad 2.3\text{-}5$$

V clearly is a tristimulus value and V_λ, a color mixture function.

Color matching by the Standard Observer corresponds to vector addition in tristimulus space. Increasing the energy of a stimulus by a constant factor will obviously change the luminance but not the ratio of tristimulus values, in effect, the chromatic quality of the stimulus. Such strictly multiplicative changes in a stimulus can be factored out by plotting the intersection of a color vector with a plane in tristimulus space

$$\alpha R + \beta G + \gamma B = 1, \quad \alpha,\beta,\gamma \neq 0 \qquad 2.3\text{-}6$$

Setting α,β,γ to 1 defines the chromaticity plane (Figure 2-4). A color vector [R,G,B] intersects the chromaticity plane at [r,g,b], where

$$r = \frac{R}{R+G+B}\ ,\ g = \frac{G}{R+G+B}\ ,\ b = 1-r-g \qquad 2.3\text{-}7$$

The chromaticity diagram is the projection onto the R-G plane in tristimulus space of the chromaticity plane. Given the definition of unit amounts of the primaries (R),(G),(B), the amount of a color (P) with tristimulus values

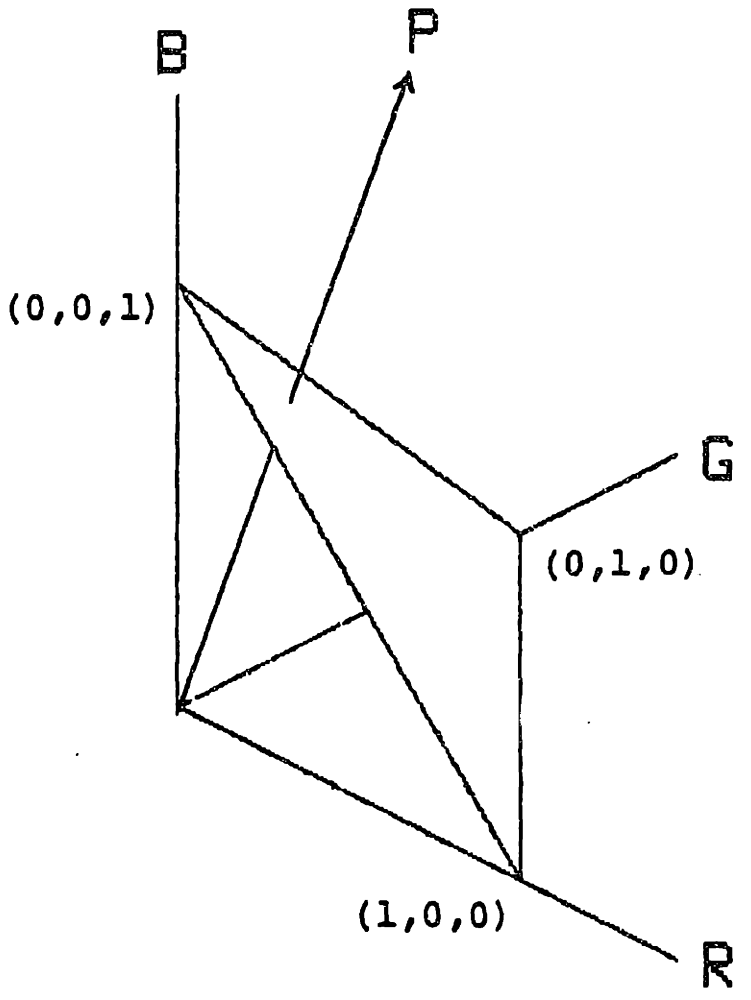

Figure 2-4. The chromaticity plane R+G+B=1 in tristimulus space.

R,G,B is R+G+B. The chromaticity diagram thus represents a normalization with respect to the quantity of light in the stimulus and in separating the quantity of the stimulus from its quality, reduces the mathematics of color matching from three dimensions to two. The color (P) can be specified on the chromaticity diagram by the point (r,g) and any one tristimulus value. The equal energy achromatic stimulus S_E has equal tristimulus values R=G=B and thus has chromaticity co-ordinates (1/3,1/3). The r-g chromaticity diagram is shown in Figure 2-5.

With the transformation of tristimulus values from R,G,B to P_1,P_2,P_3, the new chromaticity co-ordinates are

$$p_i = \frac{b_{i1}r + b_{i2}g + b_{i3}b}{(\sum_j b_{j1})r + (\sum_j b_{j2})g + (\sum_j b_{j3})b} \qquad 2.3\text{-}8$$

where the b_{ij} are the elements of the matrix $\underline{B}$ in Equation 2.3-3.

The chromaticity diagram of Figure 2-5 suggests another means of representing a color, using its dominant wavelength and excitation purity. A line joining the reference achromatic point (in this case, the equal energy white point) to (r,g) and extrapolated to the spectral locus intersects it at the dominant wavelength λ_d. The excitation purity p_e is the ratio of the distance from the white point to (r,g) to the distance from the white point to the point on the spectral locus with the same dominant wavelength as (r,g),

$$p_e = \frac{r - r_n}{r_d - r_n} = \frac{g - g_n}{g_d - g_n} \qquad 2.3\text{-}9$$

2.4 Uniform Chromaticity Space

Through the use of color space transformations, the original color matching data of the RGB system can be converted into a system that meets

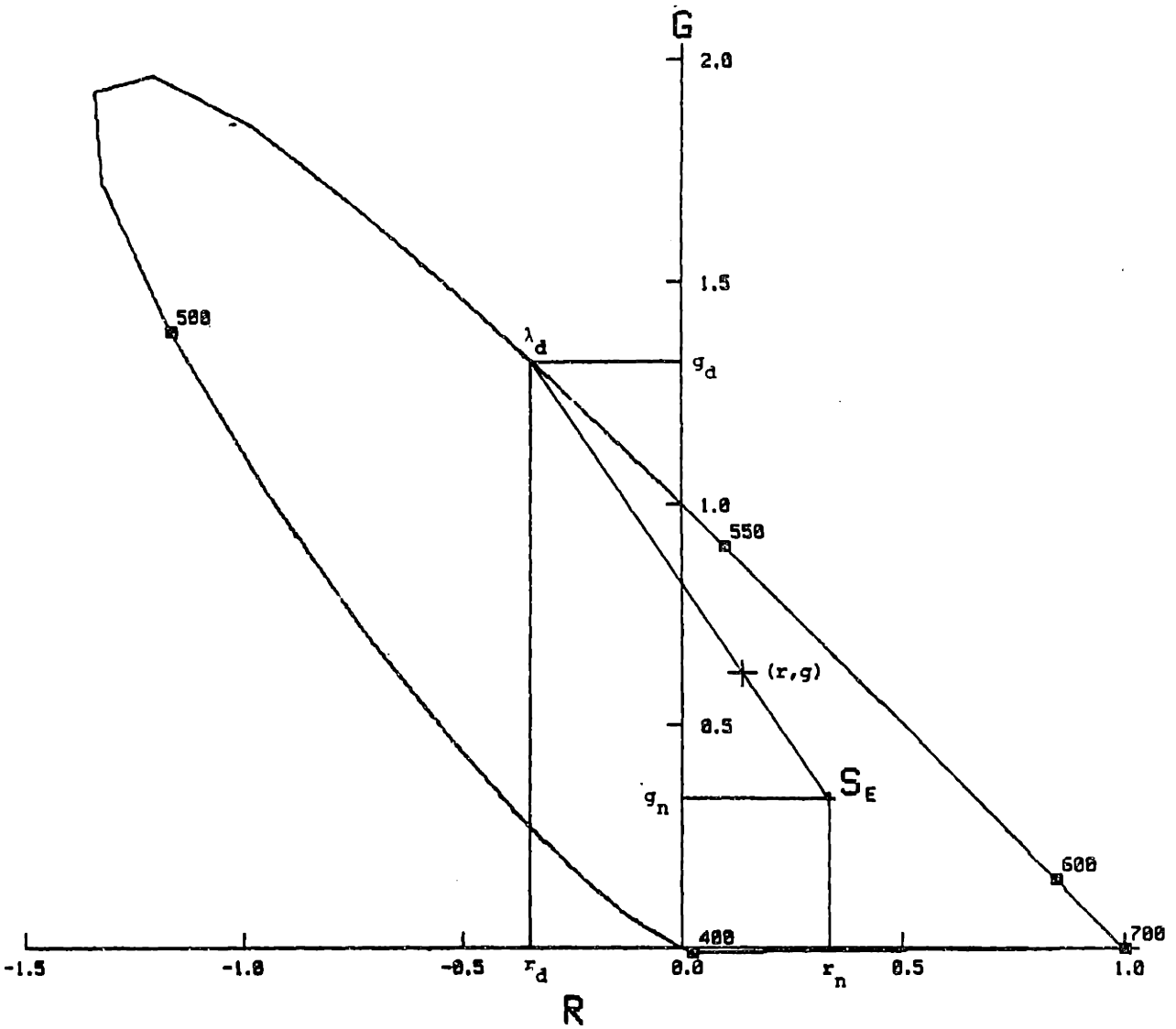

Figure 2-5. The r-g chromaticity diagram.

'desirable' criteria. The CIE XYZ system is the result of such a conversion [11]. The (Y) primary was chosen so that the corresponding color mixture function $\bar{y}$ is the luminous efficiency function: as a result, the Y tristimulus value is the luminance of the stimulus. The (X) and (Z) primaries thus have zero luminance. Another feature judged desirable was that the color mixture functions be positive-valued for all wavelengths. This specifies a primary transformation such that the spectral locus is confined entirely to one octant of tristimulus space, or alternatively, one quadrant of the chromaticity diagram. It is apparent from these conditions that the primaries (X),(Y),(Z) are imaginary, but with Equation 2.3-4, their color mixture functions can be obtained without recourse to a new experiment and the generation of imaginary primaries. As an aid to computation, a further requirement was that as many spectral stimuli as possible should be matched by two of the three primaries. The color mixture function corresponding to the third primary then would be zero over that range of wavelengths.

The primary transformation meeting these requirements is not unique; the XYZ is one solution adopted by the CIE in 1931. While computationally convenient, the XYZ system does not possess a psychophysically significant distance function: equally discriminable colors have a non-uniform distribution on the x-y chromaticity diagram [12]. This is illustrated in Figure 2-6 where the sensitivity to chromaticity differences (ten times the standard deviation of color matches) are plotted at various points on the x-y chromaticity diagram. For a given color, the chromaticity locus of just noticeably different colors at the same luminance is an ellipse whose parameters vary with (x,y). A transformation on the XYZ system that maps these ellipses into constant diameter circles would yield a uniform

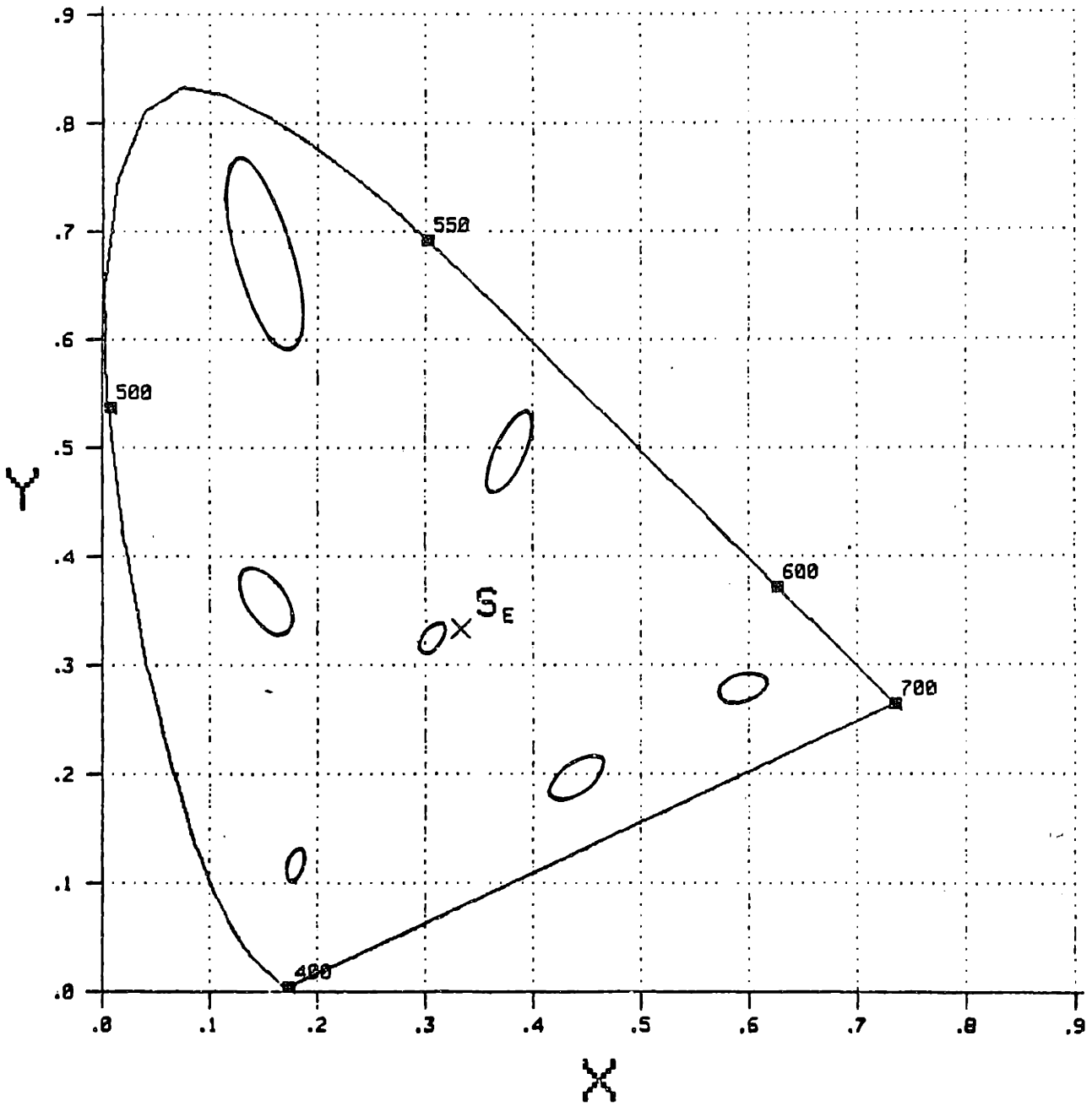

Figure 2-6. The x-y chromaticity diagram with loci of just noticeable chromaticity differences.

chromaticity space. Though no linear transformation meets these specifications, MacAdam [13] has suggested one from the XYZ to UVW primaries that significantly reduces the non-uniform distribution. This was adopted by the CIE and is the basis for the 1960 CIE-UCS (Uniform Chromaticity Scaling) diagram (Figure 2-7). The primary transformation from the RGB to the UVW primaries is given by

$$\begin{vmatrix} (U) \\ (V) \\ (W) \end{vmatrix} = \begin{vmatrix} 0.4741 & -0.1066 & 0.2536 \\ 0.0846 & 0.1934 & 0.5070 \\ -0.1560 & 0.0296 & 0.3364 \end{vmatrix} \begin{vmatrix} (R) \\ (G) \\ (B) \end{vmatrix} \qquad 2.4\text{-}1$$

The color mixture function corresponding to the (V) primary is V_λ, so that the tristimulus value V is the luminance. The chromaticity transformation is

$$u = \frac{1.96\ r + 1.24\ g + 0.8\ b}{3.1445\ r + 12.5260\ g + 3.3294\ b} \qquad 2.4\text{-}2a$$

$$v = \frac{1.0618\ r + 4.8744\ g + 0.0638\ b}{3.1445\ r + 12.5260\ g + 3.3294\ b} \qquad 2.4\text{-}2b$$

A color can thus be represented by the triplet (V,u,v).

The UCS chromaticity diagram is appropriate only for chromaticity spacing. Wyszecki recommended [14] and in 1964 the CIE adopted the U*V*W* system as the basis for the uniform three-dimensional spacing of object colors. An object color is something other than a source: its spectral distribution is due to the reflection or transmission of an irradiating flux from an object. Equal steps in luminance are not judged perceptually equal: a lightness index. that is perceptually more uniform is

$$W^* = 25\sqrt[3]{Y} - 17 \qquad 2.4\text{-}3$$

where Y is the luminous factor, the luminance normalized to 100 for a perfectly reflecting or transmitting object. The chromaticness indices are

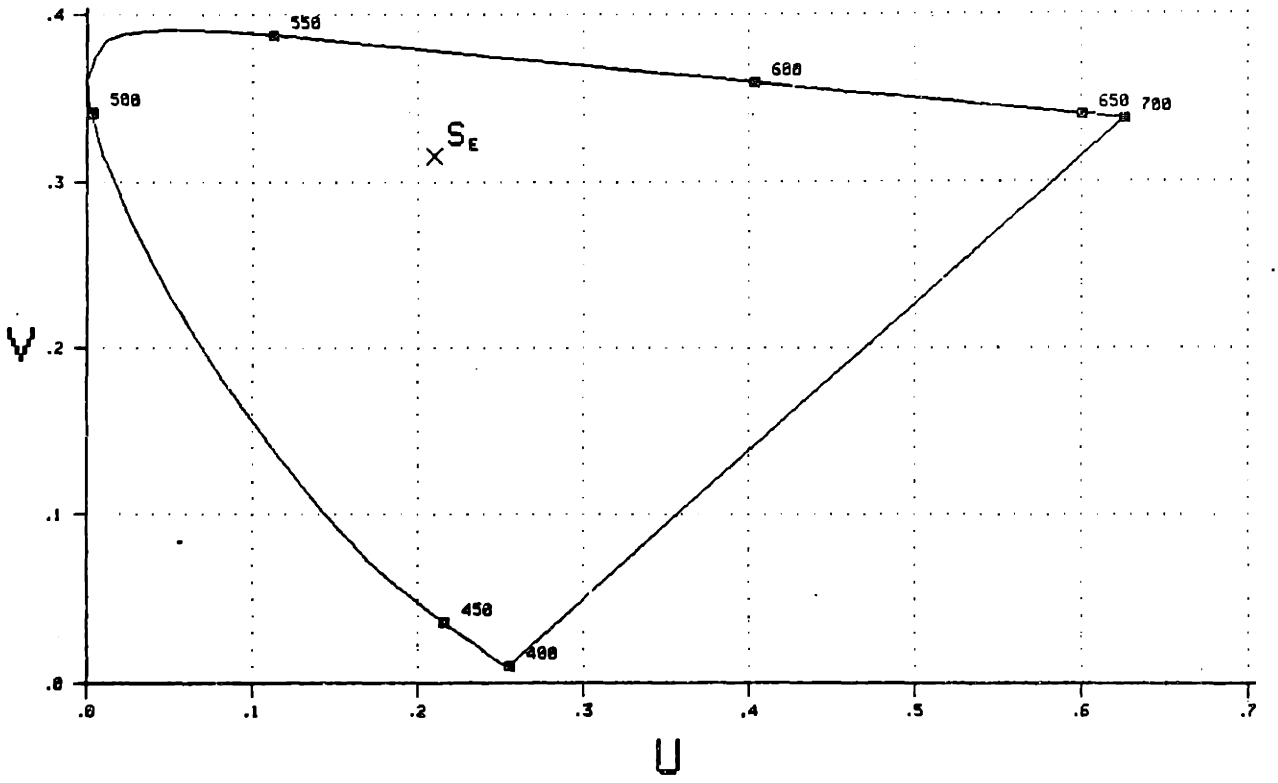

Figure 2-7. The 1960 CIE-UCS Chromaticity Diagram.

$$U^* = 13\ W^*\ (u-u_o) \qquad 2.4\text{-}4a$$

$$V^* = 13\ W^*\ (v-v_o) \qquad 2.4\text{-}4b$$

where (u_o,v_o) is the chromaticity of the achromatic reference point. The distance function for the U*V*W* space is the Euclidean norm: the distance d between two points, $[U_1^*,V_1^*,W_1^*]$ and $[U_2^*,V_2^*,W_2^*]$, is

$$d = [(U_1^*-U_2^*)^2+(V_1^*-V_2^*)^2+(W_1^*-W_2^*)^2]^{\frac{1}{2}} \qquad 2.4\text{-}5$$

2.5 Colorimetry and Sensation

Colorimetry describes the operating characteristics of the human visual system in a carefully controlled situation. The contiguous hemifields of the colorimeter subtend 2°, thereby excluding a rod component from the match. The stimuli are drawn from a range of luminances known as the photochromatic interval and are presented to the subject in Maxwellian view with a dark surround. They thus represent a particularly impoverished color stimulus, not at all like the spatially and temporally inhomogeneous fields of view we normally deal with. The Standard Observer is the artifice that averages out experimental, intra- and inter-subject variations in the matching data.

The Standard Observer is required to make no other decision than the equality of the hemifields of the colorimeter and in particular, is never asked to assign a value or attach a sensation to a given stimulus. Colloquially, a color is described in terms of its hue, saturation and brightness or lightness; it is a seductive idea that there might be a transformation from the three colorimetric variables to the three perceptual variables. There is, however,no mapping known from one to the other. A given stimulus does possess a

unique set of tristimulus values, but these do not uniquely specify the color sensation to which that stimulus gives rise.

The classic example of the inadequacy of colorimetry to predict perceptual effects was the two-color movie industry [15], now obsolete but recalled by Land's two-color demonstrations [16]. The naive application of colorimetry would predict that the additive mixture of two primaries will produce colors confined to the plane of the two primary vectors in tristimulus space, or alternatively, the line joining them on the chromaticity diagram. The sum of two color sensations is also a color sensation, but not their linear sum: psychology does not possess a conservation law. The U*V*W* representation is an attempt at a Euclidean color space but its distance function is restricted to use in the classical color matching paradigm. The range of color sensation in two-color movies was commercially acceptable, until the introduction of films incorporating three dyes in a single sheet, and confounded the strict predictions of colorimetry. An even more striking demonstration was arranged by Land and McCann [17]. Two regions in a two-color additive picture had the same tristimulus values but were surrounded by regions that between themselves had different tristimulus values: the result was that one region appeared red, and the other, green. In general then, a color sensation is a function of the tristimulus values, the recent history of visual stimulation and the spatial configuration of the visual field, as well as ill-determined psychological variables.

Chapter 3

Color Reproduction

3.1 Introduction

The block diagram of the generalized color reproduction system is shown in Figure 3-1; $Q(\lambda)$ is the spectrum of a color Q in the original and $P(\lambda)$, that of its reproduced version, P. The goal of an objective color reproduction system is $P(\lambda)=Q(\lambda)$ so that P and Q are isomers, while that of a subjective system is $P \equiv Q$, where '$\equiv$' siginifies a colorimetric match and P and Q are metamers. When all other variables of the viewing situation are equal, either condition is sufficient to insure the equal appearance of the original and its reproduction. The objective-subjective distinction of producing isomers or metamers can be restated in terms of the number of degrees of freedom, n. Subjective reproduction, with its basis in colorimetry, requires only three degrees of freedom. On the other hand, an objective system requires, in theory, an infinite number of degrees of freedom, one for each $d\lambda$. This notion is invoked in historical accounts of color photography [18], though in practice, color photographic systems are limited to three degrees of freedom.

3.2 Color Analysis and Synthesis

A reproduction system with an arbitrary set of n spectral or taking sensitivities $\{\bar{q}_i(\lambda); i=1,\ldots,n\}$ will demonstrate the phenomenon of metamerism, mapping an infinite number of spectral distributions onto the same n-tuplet $[q_1, q_2, \ldots, q_n]$, where

$$q_i = \int_{\Lambda} d\lambda \; Q(\lambda) \; \bar{q}_i(\lambda) \qquad 3.2\text{-}1$$

The metamers of such a system would not, in general, correspond to those of

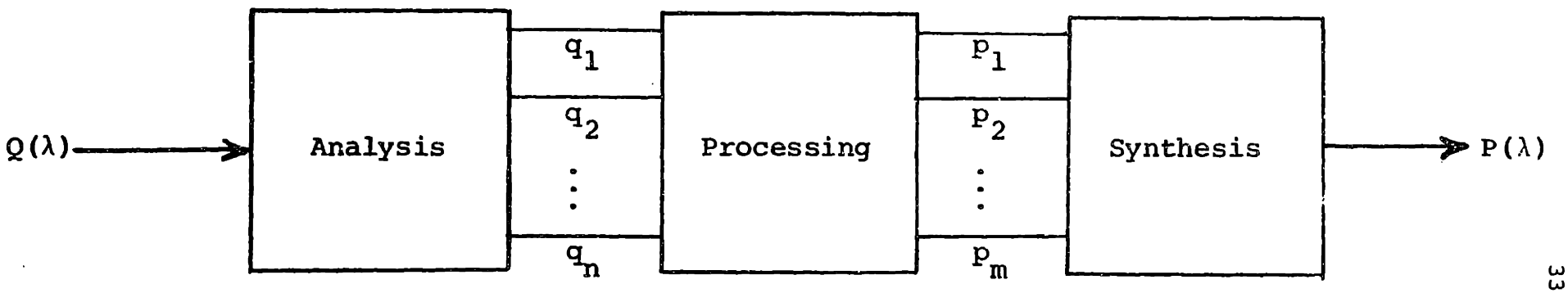

Figure 3-1. Block Diagram of the General Color Reproduction System

the Standard Observer, unless its n=3 taking sensitivities are a set of color mixture functions. Therefore, in order that metameric colors of the Standard Observer are invariant under reproduction, the results of the analysis of the input spectrum $Q(\lambda)$ must be a set of tristimulus values $[q_1,q_2,q_3]$. Then the input color Q is

$$Q \equiv q_1(Q_1) + q_2(Q_2) + q_3(Q_3) \qquad 3.2\text{-}2$$

where $(Q_1),(Q_2),(Q_3)$ are analysis primaries with color mixture functions $q_1(\lambda),q_2(\lambda),q_3(\lambda)$.

Reproduction systems are traditionally classified as additive or subtractive with regard to how they synthesize $P(\lambda)$. An additive system is the direct application of color matching experiments: the reproduced color $P(\lambda)$ is a linear combination of three fixed primaries, $(P_1)=P_1(\lambda),(P_2)=P_2(\lambda)$, $(P_3)=P_3(\lambda),(m=3)$

$$P(\lambda) = p_1P_1(\lambda) + p_2P_2(\lambda) + p_3P_3(\lambda) \qquad 3.2\text{-}3$$

taken in amounts p_1,p_2,p_3. In exact colorimetric reproduction, these amounts are tristimulus values, since $P \equiv Q$. The results of the analysis q_1,q_2,q_3 are tristimulus values for the analysis primaries $(Q_1),(Q_2),(Q_3)$ which need not be the same as the synthesis primaries $(P_1),(P_2),(P_3)$. In this case, Equation 2.3-3 applies and the processing by the system for n=m=3 can be modelled as a linear transformation $\underline{B}$,

$$[p_1,p_2,p_3]^T = \underline{B}^T\,[q_1,q_2,q_3]^T \qquad 3.2\text{-}4$$

The control signals p_1,p_2,p_3 are physically constrained to be non-negative. Given a particular set of additive primaries, this condition

restricts the range of output chromaticities and defines the gamut of the system. This is illustrated in Figure 3-2(a) for the NTSC R,G,B primaries in a color television system, the major example of additive synthesis. The gamut on the chromaticity diagram is a triangle with the R,G,B primaries at its apices: only chromaticities within the triangle can be synthesized. The chromaticity gamut gives a useful but limited view of the output. A more complete representation is given by the color solid, the convex volume in tristimulus space that contains all realizable colors, shown in Figure 3-2(b).

It would simplify the processing if $[p_1,p_2,p_3] = [q_1,q_2,q_3]$, so that $\underline{B} = \underline{I}$, the identity matrix. However, for a realizable (non-negative valued) set of primaries, as $(P_1),(P_2),(P_3)$ must be, the corresponding taking sensitivities for colorimetric reproduction would be negative valued for some λ, since there is no triangle which both contains and is contained by the spectral locus on the chromaticity diagram. This indicates a trade-off between processing complexity and the fidelity of reproduction in the choice of a set of camera taking sensitivities.

In subtractive synthesis, the spectrum of the reproduced color P is

$$P(\lambda) = I(\lambda)\tau(\lambda) \quad \text{or} \quad P(\lambda) = I(\lambda)\rho(\lambda) \qquad 3.2\text{-}5$$

where $\tau(\lambda)$ and $\rho(\lambda)$ are the transmittance and reflectance functions respectively of dyes or inks that modulate $I(\lambda)$, the spectrum of the incident illuminant. This might be more appropriately called multiplicative synthesis, given the form of Equation 3.2-5. The action of a dye is to remove energy from certain portions of the incident spectrum $I(\lambda)$, in effect, 'sculpting' the output spectrum $P(\lambda)$.

Color transparencies and reflection prints are examples of subtractive

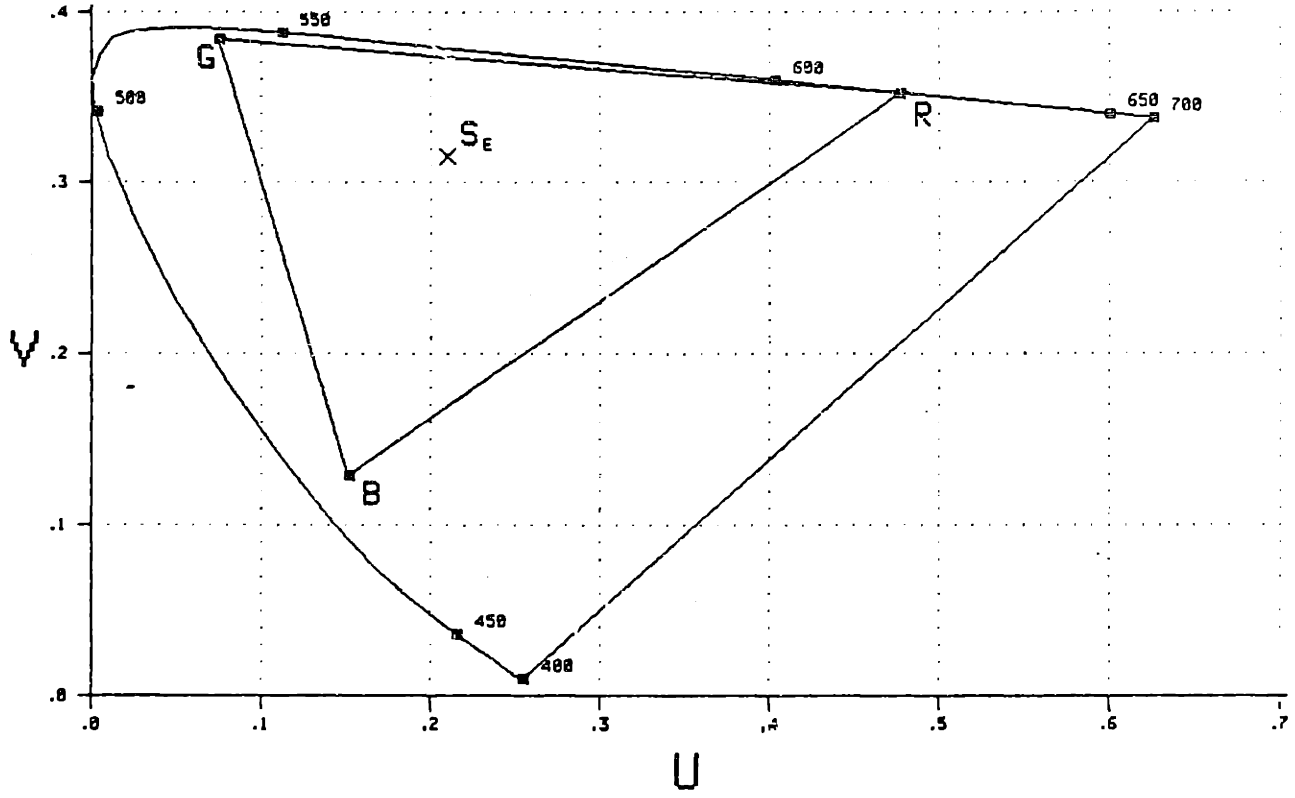

(a)

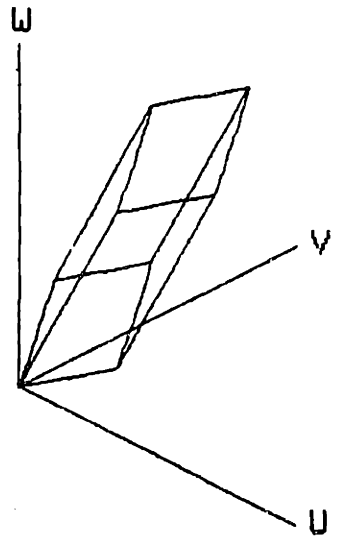

(b)

Figure 3-2. The Output Colors of the NTSC RGB Additive Primaries
(a) u-v chromaticity gamut
(b) UVW tristimulus space color solid

systems. In a transparency, the illuminant passes through dyes deposited in a thin transparent gelatin layer. The concentration or density of the dye determines the amount of light that survives to emerge from the gelatin layer: the greater the dye density at a particular wavelength, the smaller the transmittance and the less light that emerges at that wavelength. The relationship between transmittance and dye density is given by the Lambert-Beer Law [19],

$$\tau(\lambda) = 10^{-d\ D(\lambda)} \qquad 3.2\text{-}6$$

where $\tau(\lambda)$ is the transmittance function; d, the dye density or concentration and $D(\lambda)$, the spectral density function of a unit concentration of dye. In a reflectance print, the gelatin layer containing the dyes is coated on a diffusely reflecting white (spectrally non-selective) support from which light reflects back through the absorbing dye layer.

Modern photographic systems have three spatially continuous dyes (m=3) and thus, three degrees of freedom in determining $\tau(\lambda)$

$$\begin{aligned}\tau(\lambda) &= 10^{-[d_1D_1(\lambda)+d_2D_2(\lambda)+d_3D_3(\lambda)]} \\ &= 10^{-\ \underline{d}\cdot\underline{D}(\lambda)}\end{aligned} \qquad 3.2\text{-}7$$

where $\underline{d} = [d_1, d_2, d_3]$ is the dye concentration vector and $\underline{D}(\lambda) = [D_1(\lambda), D_2(\lambda), D_3(\lambda)]$ is the dye spectral density vector. Processing controls the vector $\underline{d}$. The dyes typically cited as ideal are spectral notch filters with non-overlapping stop bands, as shown in Figure 3-3. The maximum absorption of the ideal yellow block dye occurs in the blue region of the spectrum, λ = 400 to 500 nm (yellow and blue are complementary colors); for the magenta dye, in the green region from 500 to 600 nm and for the cyan dye, in the red region from 600 to 700 nm.

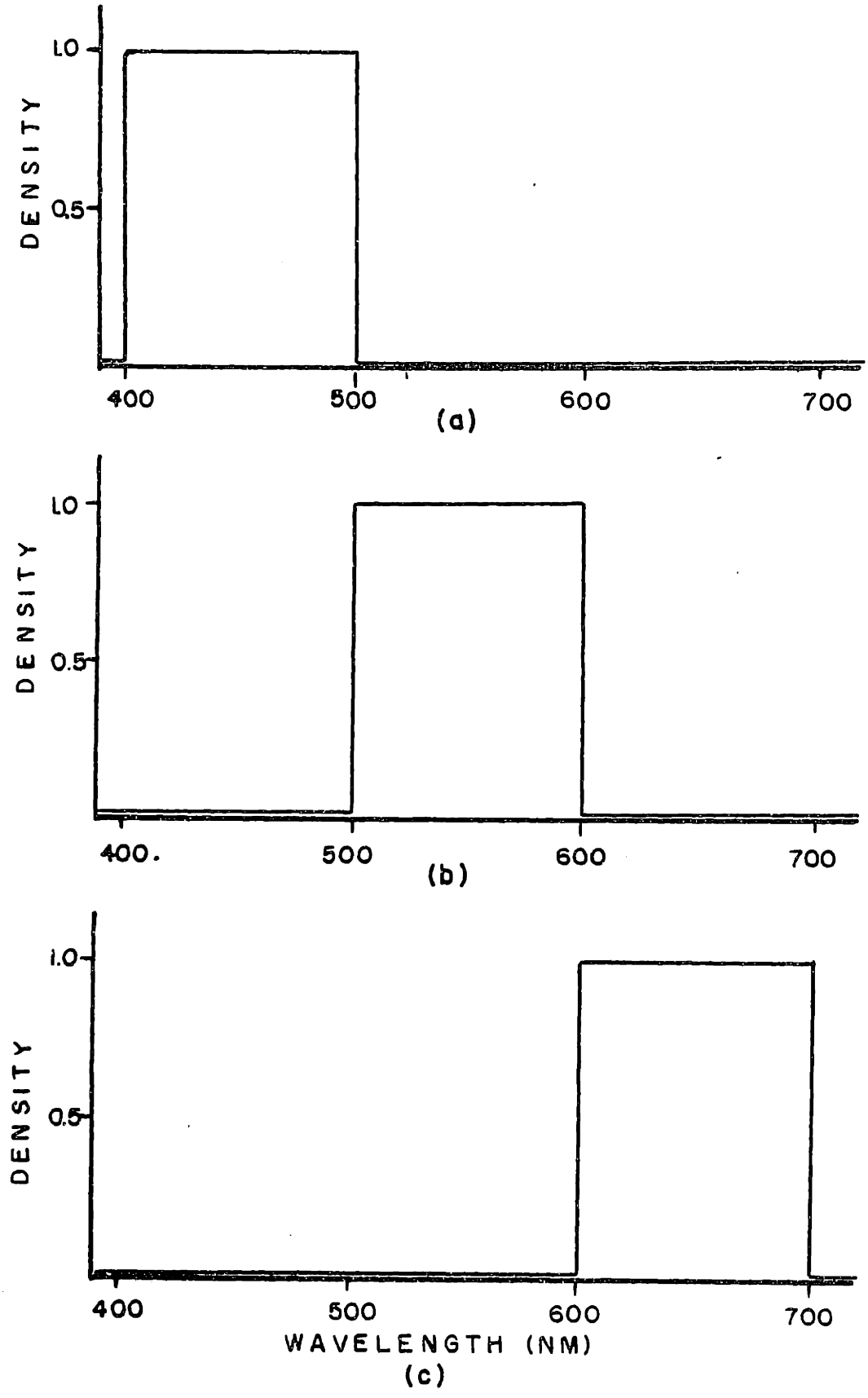

Figure 3-3. Spectral Density Functions of Ideal Block Dyes: (a) yellow, (b) magenta, (c) cyan.

The dyes in a subtractive system act as if they are controlling primaries. In an additive system, the primaries are self-evident while in a subtractive system, they are not, though it would be equally useful to know what they are [20,21]. An additive primary (P_i) can be described by its spectral distribution $P_i(\lambda)$ or by a vector of tristimulus values, $\underline{P}_i = [P_{i1}, P_{i2}, P_{i3}]$. The additively synthesized color P then has the tristimulus vector

$$\underline{P} = p_1 \underline{P}_1 + p_2 \underline{P}_2 + p_3 \underline{P}_3 \qquad 3.2\text{-}8$$

The primary controlled by p_i is

$$\frac{\partial \underline{P}}{\partial p_i} = \underline{P}_i \qquad 3.2\text{-}9$$

The tristimulus vector for a subtractively synthesized color P is

$$\underline{P} = \int_{\Lambda} d\lambda \; I(\lambda) \; 10^{-\underline{d}\cdot\underline{D}(\lambda)} \; \underline{u}(\lambda) \qquad 3.2\text{-}10$$

where $\underline{u}(\lambda) = [\bar{u}(\lambda), \bar{v}(\lambda), \bar{w}(\lambda)]$ is a vector of color mixture functions. The primary controlled by d_i is

$$\frac{\partial \underline{P}}{\partial d_i} = -2.3 \int_{\Lambda} d\lambda \; D_i(\lambda) \; I(\lambda) \; 10^{-\underline{d}\cdot\underline{D}(\lambda)} \; \underline{u}(\lambda) \qquad 3.2\text{-}11$$

The subtractive primary is clearly a function of the dye concentration $\underline{d}$ and consequently varies with the color being reproduced. For this reason, subtractive primaries have been characterized as unstable [20]. Since they are not constant functions, the simple analysis of the additive system does not carry over to the general case of subtactive synthesis, where another line of analysis must be pursued. The difference between additive and subtractive synthesis then is analogous to that between linear time-invariant

and non-linear time-varying systems. We are now in a position to appreciate the sense in which the dyes of Figure 3-3 are ideal.

The visible spectrum Λ is partitioned into three intervals, $\Lambda_1,\Lambda_2,\Lambda_3$. Over any one interval Λ_i, the unit amount of one dye has a constant spectral density D_i=1.0, while the other two dyes transmit perfectly (D=0.0). For these dyes, Equation 3.2-10 can be re-written as

$$\begin{aligned}\underline{P} &= \sum_{i=1}^{3} \int_{\Lambda_i} d\lambda\ I(\lambda)\ 10^{-d_i D_i}\ \underline{u}(\lambda) \\ &= \sum_{i=1}^{3} 10^{-d_i D_i} \int_{\Lambda_i} d\lambda\ I(\lambda)\ \underline{u}(\lambda) \\ &= \sum_{i=1}^{3} 10^{-d_i}\ \underline{I}_i \end{aligned} \qquad 3.2\text{-}12$$

This reduces to Equation 3.2-8 when $p_i=q_i=10^{-d_i}$ or $d_i = -\log(q_i)$ where q_i is a tristimulus value from the analysis. Therefore, if this relation is is satisfied and the Lambert-Beer Law holds, then subtractive color reproduction with ideal dyes is a linear system, with primaries $\underline{I}_1,\underline{I}_2,\underline{I}_3$. This is a physically impossible situation,but has nevertheless motivated modern subtractive reproduction theory [20].

Color photography has often been discussed as an imperfect though practical example of objective reproduction [18,22,23]. The visible spectrum Λ is divided into n bands of equal width $\Delta\lambda=\Lambda/n$; these n pulses correspond to a set of orthogonal basis functions. The input spectrum is analyzed over each of these bands, with the results of the analysis controlling the light in the same band of the output spectrum (m=n). In subtractive synthesis, the control is reciprocal: for example, the more light in the blue band of the original, the less yellow (minus-blue) dye in the reproduction. In the ideal

case, $n \to \infty$ and $\Delta\lambda \to d\lambda$. Practical considerations are typically cited [18] for limiting n to 3, though the trichromacy of human color vision indicates that these three degrees of freedom are sufficient to obtain a gamut that, according to the psychology of color sensation, is acceptable, as imperfect as the actual process may be.

This theoretical analysis provides the starting point for examining the photographic process used in the experimental system.

3.3 A Color Photographic Process

Polacolor 2 is a direct photographic process producing reflection prints, an example of subtractive color reproduction. The spectral density functions $D_i(\lambda)$ of its three dyes are shown in Figure 3-4 for dye amounts that yield a neutral density of 1.0 when the illuminant is S_E. The dye amounts are determined by the exposure to dye-forming layers with taking sensitivities that are approximately complementary to the spectral density function of the dye each controls. The spectral sensitivity functions of the yellow, magenta and cyan dye-forming layers are shown in Figure 3-5. The exposure E_d is given by

$$E_d = \int_0^\infty d\lambda \; H(\lambda) \; S_d(\lambda) \qquad 3.3\text{-}1$$

Allowing for the change in notation, this expression is identical to Equation 3.2-1: $S_d(\lambda)$ is the spectral sensitivity function of the emulsion controlling dye d and $H(\lambda)$ is the irradiating energy spectrum. $H(\lambda)$ is the integral of the irradiating flux over the exposure time: in as much as flux (power) can be traded off against exposure time such that their product remains constant and E_d is unchanged, the process obeys the reciprocity law. The analytic density or concentration (d_i in Equation 3.2-7) of dye d is a

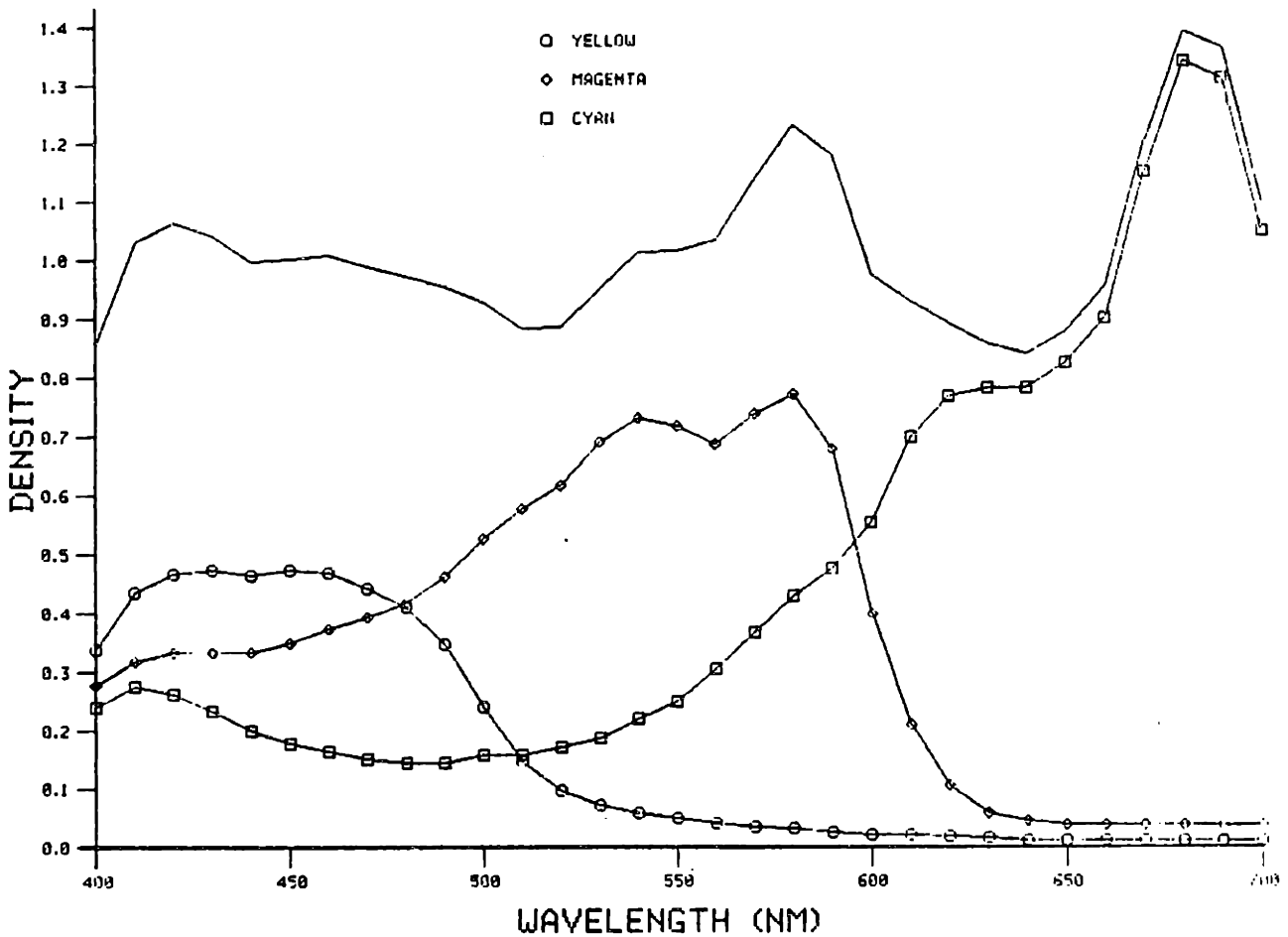

Figure 3-4. Spectral Density Functions of Polacolor 2 Dyes at an Equivalent Neutral Density of 1.0.

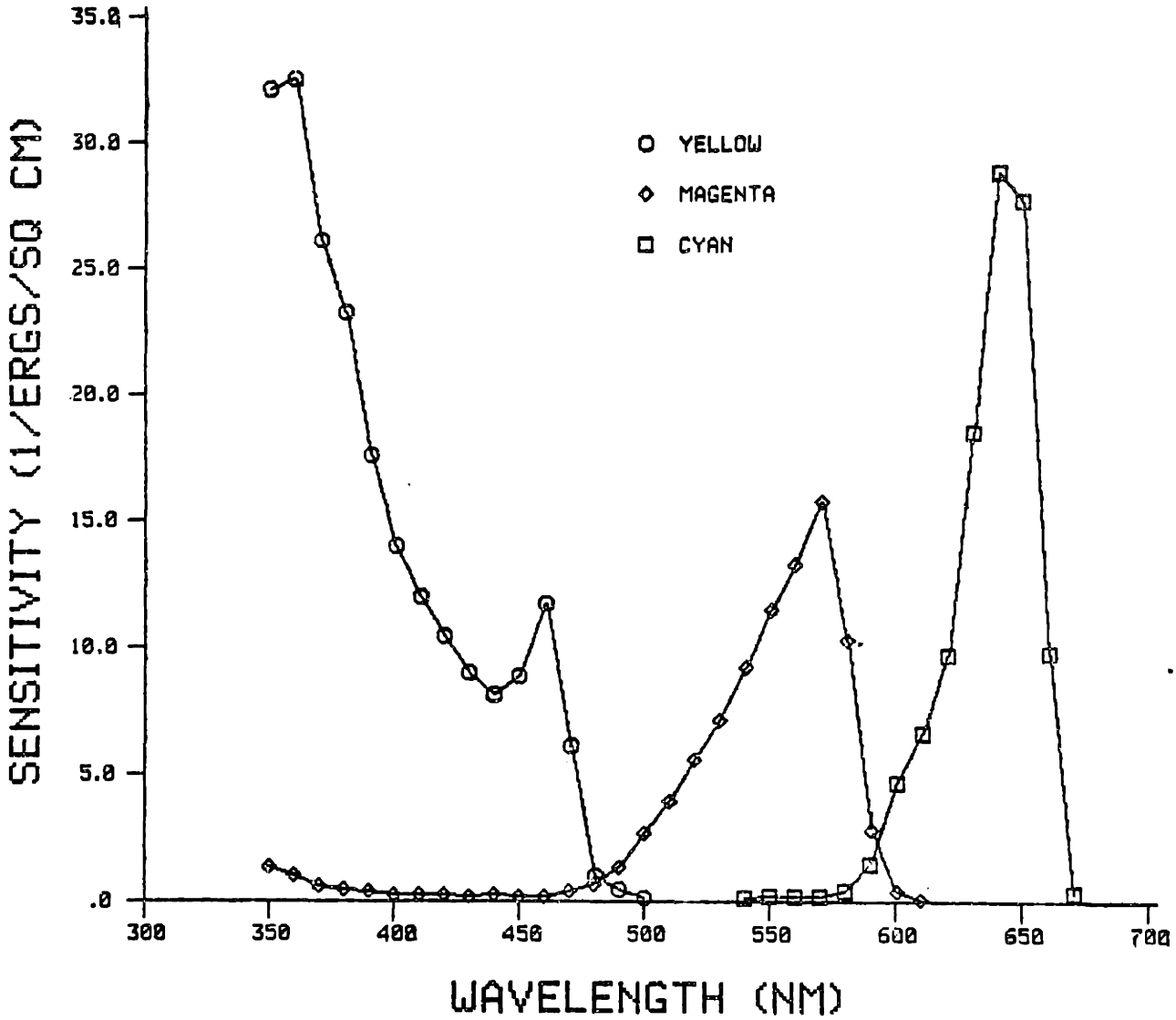

Figure 3-5. Spectral Sensitivity Functions of Polacolor 2 Emulsions at an Equivalent Neutral Density of 0.75.

function of the exposure E_d. Plotting the analytic dye density against the logarithm of the exposure gives a straight line: this is the log operation of the ideal system in the last section. The exact nature of the relationship between them is determined by the chemical processes during the development of the print.

It is implicit that this processing is described by the identity matrix $\underline{I}$ so that the cyan, magenta and yellow dye densities are controlled only by the exposures to the cyan, magenta and yellow dye-forming layers respectively. However, in Polacolor 2, as in some other films [24], there are inter-image effects and the developed dye density in one layer affects those in the other layers as well.

The antilog operation required by the ideal system is obtained optically by the way in which light intensity is controlled by an absorbing dye layer. From Equation 3.2-7, the transmission density (the logarithm of the transmittance $\tau(\lambda)$) of the dye layer is $\underline{d} \cdot \underline{D}(\lambda)$. However, when this dye layer is coated on a white reflective support, the resulting reflection density is not simply twice the transmission density of the dye layer since the support is not a perfect reflector and there are internal reflections at the gelatin-air interface [25]. The actual relationship between reflection and transmission density for a gelatin layer on a diffusely reflecting base is shown in Figure 3-6.

The overall transfer characteristic of the process, resulting from the concatenation of the analytic dye density versus log exposure and reflection density versus analytic dye density curves, is shown in Figure 3-7. This is the Hurter-Driffield [26] or D - log(E) curve, where optical density D, the logarithm of the reflectance as seen through a red, green or blue

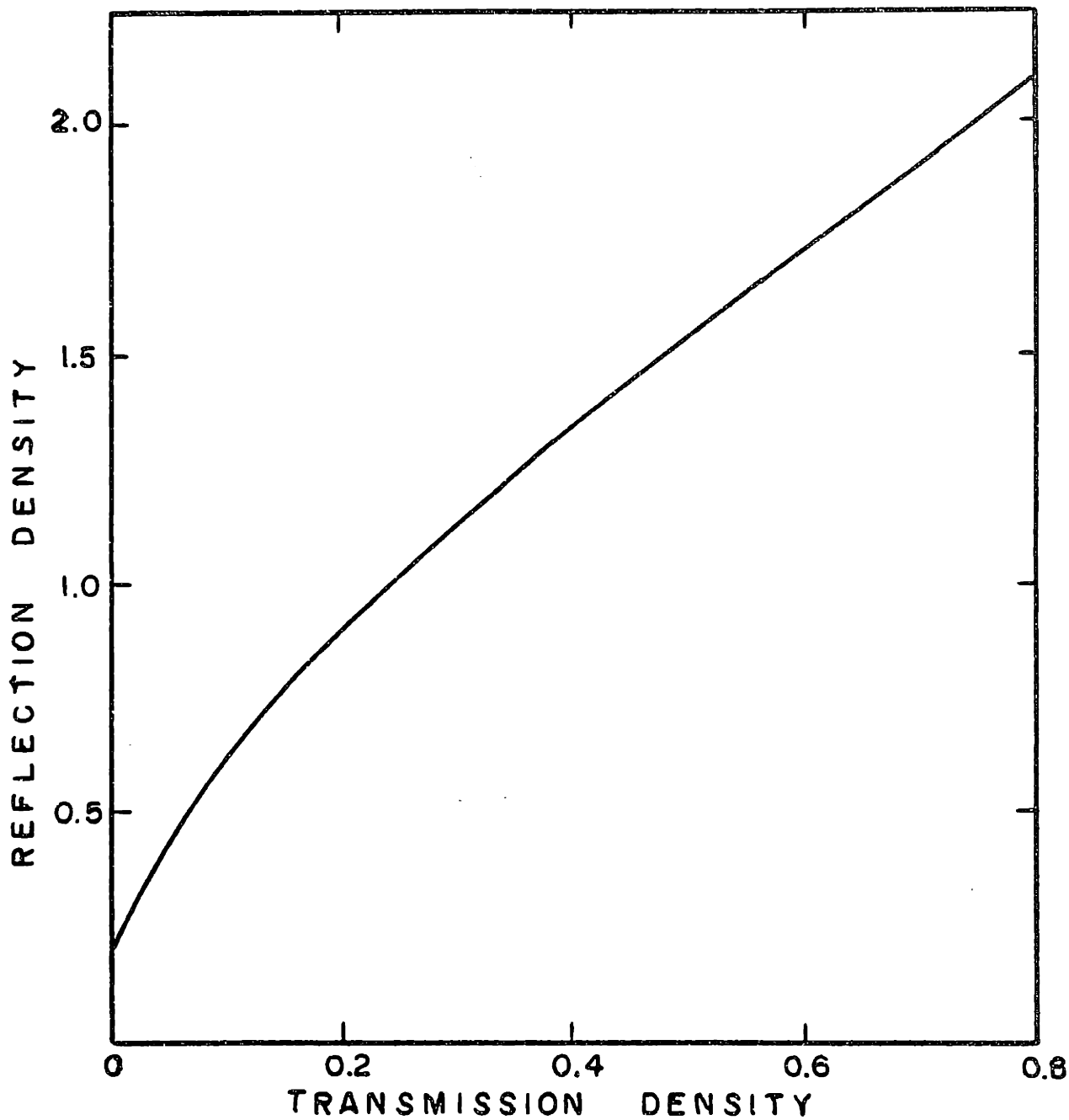

Figure 3-6. Reflection Density versus Transmission Density of a gelatin layer coated on a base with reflectance = 0.80

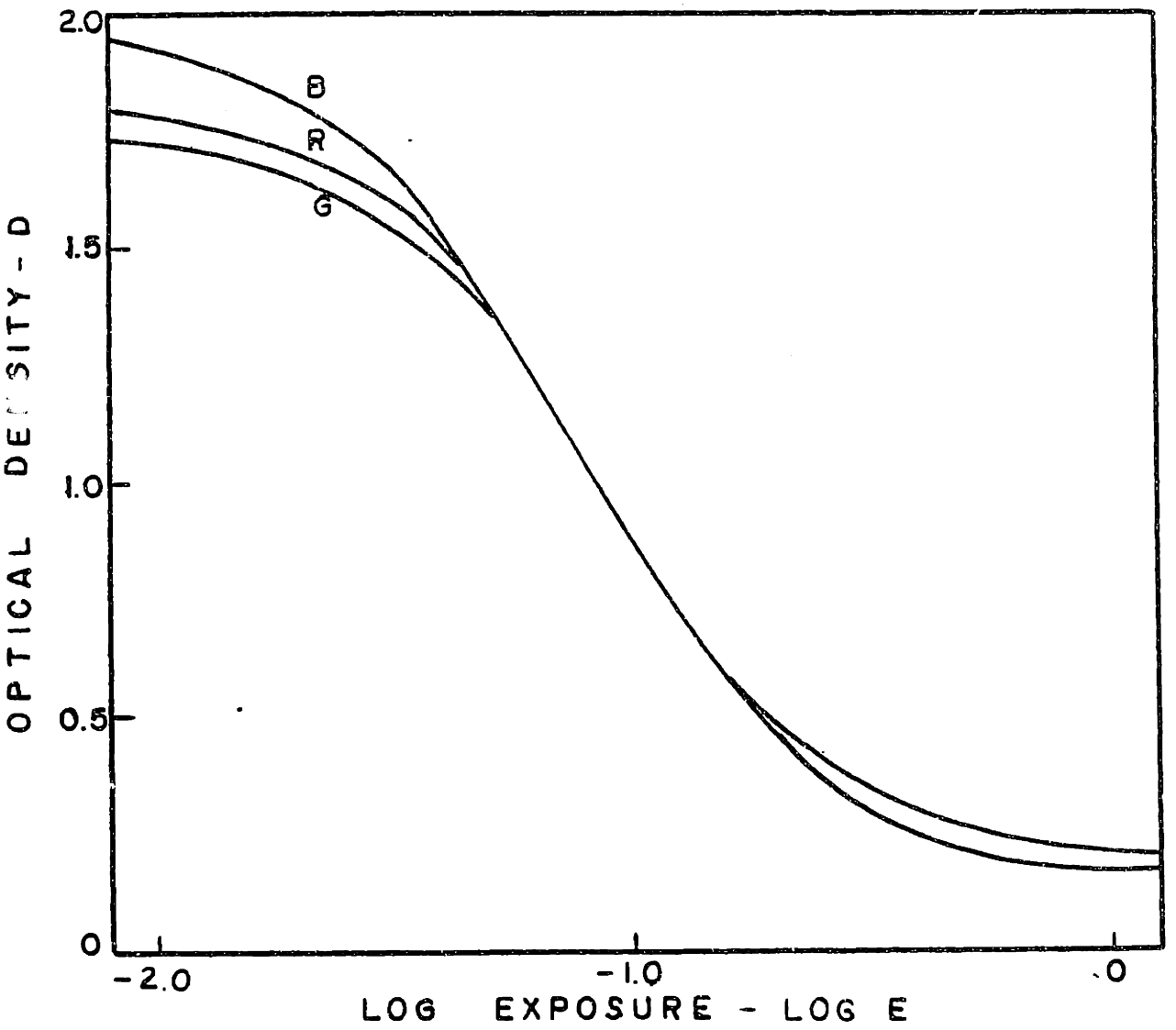

Figure 3-7. Sample D - log E curve

filter is plotted against the logarithm of the exposure. Equal exposures give equal optical densities and a neutral dye image. A portion of the D - log(E) curve can be fit by a straight line with slope gamma γ. In order to track a neutral over this portion of the exposure range, the gammas of the three D - log(E) curves must be equal.

With the spectral density functions and the relationship between transmission and reflection density, it is possible to compute the chromaticity gamut of Polacolor 2. It is shown in Figure 3-8 for a maximum print reflectance density of 2.0 .

It is clear that Polacolor 2 does not satisfy the mathematical conditions for exact colorimetric reproduction: indeed, no photographic process does. This however, has not limited the commercial success of color photography, since pleasing rather than colorimetric reproduction is the ultimate criterion of acceptance.

3.4 The Analysis of a Color Reproduction System

The previous section gave the characteristics of Polacolor 2, the photographic process used in the experimental system. Though not capable of colorimetric reproduction, it is able to give very pleasing color pictures. There are situations,however, where the former would be the goal of a reproduction system. When a photo editor selects a color picture for publication, he or she would certainly accept a reproduction that is indistinguishable from the original when the two are compared side by side. With the computer processing of pictures, it is possible to reduce the error $(\underline{P}-\underline{Q})$ in tristimulus space that the photographic process introduces with respect to the goal of colorimetric reproduction (Figure 3-9).

Color reproductions result from triple exposing 3 computer-generated

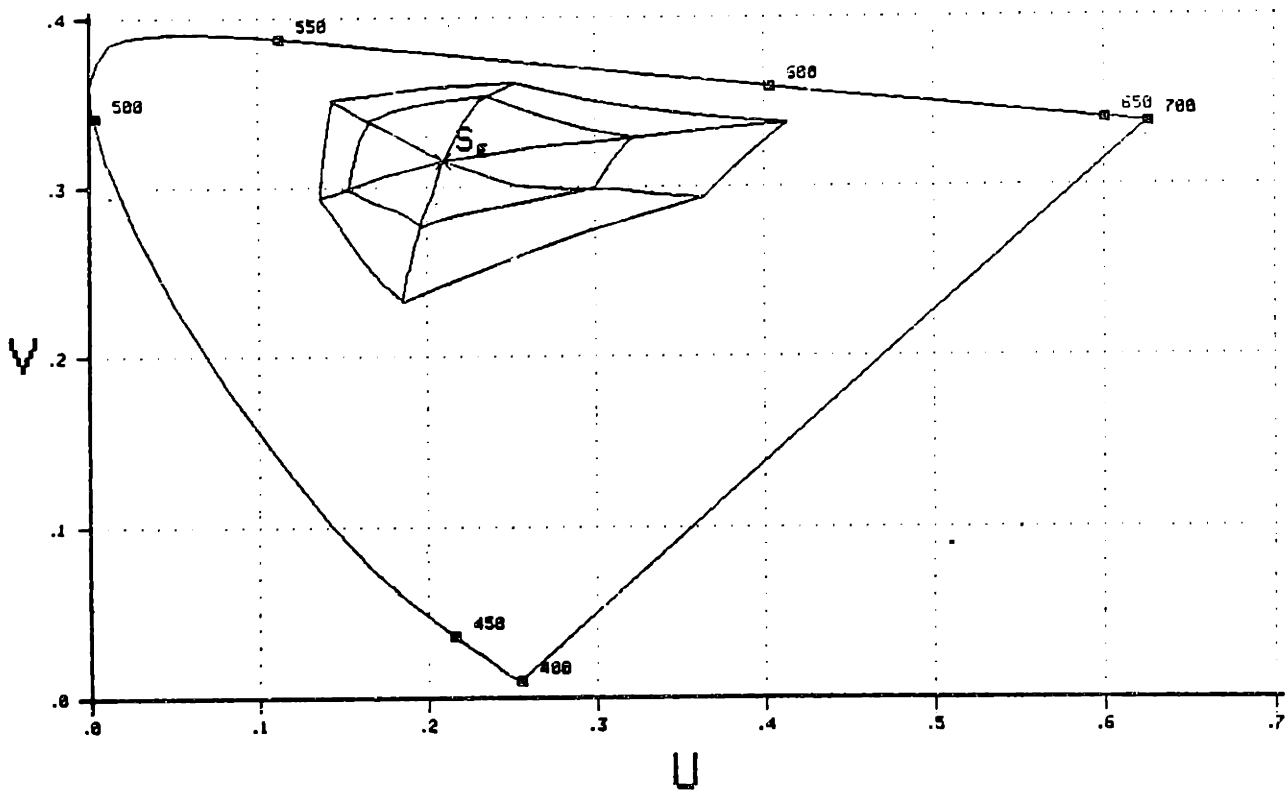

Figure 3-8. The chromaticity gamut of Polacolor 2 for a maximum reflectance density of 2.0.

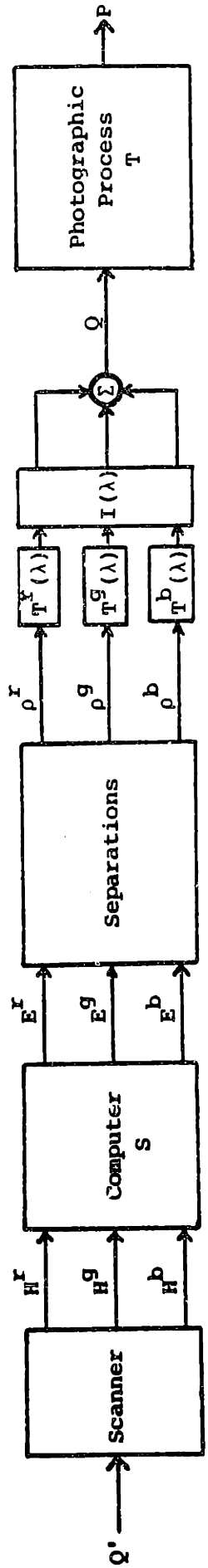

Figure 3-9. Block Diagram of the Computer Color Reproduction System.

See text for description of the variables.

separations through the appropriate filters onto film. The photographic process can be represented by a mapping T: $\underline{Q} \rightarrow \underline{P}$ and the computer processing by the mapping S: $\underline{Q}' \rightarrow \underline{Q}$, where $\underline{Q},\underline{Q}',\underline{P}$ are the tristimulus vectors of the colors Q,Q',P in Figure 3-9. For exact colorimetric reproduction, the composition of these functions $(S \circ T)$: $\underline{Q}' \rightarrow \underline{P}$ is such that $Q' \equiv P$, that is, $\underline{Q}' = \underline{P}$. Therefore, $S \circ T$ is the identity mapping in tristimulus space and S is the inverse of T.

A constraint imposed on the experimental system is that both the original reflection copy and its reproduction use the same dyes, so that $Q' \equiv P$ becomes $Q'(\lambda) = P(\lambda)$. This is referred to as duplicating, as opposed to copying. Therefore, the mapping from the set of possible input spectral distributions $Q'(\lambda)$ to tristimulus space is one to one, since the input spectra have only three degrees of freedom: once $\underline{d} = [d_1,d_2,d_3]$ is known, the input is uniquely specified. Therefore, the computer need not have spectral sensitivity functions that are a set of color mixture functions.

Computer processing is equivalent to inverting the transformation T. This can be accomplished in one of two ways. The first is to generate a large set of $\underline{Q}$ on the computer, producing points $\underline{P}$ within the color solid of the photographic process. A table is then set up, where a particular entry, accessed by co-ordinates $\underline{P} = \underline{Q}'$, is the $\underline{Q}$ that produces that $\underline{P}$. Color reproduction is thus had by table look-up; when there is no entry for a given $\underline{P}$, the corresponding $\underline{Q}$ is obtained by interpolation. The second method is to model the photographic process by a closed-form function T, where $\underline{P} = T(\underline{Q})$ and then simply invert that function to obtain T^{-1}. This was the method pursued, for the simplicity that it appeared to offer. It involves modelling three stages in the reproduction system: the computer generation

of separations, their combination onto film and the scanning of the resulting color copy by the computer. T then gives the computer input variables as a function of the computer output variables.

The three computer-generated separations are black and white reflectance copy with density D^s, where

$$D^s = - \gamma_1 \log E^s + D_{max} \qquad 3.4\text{-}1$$

E^s is the digital exposure value output by the computer; γ_1, the gamma of the process and s is either r, g, or b, referring to the red, green, or blue separation. Separation density decreases with increasing exposure from a maximum value of D_{max} at the minimum exposure, normalized to 1. The computer output is the exposure vector $[E^r, E^g, E^b]$.

In the second stage, each separation s is exposed onto film through a filter with transmittance function $T^s(\lambda)$. The resulting exposure to dye-forming layer d by separation s is E_d^s, given by

$$E_d^s = \int_0^\infty d\lambda \; I(\lambda) \; T^s(\lambda) \; \rho^s \; S_d(\lambda) \qquad 3.4\text{-}2$$

where $S_d(\lambda)$ is the taking sensitivity of dye-forming layer d and d is either c, m, or y, referring to the cyan, magenta, or yellow dye. $I(\lambda)$ is the energy spectrum of the source illuminating the separation s which has a spectrally non-selective reflectance function

$$\rho^s = 10^{-D^s} \qquad 3.4\text{-}3$$

With a judicious choice of separation filters $T^s(\lambda)$, it is possible that the products $S_d T^s I$ for different s are non-zero over mutually exclusive wavelength intervals. As a result, the exposure of a given separation

exposes only one dye layer: the red separation controls the cyan exposure; the green separation, the magenta exposure and the blue, the yellow exposure. Therefore, the only non-zero exposures are E_c^r, E_m^g and E_y^b so that the superscripts can be dropped. Equation 3.4-2 becomes

$$E_d = k_d \rho^s \qquad 3.4\text{-}4$$

where

$$k_d = \int_0^\infty d\lambda \; I(\lambda) \; T^s(\lambda) \; S_d(\lambda) \qquad 3.4\text{-}5$$

and $s = \bar{d}$, the complement of d. For example, if d is c (cyan), then s is r (red); similarly, $g = \bar{m}$ and $b = \bar{y}$. By definition, a neutral stimulus $\rho^r = \rho^g = \rho^b$ gives identical exposures to each dye-forming layer $E_c = E_m = E_y$, so that $k_c = k_m = k_y = k$. This condition is satisfied experimentally by combining neutral density filters with the separation filters and varying the exposure time for each so that triple exposing equal separations does indeed give a neutral.

Analogous to Equation 3.4-1, the analytic density d_d of dye d is

$$d_d = - \gamma_2 \log E_d + d_{max} \qquad 3.4\text{-}6$$

where γ_2 is the gamma of the photographic process and d_{max}, the maximum analytic dye density. Subscript d refers to a particular dye, either c, m or y. Substituting Equations 3.4-1 and 3.4-4 in 3.4-6 and then simplifying gives the analytic density d_d in terms of the computer output exposure

$$d_d = - \gamma_1 \gamma_2 \log E^{\bar{d}} + d'_{max} \qquad 3.4\text{-}7$$

where

$$d'_{max} = d_{max} + \gamma_2 (D_{max} - \log k) \qquad 3.4\text{-}8$$

This means that the plot of analytic dye density versus the logarithm of the computer output exposure is a straight line.

The simplest model for the reflectance function of the output print is

$$\rho(\lambda) = 10^{-\underline{d}\cdot\underline{D}(\lambda)} \qquad 3.4\text{-}9$$

where '·' signifies the dot product of the analytic dye density vector $\underline{d} = [d_c, d_m, d_y]$ and the spectral density function vector $\underline{D}(\lambda) = [D_c(\lambda), D_m(\lambda), D_y(\lambda)]$.

In the last of the three processes to be modelled, the computers scans the reflection copy using an optical head with spectral sensitivity functions $\{h^s(\lambda); s=r,g,b\}$. The input to the computer is a color head vector $\underline{H} = [H^r, H^g, H^b]$, where

$$H^s = \int_0^\infty d\lambda\ \rho(\lambda)\ h^s(\lambda) \qquad 3.4\text{-}10$$

In order to obtain a closed form expression for H^s, one of two assumptions can be made. The first is that the color head uses narrowband filters, approaching $\delta(\lambda-\lambda^s)$ in the limit. The alternative is that the process has 'non-ideal' block dyes (Figure 3-10). The spectral density function $D_d(\lambda)$ of dye d is a constant D_d^r, D_d^g, D_d^b over the three wavelength intervals Λ^r, Λ^g, Λ^b respectively, corresponding to the mutually exclusive passbands $h^s(\lambda)$ of the computer color head. Pursuing this assumption yields

$$\begin{aligned} H^s &= \int_{\Lambda^s} d\lambda\ h^s(\lambda)\ 10^{-\underline{d}\cdot\underline{D}(\lambda)} \\ &= 10^{-\underline{d}\cdot\underline{D}^s} \int_{\Lambda^s} d\lambda\ h^s(\lambda) \end{aligned} \qquad 3.4\text{-}11$$

$\underline{D}^s = [D_c^s, D_m^s, D_y^s]$ is the dye spectral density vector in the interval Λ^s.

Substituting Equation 3.4-7 in 3.4-11 gives

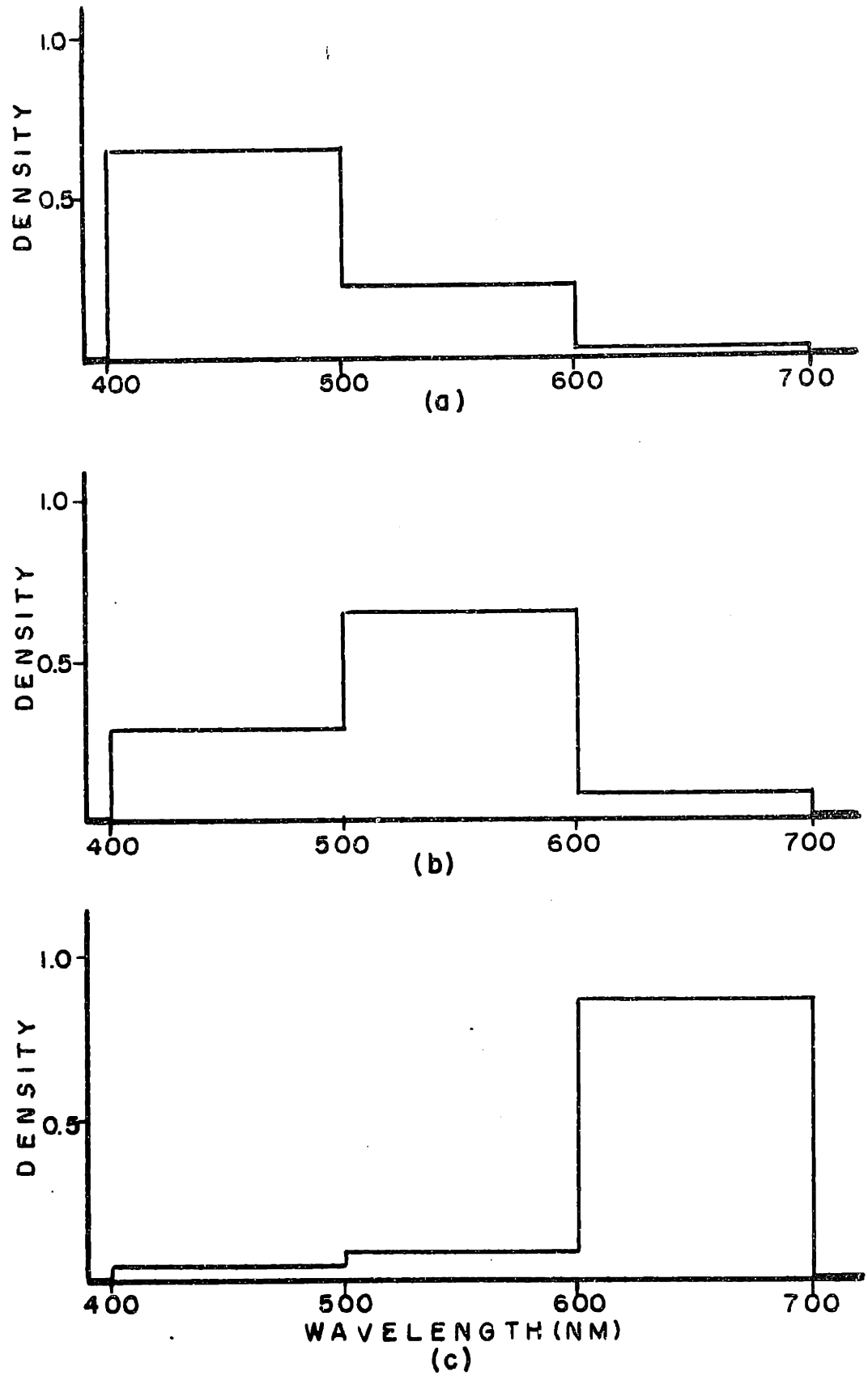

Figure 3-10. Spectral Density Functions of 'Non-Ideal' Block Dyes: (a) yellow, (b) magenta, (c) cyan.

$$H^s = 10^{\gamma_1\gamma_2 \log \underline{E}^{\bar{d}} \cdot \underline{D}^s} \; 10^{-d'_{max} \int_{\Lambda^s} d\lambda \; h^s(\lambda)}$$

$$= k^s \; 10^{\gamma_1\gamma_2 \log \underline{E}^{\bar{d}} \cdot \underline{D}^s} \qquad 3.4\text{-}12$$

k^s is the color head calibration so that the minimum exposure, resulting in the maximum optical density d'_{max}, gives $H^s = 1$. Therefore,

$$H^s = 10^{\gamma_1\gamma_2 \log \underline{E}^{\bar{d}} \cdot \underline{D}^s} \qquad 3.4\text{-}13$$

This is the desired closed form expression, relating the computer input to the computer output, via photographic reproduction. Taking the logarithm of both sides of Equation 3.4-13 for s equal to r, g and b gives

$$\begin{vmatrix} \log H^r \\ \log H^g \\ \log H^b \end{vmatrix} = \gamma_1\gamma_2 \begin{vmatrix} D_c^r & D_m^r & D_y^r \\ D_c^g & D_m^g & D_y^g \\ D_c^b & D_m^b & D_y^b \end{vmatrix} \begin{vmatrix} \log E^r \\ \log E^g \\ \log E^b \end{vmatrix} \qquad 3.4\text{-}14$$

This makes intuitive sense: each color head value is controlled by all three exposures due to the overlapping absorption curves of the dyes.

For the model of the photographic process described here, the mapping $T: \underline{E} \rightarrow \underline{H}$ is a linear transformation in the log (density) domain

$$\log \underline{H} = \underline{A} \log \underline{E} \qquad 3.4\text{-}15$$

where $\underline{A}$ is a 3x3 matrix with elements $\gamma_1\gamma_2 D_d^s$. The inverse mapping, $S: \underline{H} \rightarrow \underline{E}$ can be had by inverting $\underline{A}$ to obtain $\underline{B} = [b_{ij}]$

$$\log \underline{E} = \underline{B} \log \underline{H} \qquad 3.4\text{-}16$$

According to Equation 3.4-16, color correction for a subtractive system with

spatially-continuous non-ideal block dyes obeying the Lambert-Beer Law is a multiplicative homomorphic system [27].

This is the mathematical expression of masking for color correction as it is performed in the darkroom [28]. Consider the exposure E_m to the magenta dye. From Equation 3.4-16,

$$E_m = H_r^{b_{21}} H_g^{b_{22}} H_b^{b_{23}} \qquad 3.4\text{-}17$$

For convenience, H^s is written H_s here. In a negative-positive process, this exposure is obtained by sandwiching together three negatives, developed to have gammas of b_{21}, b_{22}, b_{23}, and then exposing the print paper through them. When the gamma b_{ij} is negative, the corresponding mask $H_s^{b_{ij}}$ is a positive rather than a negative. The masking equation for the magenta exposure E_m indicates that it is not what one would expect from the green record H_g alone. The green record of the original is not determined solely by the magenta dye density, but also by the cyan and yellow dye densities, due to their unwanted absorptions (with respect to the ideal dyes) in the band of H_g. Therefore, in using the green record to print the magenta dye, it must first be corrected for the unwanted absorptions of the other dyes.

Allowing for a change in notation, Equation 3.4-16 occurs in almost every treatment of color correction. Its standard form is

$$\begin{vmatrix} D_c \\ D_m \\ D_y \end{vmatrix} = \begin{vmatrix} b_{11} & b_{12} & b_{13} \\ b_{21} & b_{22} & b_{23} \\ b_{31} & b_{32} & b_{33} \end{vmatrix} \begin{vmatrix} D_r \\ D_g \\ D_b \end{vmatrix} \qquad 3.4\text{-}18$$

On the right-hand side, D_s is the optical density ($\log H^s$) and on the left-hand side, D_d is the printing density ($\log E^{\bar{d}} = \log E_{\bar{d}}$). The derivation of

this result is useful in making explicit four assumptions that had to be made along the way [29].

One is that the system is operating over the linear portions of the characteristic curves of its constituent processes. This can be examined for the reproduction of a neutral grey scale. Equal exposures $E^r = E^g = E^b = E$ give a non-selective (flat) reflectance function, so that

$$\sum_d D_d^s = 1.0 \qquad 3.4\text{-}19$$

for each wavelength band s, where D_d^s is the spectral density of dye d in band s. Therefore, $H^r = H^g = H^b = H$ and taking the log of both sides of Equation 3.4-13 gives

$$\log H = \gamma_1 \gamma_2 \log E \qquad 3.4\text{-}20$$

The gamma γ of the system is the product of the gammas of its two stages, γ_1 and γ_2. This equation is the linear approximation to

$$\log H = f(\log E) \qquad 3.4\text{-}21$$

where f is the function described by the D - log E curve of the system, as log H is the optical density. To reproduce a given H, the computer exposure E that yields a print with that same H must be calculated. This calculation corresponds to the inversion of Equation 3.4-21 and is equivalent to the use of the classical Jones diagram of black and white picture reproduction [26]. The function f can be obtained experimentally by generating and then scanning a neutral grey scale, thus avoiding explicit consideration of the non-linearities of the individual D - log E curves and flare in the system.

The second and third assumptions are that the system is additive and proportional. As a result, it is linear in the log domain so that

$$T(\alpha \cdot \log \underline{E}_1 + \beta \cdot \log \underline{E}_2) = \alpha \cdot T(\log \underline{E}_1) + \beta \cdot T(\log \underline{E}_2) \qquad 3.4\text{-}22$$

and the mapping T can be partitioned into rows and columns. According to the additivity rule, the density of the sum of a number of dyes is equal to the sum of densities taken one at a time. The proportionality rule states that the ratio of the densities of a given dye, as measured through two different filters, is independent of the concentration of that dye [30]. Failure to obey these rules is due to the spectral characteristics of the dyes and the color head as well as optical effects within the reproduction medium. For example, Equations 3.2-12 and 3.4-12 describe systems that are additive and proportional, contingent on the use of ideal dyes and narrowband color head filters respectively.

The final assumption is that the printing filter $T^s(\lambda)$ and film spectral sensitivity $S_d(\lambda)$ products are non-zero over mutually exclusive wavelength intervals so that a given separation exposes one and only one emulsion. This is analogous to assuming there is no crosstalk in the formation of the dye images. As a result, we are dealing with the sum of logs rather than the intractable log of a sum. Dye interactions did not enter into the model. They correspond to a linear transformation on the analytic density vector $\underline{d}$ in Equation 3.4-9 and thus do not change the form of the mapping from $\underline{H}$ to $\underline{E}$.

3.5 The Engineering of Color Correction Systems

In spite of the assumptions implicit in the equation

$$\log \underline{E} = \underline{B} \log \underline{H} \qquad 3.5\text{-}1$$

it remains the basis of a large number of color correction schemes.

They differ in detail as to how they propose to deal with these assumptions, if at all, while preserving the basic notion of a transformation in the log domain.

Rather than using narrowband spectral sensitivities, the color head could have a set of color mixture curves so that $\underline{H}$ would be a vector of tristimulus values. This would eliminate the constraint of the original and its reproduction using the same dyes. The log of the exposure vector $\underline{E}$ then would be a linear transformation on the logarithm of tristimulus values or colorimetric densities. However, the use of color mixture functions implies broad-band color head filters which means an increase in additivity and proportionality failure. As a result, the power of a tristimulus analysis of the input is traded off against the accuracy of Equation 3.5-1.

There are three lines of approach to computing the matrix $\underline{B}$. The first stems from the analogue interpretation of Equation 3.4-14. Consider the image of a single dye d, obtained by an exposure through the appropriate filter, sandwiched with a neutral density step wedge. This image is scanned and three D^s- log E_d curves obtained, for s = r, g and b. Over the linear portion of the curve, the slope is $\gamma_1\gamma_2 D_d^s$. Doing the same for similar images of the other two dyes will give the other two rows of $\underline{A}$ and then inverting $\underline{A}$ will give $\underline{B}$ [28,31]. An alternative [21] is to compute the best fit of the dye spectral density functions to a set of non-ideal block dyes, returning the matrix $\underline{D}^s$ that, when combined with the gamma of the overall process, gives $\underline{A}$.

A second approach recognizes that the parameters of the masking matrix $\underline{B}$ can be selected experimentally so that three colors are reproduced exactly. For example, three sets of exposures are made and the resulting colors scanned.

The elements $[b_{ij}]$ are then computed by solving three sets of three linear simultaneous equations so that these colors are reproduced exactly: it can only be hoped that the remaining colors are not reproduced too far wrong. Three typical colors for calibrating the system are a neutral, flesh tone and a patch of grass or sky, colors to whose correct reproduction most observers through experience are very sensitive. The set of colors reproduced optimally can be increased beyond three by choosing $[b_{ij}]$ so as to minimize the mean squared density error in the reproduction of the given set of colors [32]. Another alternative is a piecewise linear transform $\underline{B}$ [33]: over different regions of the gamut, different $\underline{B}$ matrices are used. The parameters of each are chosen so that three colors within each region are reproduced exactly.

None of these approaches to the application of the basic masking equation deals explicitly with its shortcomings. Color correction schemes that attempt to account for additivity and proportionality failure do so by increasing the dimensions of the optical density vector in Equation 3.4-18. For example,

$$\begin{vmatrix} D_c \\ D_m \\ D_y \end{vmatrix} = \underline{B}' \begin{vmatrix} D_r \\ D_g \\ D_b \\ D_r^2 \\ D_g^2 \\ D_b^2 \\ D_r D_g \\ D_r D_b \\ D_g D_b \end{vmatrix} \qquad 3.5\text{-}2$$

The vector on the right-hand side is a truncated Taylor series approximation to the relationship between printing density D_d and optical density D_s. In this case, $\underline{B}'$ is a 3x9 matrix. Its elements can be computed from a simulation of the reproduction system [34], from the scan of 27 sample colors or from the least squares best fit to an even larger set of colors [35].

These approaches stem from the observation that a subtractive system in general does not possess stable primaries. In other words, the locus of the synthesized color P on the chromaticity diagram is not a straight line as the concentration of a given dye is changed (compare Figures 3-8 and 3-2(a)). It is possible however, to combine non-ideal block dye density functions in pairs $aD_i(\lambda) + bD_j(\lambda)$ such that, as the concentration of the combination is varied, the trajectory of the resulting chromaticity is a straight line. In the limit, as the concentration approaches infinity, the chromaticity of the dye pair goes to a value that does not depend on the exact nature of the spectral density functions but rather on how they are partitioned along the wavelength axis and the illuminant, that is, on $\underline{I}_i$ in Equation 3.2-12. The three limiting chromaticities,resulting from the possible combinations of three dyes taken two at a time,are identical to those for a set of ideal block dyes and specify a set of primaries. MacAdam [36] has suggested that improved color correction results when the color head vector is the set of tristimulus values corresponding to the primaries defined by the chromaticities on which the pairwise combinations of real dyes converge. It must still be postulated that the process obeys the additivity rule.

Chapter 4

Color Picture Processing

4.1 Introduction

The last chapter assumed that the tone reproduction curve of the system was a straight line with a slope γ of 1 (Figure 4-1). Typically, the characteristic curve of the reproduction medium, whether chemical dyes on photographic paper or printing inks on newsprint, is a straight line over only a portion of the curve and flattens out at the extremes of the output density range, with a distinct 'toe' and 'shoulder'. This toe and shoulder limit the maximum and minimum densities obtainable so that input densities on those parts of the curve cannot be reproduced exactly. Colors in the input image that call for dye densities that exceed the output dynamic range $[D_{min}, D_{max}]$ are therefore non-reproducible. They will saturate the output so that tone separation will be lost in the highlight and shadow regions. Distortion will also result for the saturated colors that require a high density of one or two of the dyes and a low density of the others. In terms of the color correction algorithm (Equation 3.4 - 18), only densities D_c, D_m, D_y on the interval $[D_{min}, D_{max}]$ are obtainable.

The problem then is the optimal use of an output dynamic range smaller than that of the input. There is already a large literature on this problem in black and white reproduction. An obvious approach is a linear compression in density, where the characteristic curve is a straight line of slope less than 1 (Figure 4-2). The minimum input density is reproduced at the minimum output density; similarly, the maximum input density maps to the maximum output density. Obviously tone separation is preserved, if diminished in this case, with the

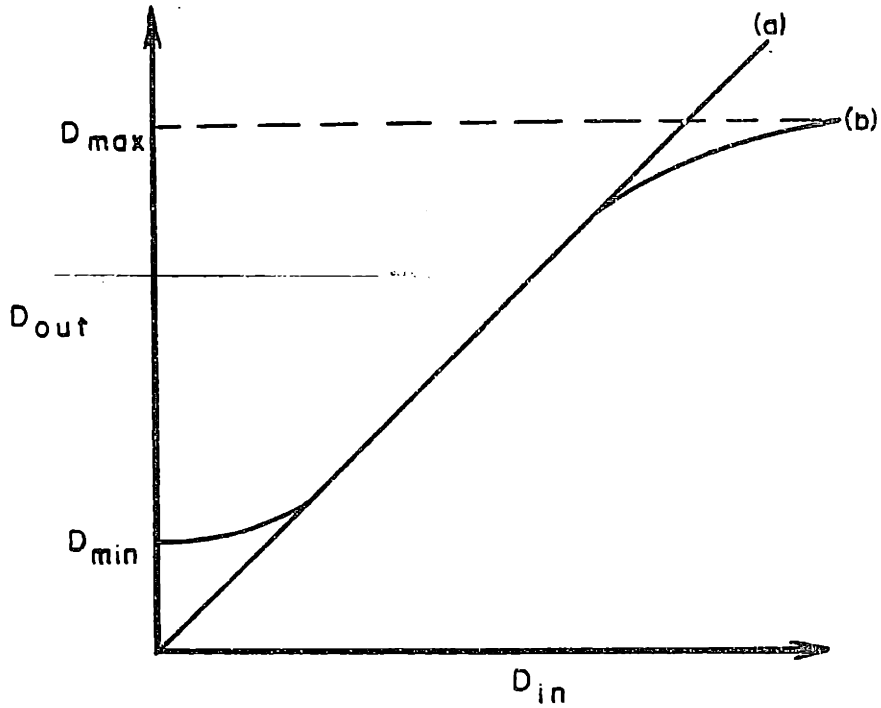

Figure 4-1. Tone Reproduction Curve
(a) ideal
(b) actual

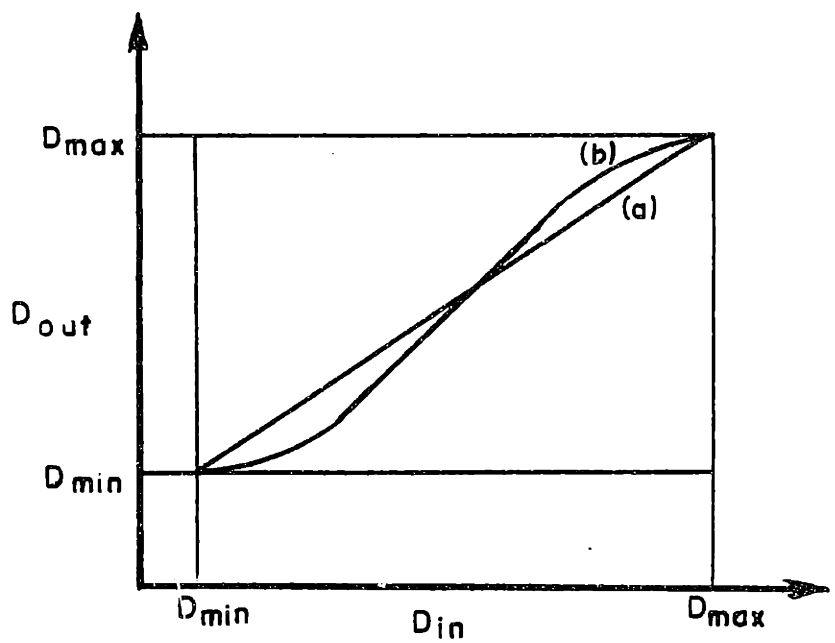

Figure 4-2. Black and White Tone Compression
(a) linear in density
(b) non-linear, midtone $\gamma = 1$

possibility that the picture reproduced will look 'washed-out'. A second approach that has been found to yield better pictures reproduces the midtones with a γ of 1 or greater while confining the compression to the highlights and shadows (Figure 4-2). The difficulty arises in deciding whether or not this scheme, or indeed any other, is optimal where the optimization occurs in what can only be labelled imprecisely as the 'preference' space of a typical human observer.

4.2 Dynamic Range Compression in Color Pictures

A smaller dynamic range in an output color picture vis-a-vis the original input will restrict the range of luminances that can be obtained as well as the chromaticity gamut. The limiting of the chromaticities is illustrated in Figure 4-3 where the input gamut on Polacolor 2 is plotted for a maximum density of 2.0 and the output gamut for a maximum density of 1.5. In order to preserve the separation of input luminance and chromaticity, they must be mapped into the restricted gumut of the output. The simplest solution, an extension of black and white picture reproduction, is to compress the cyan D_c, magenta D_m and yellow D_y separations individually, as if each were a black and white picture. The effect of this approach, using the linear compression scheme of Figure 4.2, is shown in Figure 4-4 for a set of sample colors generated with the Polacolor 2 dyes. The results show that this approach leads to shift in the dominant wavelength λ_d (and presumably in its perceptual correlate, hue) for some colors in the reproduction with respect to the original. Further, the decrease in excitation purity p_e (and its perceptual correlate, saturation) is not uniform over the input colors. This is not surprising as we have no reason to expect that linear changes in the density domain

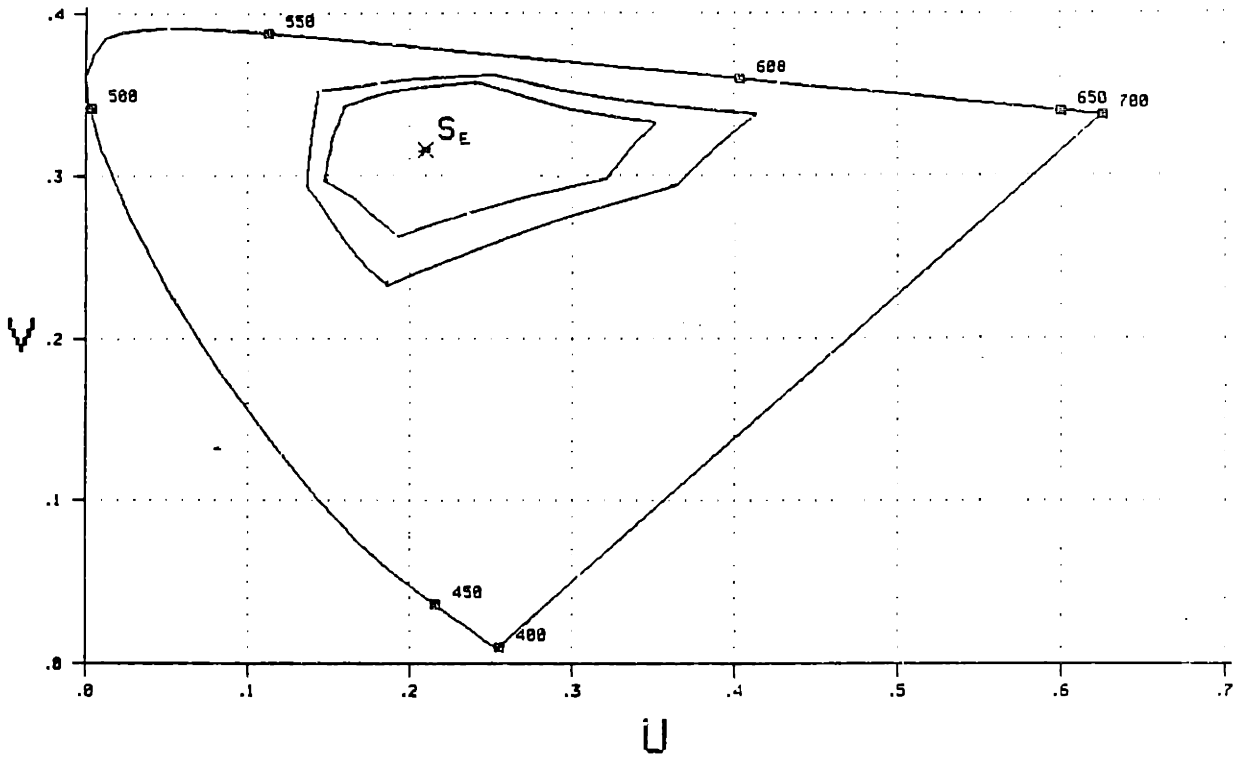

Figure 4-3. The output gamut for D_{max}=1.5 within the larger input gamut for D_{max}=2.0 on Polacolor 2.

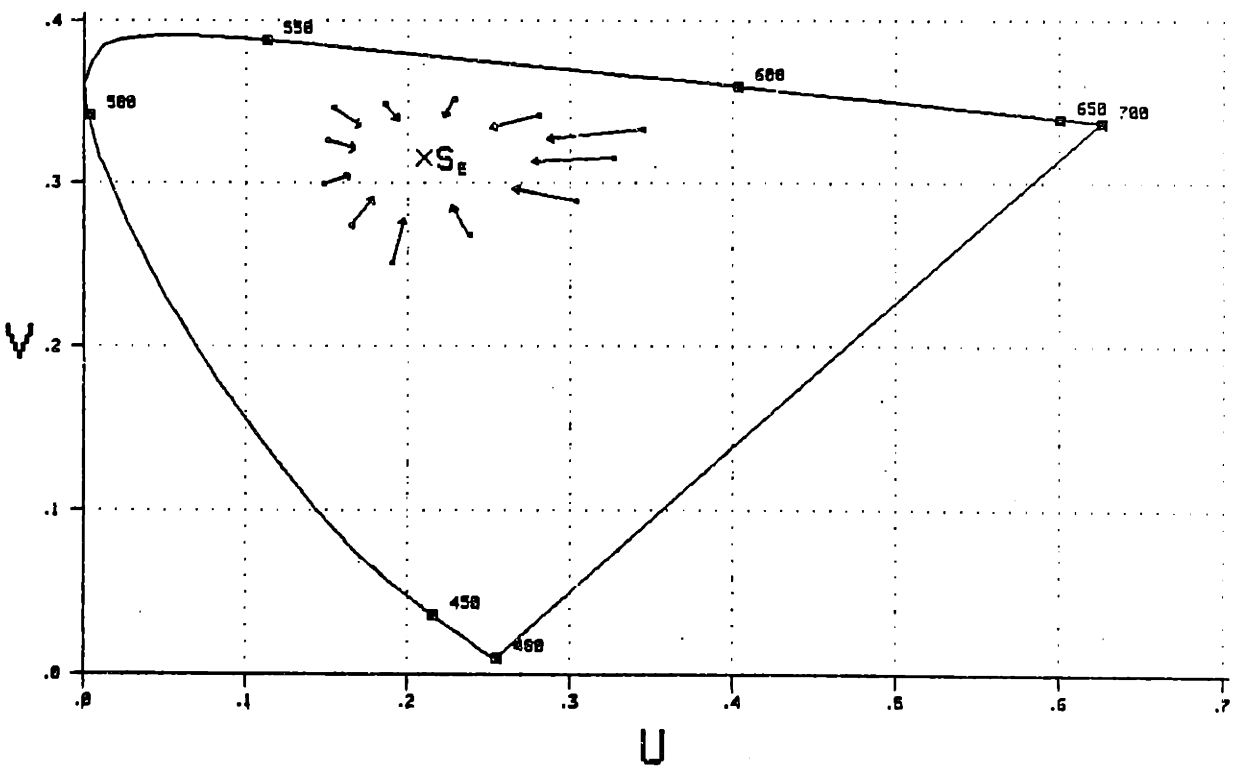

Figure 4-4. Chromaticity mapping with a linear compression in density from D_{max}=1.8 to D_{max}=1.2.

would give linear changes in chromaticity space.

Compression in the density domain, however, is capable of yielding acceptable color pictures, though there may well be another approach that would yield improved results. By the subjective nature of what constitutes an improvement in a complex visual stimulus such as a color picture, the criteria that the solution must satisfy are necessarily qualitative. For example, there is Evans' Consistency Principle [37]: it states that the colors of the preferred reproduction are 'internally consistent', that is, no color should be reproduced better than any other. Bartleson [1] has stated that the optimum black and white tone reproduction curve preserves the relative brighnesses of the original picture. He has generalized this to the three dimensions of color as a 'Relativity Principle' where the stimuli in the reproduction need not match those in the original absolutely, but must instead be congruent with the oberver's frame of reference.

A more specific criterion is the Ives-Yule-Abney compromise [2]. It was originally formulated for selecting a set of spectral sensitivities for input color analysis in an additive reproduction system, when it is not possible to realize the negative portions of the color mixture functions of a set of real primaries. The best compromise in this situation is a set of non-negative color mixture functions corresponding to imaginary primaries which are super-saturated versions of the actual primaries. As a result, the colors reproduced by this system are desaturated versions of the original hues. When there is a corresponding limitation on the magnitude of the output signals, then the most tolerable degradation in the reproduced color is desaturation without the hue shifts to which human observers are particularly sensitive [2]. Pobboravsky,

Pearson and Yule [38] found that the ratio of the saturation of colors in an original to the saturation of the reproduced versions of those colors was approximately constant in what were judged to be good reproductions. On the other hand, poor reproductions showed a large variation in the saturation ratio.

The implication is that the compression from input to output should be performed in color (or more precisely, sensation) space rather than in the density domain. In particular, the input picture, represented as a set of points in an appropriate three-dimensional color space, should be smoothly mapped into the restricted output color solid. This mapping can be viewed as separable for black and white compatible processing, with the compression performed first in the achromatic luminance domain and then in the chromatic domain.

Sensation does not vary linearly with luminance but rather with the lightness index W*. Consequently, a linear mapping of the W* range from input to output preserves the relative lightnesses of the original. To preserve the color balance, chromatic compression in UCS space takes the form of a single multiplicative constant, applied to all chromaticities, and compressing the excitation purity of each by the same factor along lines of constant hue. This corresponds to specifying a 'purity gamma' [11]. When the input and output dynamic ranges are the same, the colors in the original are reproducible with the same excitation purity, so that the purity gamma is 1. When compression is required, the purity gamma is reduced in order to fit the input chromaticities within the output gamut. This notion can be extended to U*V* space where $[(U^*)^2+(V^*)^2]^{\frac{1}{2}}$ shows a better correlation with saturation than does $[(u-u_o)^2+(v-v_o)^2]^{\frac{1}{2}}$. The dependence of U* and V* on W* accounts for the apparent change in

saturation with lightness as chromaticity (u,v) is held constant [14].

Therefore, it would appear that the most appropriate color space for the compression of the input picture, in anticipation of a diminished output color solid, is the U*V*W* space. Compression of the lightness index W* occurs first, followed by that of the chromaticness indices U* and V* along loci of constant V*/U*, corresponding to constant hue.

The choice of U*V*W* space is computationally fortuitous since the color solid of a subtractive system with spatially-continuous dyes is to a quite good approximation polyhedral. As shown in the two views of Figure 4-5, the color solid generated by the Polacolor 2 dyes can be represented as a dodecahedron with 12 triangular faces and 8 vertices, corresponding to all possible combinations (2^3) of three dyes at two concentrations, D_{min} and D_{max}. Achromatic stimuli are distributed along the W* axis, with a maximum (white) and minimum (black) occurring with densities D_{min} and D_{max} respectively. The other six vertices are the colors red, magenta, blue, cyan, green and yellow at equivalent neutral densities D_{max}. For the color solid of Figure 4-5, D_{max} is 1.5: the accuracy of the polyhedral fit declines with increasing D_{max}. As it stands, the most significant errors occur on the white-blue-cyan face in the way of points that, though outside the polyhedral solid, are nevertheless reproducible. Even then, the surface of the color solid is well-represented by a set of 12 planes,

$$W^* + a_i U^* + b_i V^* = c_i \quad i=1,2,\ldots,12 \qquad 4.2\text{-}1$$

The compression algorithm is a mapping from the set of input points $[U^*_{in}, V^*_{in}, W^*_{in}]$ to a set $[U^*_{out}, V^*_{out}, W^*_{out}]$ contained by the output color solid.

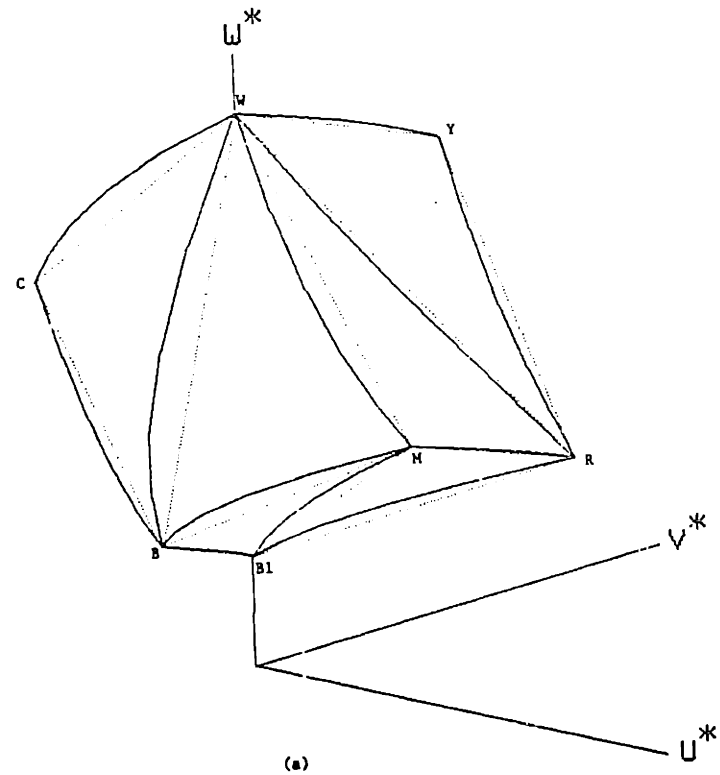

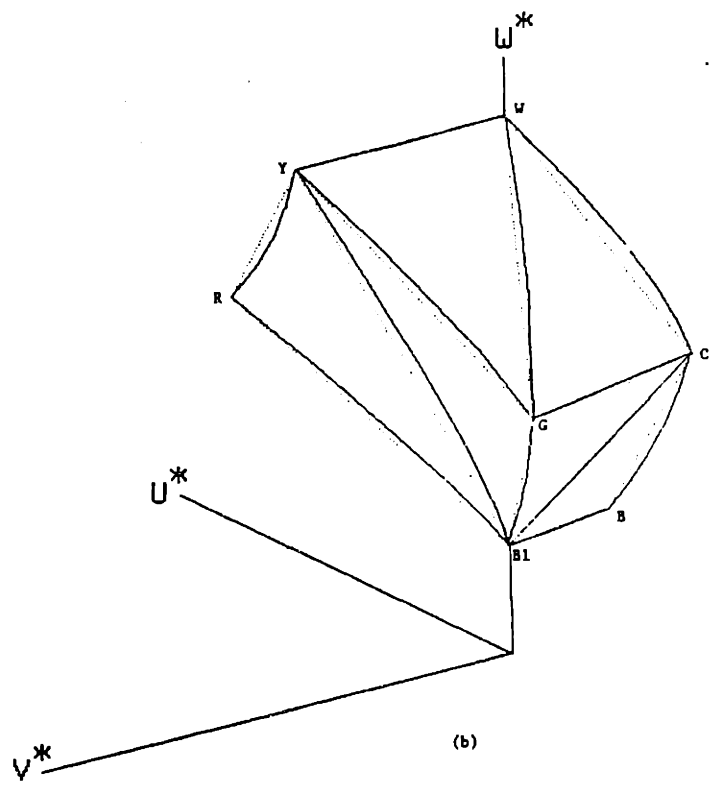

Figure 4-5. Two views of the Polacolor 2 color solid in U*V*W* space for D_{max}=1.5. Solid line: actual color solid; dotted line: polyhedral approximation. W - White, Bl - Black, R - Red, M - Magenta, B - Blue, C - Cyan, G - Green, Y - Yellow.

The compression has two components: the first is a linear affine transform on lightness W*,

$$W^*_{out} = \alpha W^*_{in} + \beta \qquad 4.2\text{-}2$$

The parameters α and β are chosen to map the maximum and minimum input lightnesses onto the maximum and minimum output lightnesses respectively.

The second component is the chromaticness mapping. It first looks at each lightness-compressed point $[U^*_{in},V^*_{in},W^*_{out}]$ to see if it is reproducible. To do this, it examines the plane $W^* = W^*_{out}$. The intersection of this plane with the output color solid is an irregular hexagon in the U*-V* plane (Figure 4-6). If (U^*_{in},V^*_{in}) is on or within the boundary of the hexagon, then the point is reproducible. Otherwise, it is not and a compression factor γ is computed so that $\gamma(U^*_{in},V^*_{in})$ is on the boundary of the hexagon and $[\gamma U^*_{in},\gamma V^*_{in},W^*_{out}]$, on the surface of the output color solid. Computing γ is a fairly simple procedure. Consider the point (U^*_k,V^*_k) in Figure 4-6; the line joining it to the origin of the U*-V* plane intersects the side of the hexagon described by the equation

$$a_jU^* + b_jV^* = c_j - W^*_{out} = d_j \qquad 4.2\text{-}3$$

This is the equation of the line resulting from the intersection of the plane $W^* = W^*_{out}$ and the plane of the j^{th} face of the color solid. If

$$|a_jU^*_k + b_jV^*_k| > |d_j| \qquad 4.2\text{-}4$$

then (U^*_k,V^*_k) is outside the hexagon and therefore not reproducible. The compression factor γ that maps it onto the boundary of the hexagon is

$$\gamma = \frac{|d_j|}{|a_jU^*_k + b_jV^*_k|} \qquad 4.2\text{-}5$$

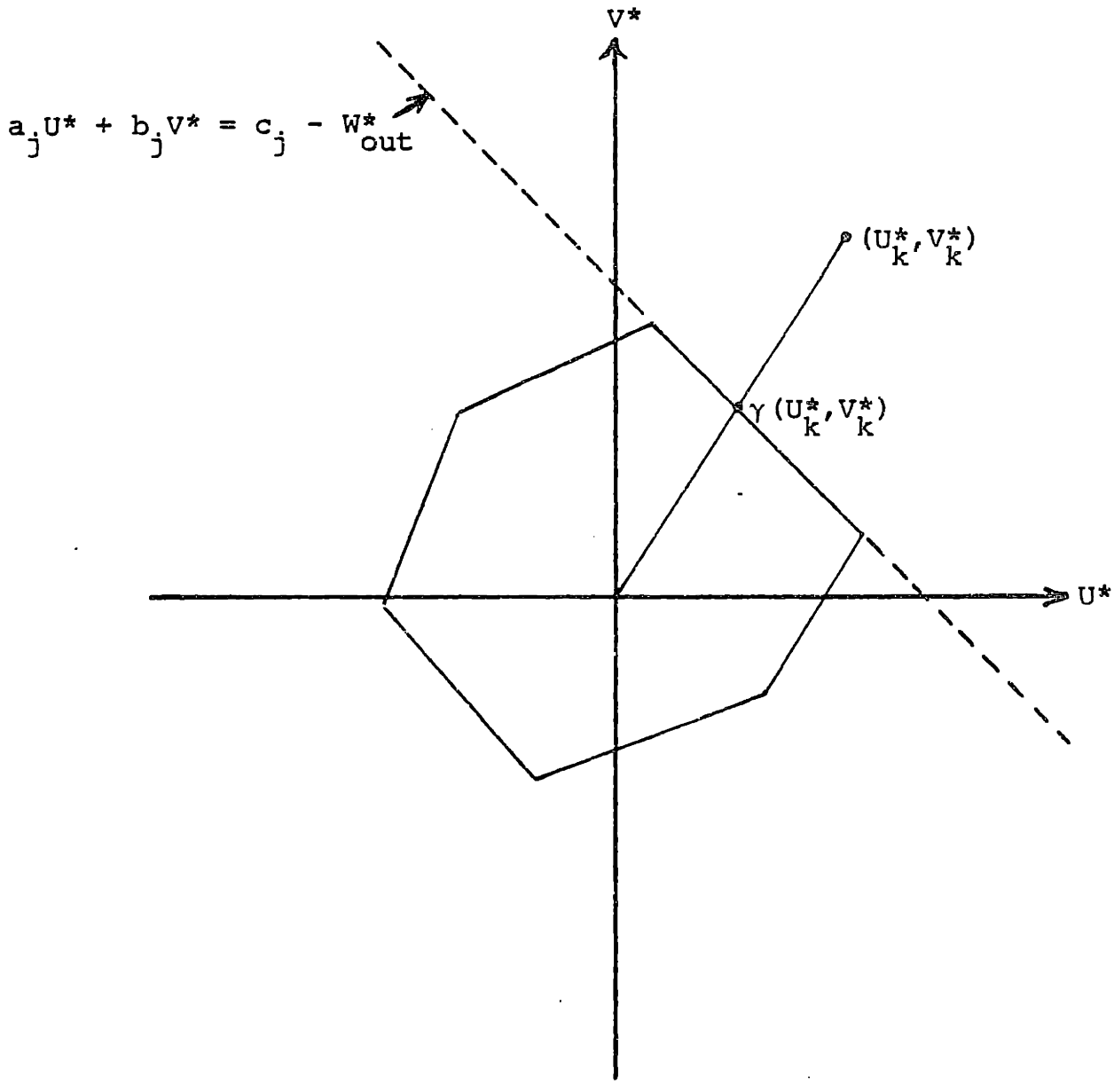

Figure 4-6. Cross-section of the U*V*W* color solid on the plane of constant lightness $W^* = W^*_{out}$.

After a search over all the input picture points, the smallest compression factor is returned; a second iteration follows, during which all chromaticness indices are compressed by that factor. The final result is a set of picture points within the output color solid.

4.3 Colorimetry without a Colorimeter

The output color solid is specified in the density domain by eight vectors $[D_c, D_m, D_y]$, equivalent to log $\underline{E}$ of the color correction transformation, where D_c, D_m and D_y equal either D_{min} or D_{max}. It is required to transform these into eight [U*,V*,W*] vectors. The first step is the inversion of the color correction equation to get the corresponding color head vectors $[H^r, H^g, H^b]$. Their transformation to [U*,V*,W*] would be a simple matter if the color head spectral sensitivities $\{h^r(\lambda), h^g(\lambda), h^b(\lambda)\}$, shown in Figure 4-7, were a set of color mixture functions. However, in choosing a set of spectral sensitivities for the color reproduction system, there is a trade-off between masking and colorimetric efficiency (see Chapter 3.5). One proposed measure of the colorimetric efficiency of an arbitrary sensitivity curve is the Colorimetric Quality Factor [39], its correlation coefficient with a set of orthogonal color mixture curves. The Quality factors for the red, green and blue color head filters used here are 0.32, 0.89 and 0.93 respectively. These filters were in fact chosen for their masking efficiency.

The problem of obtaining tristimulus values with an arbitrary set of spectral sensitivities can in general only be solved in a statistical sense. If, however, the input spectra are generated by a known set of dyes, then the mapping from the color head to the tristimulus values is 1:1 and can be performed by table look-up. The alternative, in direct analogy to the

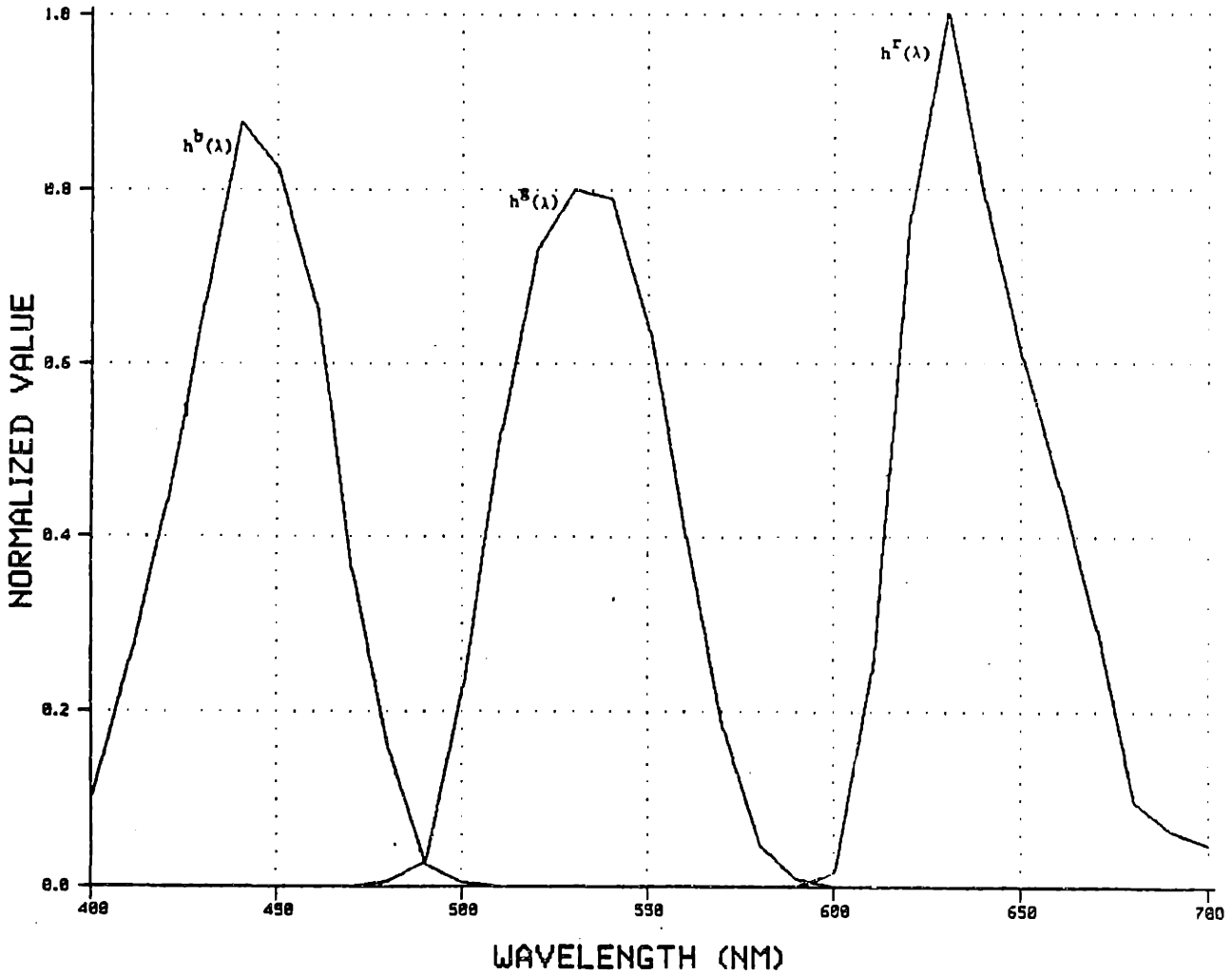

Figure 4-7. Color Head Spectral Sensitivity Functions.

problem of color correction in Chapter 3, is to seek a closed form solution by modelling the scanning process, in terms of either the input spectra or the spectral sensitivities of the scanner.

The reflectance spectra $\rho(\lambda)$ scanned can be approximated as $\tilde{\rho}(\lambda)$, the linear combination of a set of basis functions $\{f_j(\lambda)\}$ [40],

$$\tilde{\rho}(\lambda) = \sum_{j=1}^{3} x_j \, f_j(\lambda) \qquad 4.3\text{-}1$$

The error in the estimate $\tilde{\rho}(\lambda)$ is

$$\varepsilon(\lambda) = \rho(\lambda) - \tilde{\rho}(\lambda) \qquad 4.3\text{-}2$$

The integral of the error $\varepsilon(\lambda)$ weighted by the spectral sensitivity $h_i(\lambda)$ is

$$\begin{aligned} e_i &= \int_0^\infty d\lambda \; \rho(\lambda) \; h_i(\lambda) - \int_0^\infty d\lambda \; \tilde{\rho}(\lambda) \; h_i(\lambda) \\ &= H_i - \int_0^\infty d\lambda \; h_i(\lambda) \left(\sum_{j=1}^{3} x_j \, f_j(\lambda) \right) \\ &= H_i - \sum_{j=1}^{3} x_j \int_0^\infty d\lambda \; h_i(\lambda) \; f_j(\lambda) \\ &= H_i - \sum_{j=1}^{3} a_{ij} \, x_j \end{aligned} \qquad 4.3\text{-}3$$

where H_i is the i^{th} color head value. Setting the integral weighted error e_i to zero for i equal to 1, 2 and 3 gives

$$\underline{H} = \underline{a} \; \underline{x} \qquad 4.3\text{-}4$$

where $\underline{H}$ is the color head vector and $\underline{a}$ is a 3x3 matrix with elements a_{ij},

$$a_{ij} = \int_0^\infty d\lambda \; h_i(\lambda) \; f_j(\lambda) \qquad 4.3\text{-}5$$

The 'best' reflectance estimate $\tilde{\rho}(\lambda)$ then is

$$\tilde{\rho}(\lambda) = \underline{x}^T \cdot \underline{f}(\lambda) \qquad 4.3\text{-}6$$

where $\underline{f}(\lambda) = [f_1(\lambda), f_2(\lambda), f_3(\lambda)]$ and

$$\underline{x} = \underline{a}^{-1} \underline{H} \qquad 4.3\text{-}7$$

The estimate of the tristimulus vector corresponding to the color mixture functions $\underline{u} = [\bar{u}, \bar{v}, \bar{w}]$ is

$$\begin{aligned} \tilde{\underline{U}} &= \int_0^\infty d\lambda \left(\sum_{j=1}^{3} x_j f_j(\lambda) \right) \underline{u}(\lambda) \\ &= \sum_{j=1}^{3} x_j \int_0^\infty d\lambda \, f_j(\lambda) \, \underline{u}(\lambda) \\ &= \underline{x}^T \cdot \underline{U}_j \end{aligned} \qquad 4.3\text{-}8$$

where $\underline{U}_j$ is the tristimulus vector of the basis function $f_j(\lambda)$. Since $\{f_j(\lambda)\}$ and $\{h_i(\lambda)\}$ are known in advance, $\underline{a}$ and $\underline{U}_j$ can be pre-computed. This scheme was implemented for $\{f_j\}$ equal to a set of power law functions $\{\lambda^{j-1}\}$ and a set of orthogonal block functions. An error analysis was carried out over the color solid generated by the model for Polacolor 2 prints from Chapter 3. The errors between the actual and estimated color co-ordinates are shown in Table 4-1.

The second approach is to model the color head spectral sensitivities as a set of color mixture curves. In particular, since the color head sensitivities are normalized so that they give equal color head values for neutral stimuli, as do the color mixture functions $\bar{r}$, $\bar{g}$ and $\bar{b}$, the color head vector $[H^r, H^g, H^b]$ is taken as the estimate of the tristimulus vector [R,G,B]. The approximation is exact for achromatic stimuli but introduces

Table 4-1 Error Analysis of the Color Estimation Algorithms

Algorithm	RMS Error U*V*W*	RMS Error uv	RMS Error Y^1	RMS Error W^{*2}	Average % Error Y	Average % Error W*
1. Power law function fit to $\rho(\lambda)$	7.52	0.0148	0.020	2.67	13.3	6.8
2. Orthogonal block function fit to $\rho(\lambda)$	8.27	0.0131	0.019	2.62	14.2	7.5
3. Assume $[H^r,H^g,H^b]=[R,G,B]$	19.71	0.0334	0.017	2.23	12.2	6.5
4. Best fit of $\{h^r(\lambda),h^g(\lambda),h^b(\lambda)\}$ to V_λ	-	-	0.018	2.61	12.0	6.3
5. Algorithm 1 with HAT	4.59	0.0072	0.020	2.67	13.3	6.8
6. Algorithm 3 with HAT	3.85	0.0058	0.017	2.23	12.2	6.5

[1] $Y_{max} = 1.00$

[2] $W^*_{max} = 100.0$

significant errors for strongly chromatic stimuli. The overall error performance is summarized in Table 4-1. Figure 4-8 shows the effects of this scheme on the u-v chromaticity diagram. The solid line is the chromaticity gamut of Polacolor 2 for D_{max} equal to 2.0; the dotted line shows the gamut that would be obtained if the color head were fitted with the sensitivity curves $\{h^r,h^g,h^b\}$, rather than the set $\{\bar{r},\bar{g},\bar{b}\}$.

The results of Table 4-1 show that no single scheme gives a superior estimate $(\tilde{Y},\tilde{u},\tilde{v})$. In an attempt to improve the luminance estimate $\tilde{Y}$, $\{l_r,l_g,l_b\}$ were chosen to give the least squares best fit of

$$\tilde{V}_\lambda = l_r h^r(\lambda) + l_g h^g(\lambda) + l_b h^b(\lambda) \qquad 4.3\text{-}9$$

to the luminous efficiency function V_λ, subject to the constraint $l_r + l_g + l_b = 1$. Surprisingly, the result was only slightly better than that to be had using the coefficients of Equation 2.3-5.

The chromaticity estimate $(\tilde{u},\tilde{v})$ can be significantly improved by the use of a linear affine transformation in the chromaticity domain to update the original estimate [33]. The transformation is a combined rotation and scaling about the neutral point $(u_o,v_o) = (\tilde{u}_o,\tilde{v}_o)$

$$\begin{vmatrix} u - u_o \\ v - v_o \end{vmatrix} = \underline{T} \begin{vmatrix} \tilde{u} - u_o \\ \tilde{v} - v_o \end{vmatrix} \qquad 4.3\text{-}10$$

where (u,v) is the updated chromaticity estimate. The four elements of the matrix $\underline{T} = [T_{ij}]$ can be chosen so as to map two chromaticity estimates $(\tilde{u},\tilde{v})$ onto their exact chromaticity values. It is a simple matter for a digital computer to implement $\underline{T}$ as a piecewise linear transform, gaining significant flexibility in the choice of T_{ij} at a small computational cost.

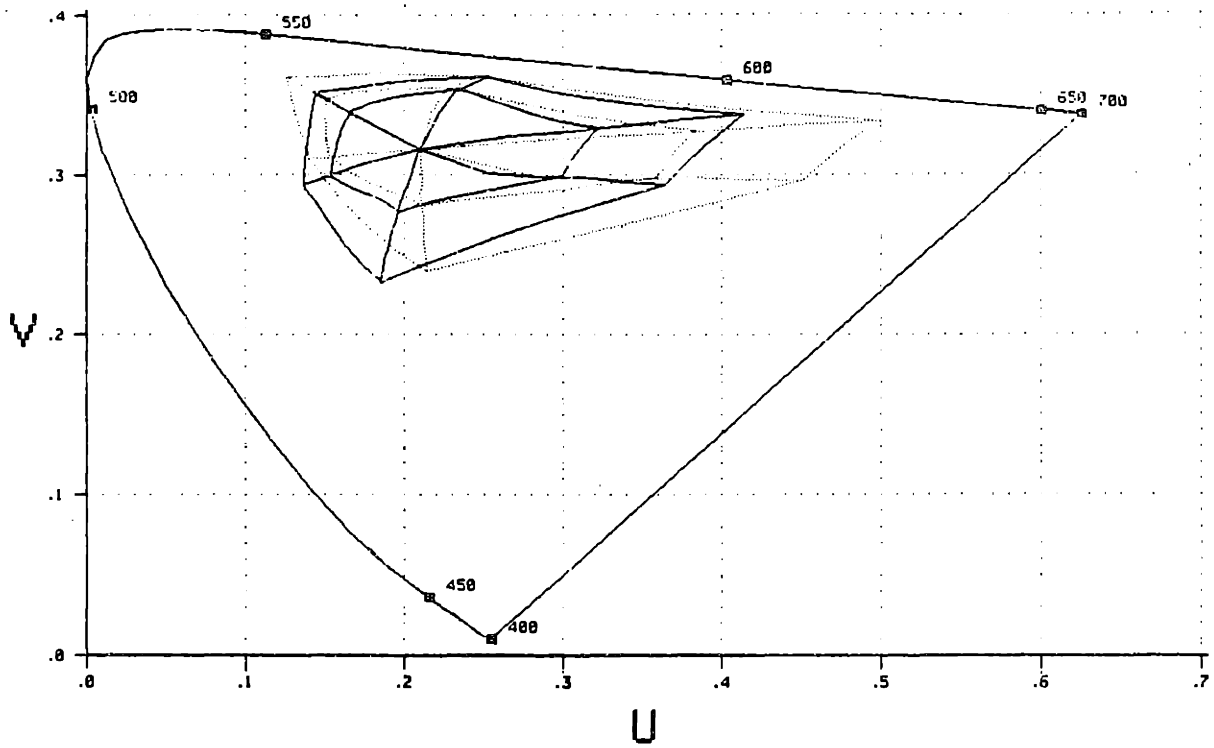

Figure 4-8. Chromaticity Gamut of Polacolor 2 for D_{max}=2.0. Dotted line is the gamut when (h^r,h^g,h^b) replace $(\bar{r},\bar{g},\bar{b})$ as colorimeter spectral sensitivity functions.

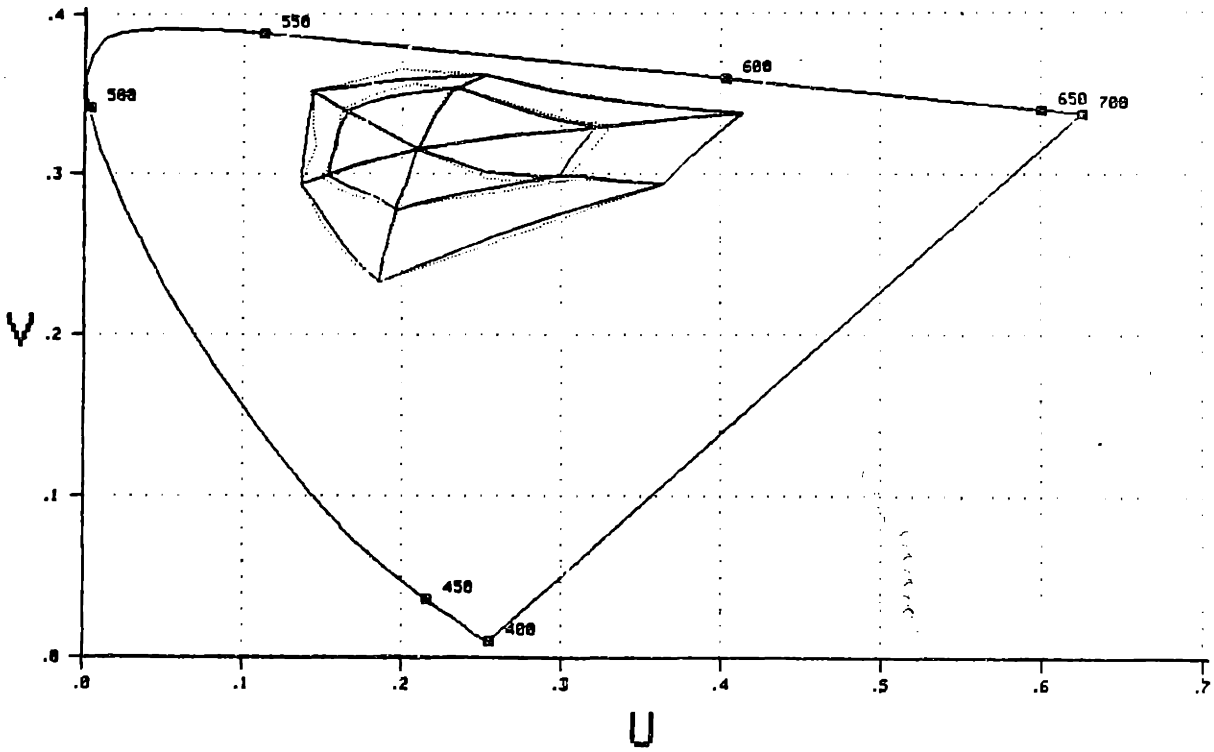

Figure 4-9. Chromaticity Gamut of Polacolor 2 for D_{max}=2.0. Dotted line is the gamut with (h^r,h^g,h^b) replacing $(\bar{r},\bar{g},\bar{b})$ and using the Hexagonal Affine Transform (HAT).

Accordingly, the chromaticity gamut of Figure 4-8 was divided into six triangular regions, with the apex of each triangle at the neutral point (u_o, v_o) and the base joining two 'adjacent' colors with an equivalent neutral density of 2.0. For example, red and yellow are adjacent colors: They have identical cyan and yellow dye densities and differ only in the magenta dye density - for red, D_m is maximum; for yellow, minimum. For each triangular region, a mapping $\underline{T}_k$ was computed so that the endpoints of the base were mapped onto their exact chromaticity values. Each region is specified by the slopes of the sides of the triangle. When the slope m

$$m = \frac{\tilde{v} - v_o}{\tilde{u} - u_o} \qquad 4.3\text{-}11$$

of the estimate $(\tilde{u},\tilde{v})$ lay between the slopes bounding the k^{th} region, $\underline{T}_k$ was applied to that chromaticity estimate.

This algorithm, the Hexagonal Affine Transform (HAT), due to Solomon [33], was used in the cases where the chromaticity estimates were had by a power law fit to the scanned reflectances and by assuming the color head sensitivities were a set of color mixture functions. The error performance in Table 4-1 shows a marked improvement in the chromaticity estimates. This is shown more clearly on comparing Figure 4-9 with Figure 4-8, the estimates of the chromaticity gamut with and without the HAT.

Upon comparison of the errors of these various schemes, it was decided to generates $(\tilde{Y},\tilde{u},\tilde{v})$ by equating the color head vector $[H^r,H^g,H^b]$ to the tristimulus vector [R,G,B] and then following up the chromaticity estimates with the Hexagonal Affine Transform. The predicted rms error in chromaticity is 0.0058, which compares favorably with the just noticeable

difference in chromaticity, 0.004 [2].

In practice, the coefficients of $\{\underline{T}_k\}$ were obtained by generating six sample colors on Polacolor 2. They were scanned on the color head to obtain the chromaticity estimates $(\tilde{u},\tilde{v})$ and then scanned on a spectrophotometer to obtain the actual (u,v).

4.4 Color Correction

The application of the color correction algorithm has two parts: the first is the linearization of the photographic tone reproduction curve over the output density range. This is accomplished by generating and then scanning a neutral scale on the system. In theory, H should equal E, though in practice, H is a function f of E other than the identity function. To obtain a characteristic curve with a gamma γ of 1, the inverse mapping f^{-1}: E → E' is realized by table look-up, so that when the computed exposure is E, the actual exposure output is E' which gives the color head value H = E.

The second part is the implementation of the color correction transformation of Equation 3.4-16, computing the dye exposure vector $\underline{E}$ from the color head vector $\underline{H}$. Given the assumptions of the closed form solution, there is a trade-off between simplicity and accuracy in the possible approaches. Given the need to compute the output color solid from known limits on $\underline{E}$, one requirement is that the approach taken be easily invertible. For this reason, a linear transform $\underline{B}$ is chosen. To improve its accuracy, in view of the requirement to reproduce a specified color whether it is the result of compression or not, $\underline{B}$ is made piecewise linear, using the HAT algorithm of the last section. For a given color head vector $\underline{H}$, the choice of $\underline{B}_k$, k=1,...,6 is made on the basis of the region of the

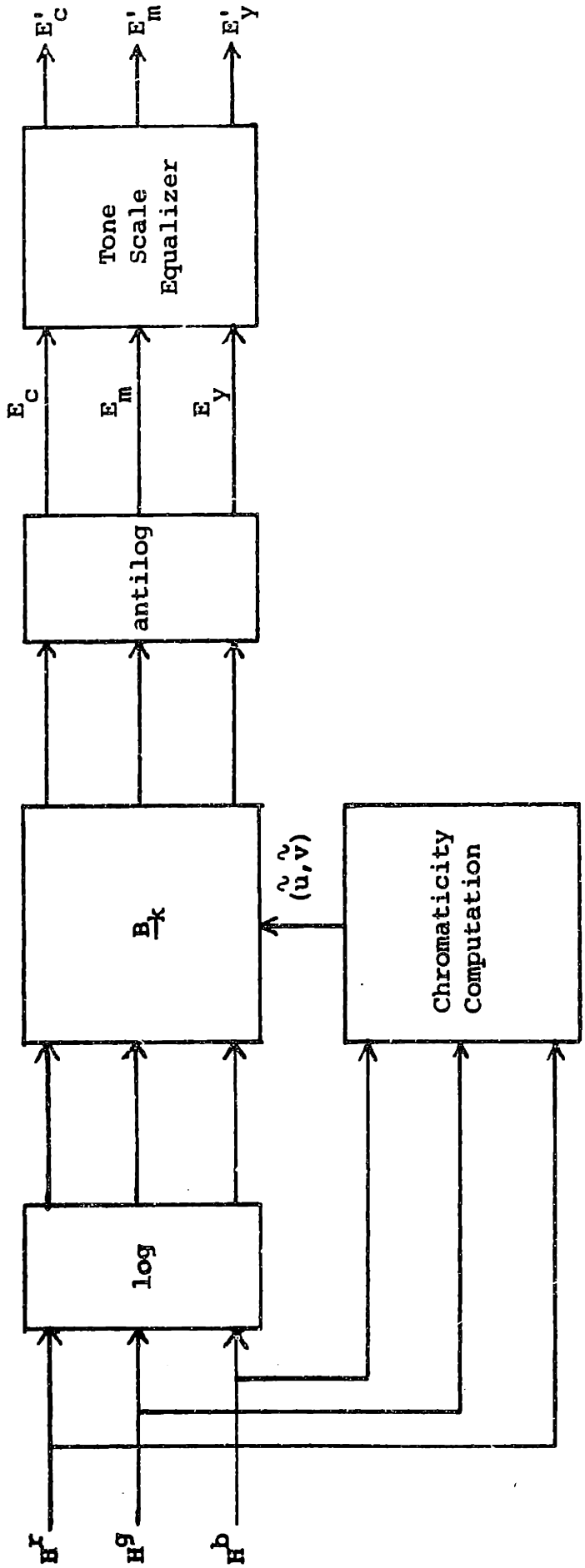

Figure 4-10. Block Diagram of the Color and Tone Correction System

chromaticity gamut that contains that point, as determined by the slope of the chromaticity estimate m in Equation 4.3-11. For each $\underline{B}_k = [b_{ij}]_k$, the reproduction of the neutral scale, where $\underline{E} = \underline{H}$, imposes the constraint

$$\sum_{j=1}^{3} b_{ij} = 1.0 \qquad 4.4\text{-}1$$

The six remaining degrees of freedom in choosing the coefficients b_{ij} of the k^{th} region are sufficient to reproduce exactly two colors in that region.

The matrices $\{\underline{B}_k\}$ are, in practice, computed by generating six sample colors (red, magenta, blue, cyan, green and yellow) with various combinations of known exposure vectors. These colors are then scanned to obtain their color head vectors. The resultant six sets of six simultaneous linear equations are then solved for the coefficients of $\{\underline{B}_k\}$.

The block diagram of the color correction system is shown in Figure 4-10. The system incorporates a great deal of flexibility since any desired tone characteristic can be obtained by another look-up table, inserted after the tone scale linearizer.

4.5 Color Picture Enhancement

So far, the discussion has dealt exclusively with the specification of a visual stimulus in terms of dye densities. These, however, are only some of the factors that determine the perception of a visual stimulus in the presence of other stimuli in the same field of view, in short, the perception of a color picture. Certainly, decreasing the incremental contrast γ or the overall contrast (dynamic range) of the system will lower the visual (apparent) contrast of the output, so that it appears 'flat' or 'soft'. But visual contrast is also affected by the sharpness of the picture, where

sharpness is a spatial variable related to the high spatial frequency content and the magnitude of edge gradients in the image. In fact, contrast and sharpness can be traded off against each other in obtaining a specified image quality. For example, the low spatial resolution and inherently low sharpness of color television is partially offset by the high contrast of the image [1]. In the other direction, a sharper picture appears to have a higher visual contrast, even though the γ of the process is unchanged [41]. This effect is illustrated in Figure 4-11 for a black and white picture that is the luminance component of a color picture.

The sharpened image $Y'(i,j)$ is given by

$$Y'(i,j) = Y(i,j) + \alpha[f(i,j) \circledast Y(i,j)] \qquad 4.5\text{-}1$$

where $Y(i,j)$ is the original digital image and $f(i,j)$ is the impulse response of a two-dimensional high pass filter. $\circledast$ is the convolution operator. In Figure 4-11(b), $f(i,j)$ is a digital Laplacian [42] for a square picture sampling lattice, with the 3x3 impulse response shown below.

0	-1	0
-1	4	-1
0	-1	0

Since

$$\sum_i \sum_j f(i,j) = 0 \qquad 4.5\text{-}2$$

the average level of the picture and hence, the gamma γ, are unchanged.

Sharpening is typically achieved by unsharp masking [43], where

$$Y'(i,j) = Y(i,j) - \beta[g(i,j) \circledast Y(i,j)] \qquad 4.5\text{-}3$$

(a)

(b)

Figure 4-11. Sharpening of the Luminance Component of a Color Picture
(a) original
(b) filtered with Laplacian

(a)

(b)

Figure 4-11. Sharpening of the Luminance Component of a Color Picture
(a) original
(b) filtered with Laplacian

g(i,j) is a unit energy low pass filter. In this case, the increase in the high spatial frequency content of the image is relative to the average level which is compressed by the factor 1-β.

While the filter implementations can be quite complicated (see [44] for example), even the simple filter described here can regain all or some of the visual contrast that would otherwise be lost with dynamic range compression. Sharpening to increase the edge gradients in color pictures increases the saturation of colored areas [41,45]. Both the achromatic and chromatic effects of edge enhancement are due to simultaneous contrast. The operational characteristics of contrast phenomena have been investigated for simple configurations, so that the results extrapolate to complex visual stimuli, such as pictures, in only a qualitative fashion. The basic result is that contiguous areas interact to increase the differences perceived between them in luminance, saturation and hue. This induction effect is strongest adjacent to the border separating the areas and increases with the edge gradient [46,47]. In as much as Mach bands are another facet of simultaneous contrast, the evidence is that luminance, rather than chromaticity, gradients are sufficient for their existence [48,49].

The benefits of sharpening can be had by filtering in any one of a number of domains. Yule [30] suggests the use of unsharp masks in color correction: this corresponds to filtering in the density (log) domain, that is,homomorphic filtering [50]. In a digital color system, this would require three filters. It may well be that a single filter, in either the luminance or lightness domain, would achieve most of the desired effects of sharpening. In any case, the degradation in picture quality due to a compressed dynamic range can be compensated for, in part, by the manipulation of spatial variables.

Chapter 5

The Experimental System

5.1 Introduction

The proposed scheme for reproducing pictures with colors not reproducible at a smaller dynamic range consists of five steps:

1. scanning the original picture
2. transforming it into U*V*W* space
3. modifying the original colors to the desired output colors
4. computing three color separations
5. preparing the reproduction

The original reflection copy is scanned on a TOHO facsimile transmitter with an optical and electronic system modified for color input [33]. Once scanned, pictures are stored on magnetic tape. The black and white separations are produced on a Laserphoto facsimile receiver. Intervening between these steps and performing the transformations on the original picture is a DEC PDP-9 digital computer with 32,000 words of 18-bit core memory, supplemented by six disks with a capacity of over one million words. The separations are used to reproduce the hard copy output directly by triple exposure onto Polacolor 2 film.

5.2 The Color Scanner

The original picture is scanned on a TOHO facsimile transmitter, a rotating drum scanner. As the drum rotates at 120 rpm, a lead screw advances the optical head 0.0107 inches per revolution, perpendicular to the direction of the scan. This gives a resolution of 93 lines per inch; along a line, the resolution is 98 picture elements (pels) per inch. The optical

system of the scanner was modified for color copy; it images a 0.01 diameter area of the print through dichroic mirrors and color filters onto three identical phototransistor detectors. The spectral response $h^s(\lambda)$ of a color head sensor is

$$h^s(\lambda) = I(\lambda)\ L(\lambda)\ F^s(\lambda)\ S(\lambda) \qquad 5.2\text{-}1$$

where s is either r, g, or b. $I(\lambda)$ is the energy spectrum of the source illuminating the copy; $L(\lambda)$, the transmittance function of the imaging lens; and $F^s(\lambda)$, the transmittance function of the infrared cutoff, dichroic, and color filters in the optical path of a photodetector with a spectral sensitivity $S(\lambda)$. The color head spectral senstivities were computed from the known characteristics of the components specified in the design [51] and are shown in Figure 4-7.

The photodetector signals are amplified by three low noise FET pre-amps, sampled and then converted to six-bit bytes; the red, green, and blue bytes for one pel are packed into an 18-bit computer word. The pre-amps have bias and gain controls that are adjusted so that maximum and minimum print neutral densities give digital values of 1 and 63 respectively for all three color bytes.

The reflection copy is Polacolor 2 prints. Since they are 3¼"x4¼", a convenient size for the sampled pictures is 256 pels by 256 lines.

5.3 The Software System

The Color Picture Handler (CPH) reads a picture onto disk from either the TOHO scanner or DEC tape. Any residual misalignment of the color head photodetectors is corrected with software that unpacks the red, green, and blue input images and translates one or two of them with respect to the

third. CPH does the pel transforms, spatial filtering, and picture file management and then outputs the color separations to either a facsimile receiver or a black and white picture monitor, PIXMON. PIXMON is a 256 pel by 256 line television frame freeze memory that provides convenient soft copy for debugging the processing routines.

The block diagram of CPH is shown in Figure 5-1. The color head bytes are unpacked and used to calculate an estimate of the luminance Y, using Equation 2.3-5, and an estimate of the chromaticity (u,v), using the bilinear transformation of Equation 2.4-2. Each estimate is quantized to eight bits. A Hexagonal Affine Transform (HAT) is then applied to the chromaticities and the (Y,u,v) triplets are transformed to [U*,V*,W*] vectors via Equations 2.4-3 and 2.4-4. The lightness and chromaticness indices are each quantized to 10 bits. These transformations are executed in fixed point arithmetic using Fortran, with the intermediate results of the calculations scaled up to give an overall accuracy comparable to that of floating point computation, but at a significant saving in computation time. When transcendental functions are required (as, for example, in the cube root formula for the lightness index W*), table look-up is used to implement them. The pel manipulation, picture file management, and system input and output routines are written in Macro assembly language for optimal speed. In addition, the transformation from the three color head values to the luminance and chromaticity estimates is written in Macro, with the result that the transformation takes 64 μs per pel.

The compression factors (α,β,γ in Equations 4.2-2 and 4.2-5) are computed in one pass over the picture and then applied during a second pass. An interactive system permits the user to select compression factors re-

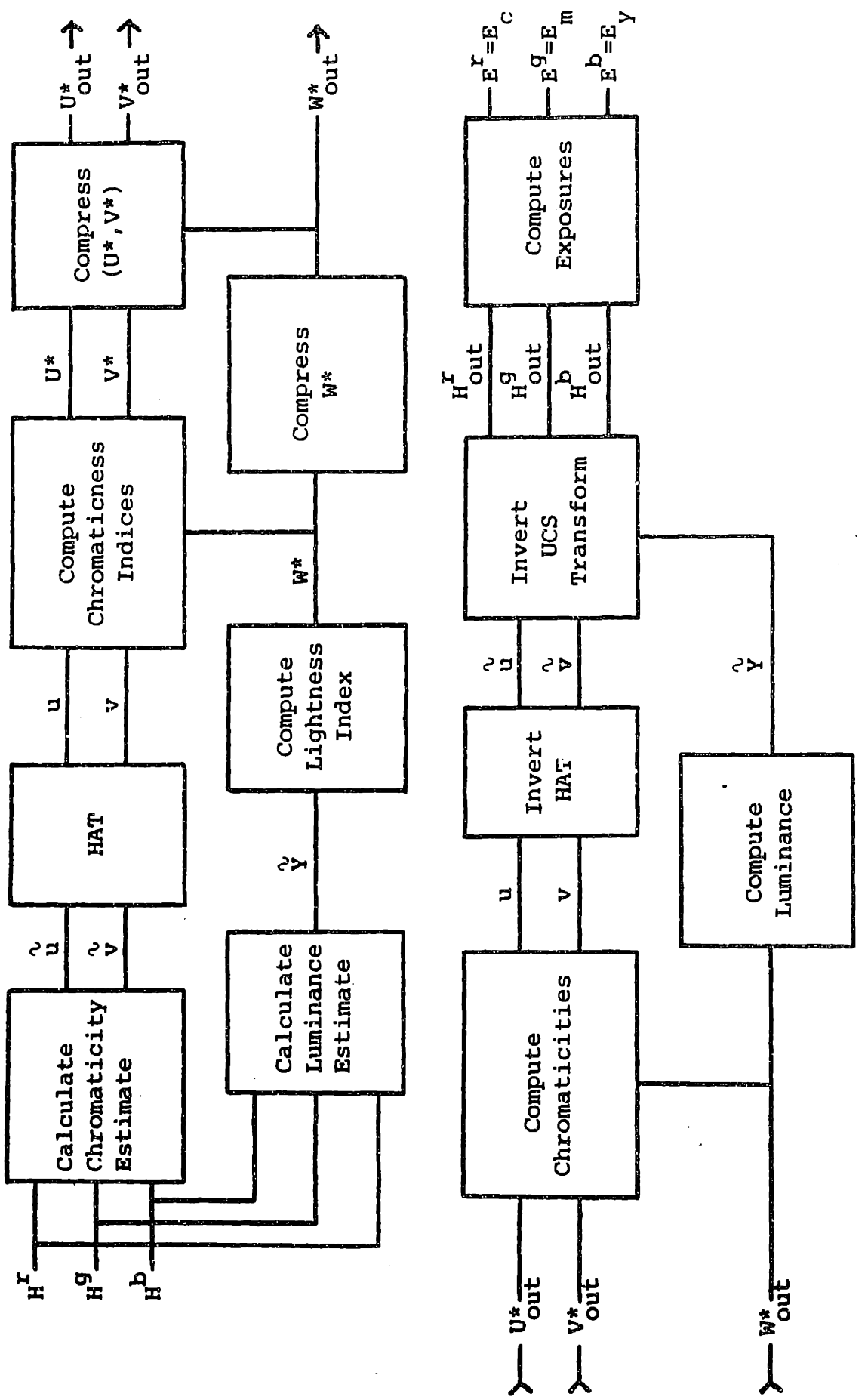

Figure 5-1. Block Diagram of the Computer Color Processing System

turned from a search over only a portion of the two-dimensional picture or the three-dimensional color solid. In this way, the compression of the input picture into the output color solid need not be determined by a relatively unimportant area of the picture or by a non-reproducible but insignificant color.

The conversion of the compressed picture from U*V*W* space back to the color head signals is had by inverting the transformations of Step 2 (the upper line in Figure 5-1). The output exposures are then computed from the color head signals using a piecewise linear implementation of the color correction transform of Equation 3.4-16. The log and antilog functions required are obtained by table look-up and the calculations themselves performed in fixed point arithmetic.

A one-dimensional compression routine or a digital filtering routine using spatial convolution can be called at any point in the sequence of Figure 5-1 to compress or filter any given color variable. In particular, it is possible to operate on the output exposures or their logarithms, the domains in which range compression and unsharp masking are currently performed.

5.4 The Preparation of the Reproduction

The red, green, and blue exposures are output to a facsimile receiver that produces separations which are then triple-exposed onto film. Since the D - log E (or alternatively, H - E) curve of the separation-film combination is not linear, a look-up table is used to linearize it. The optical densities and exposures of a computer generated step wedge are fed to a tone scale correction program that generates the table by piecewise linear interpolation over the actual H - E curve of the system. The six-bit exposure

value then refers to this table to obtain an eight-bit value output to the receiver interface for signal conditioning. It is converted to an analogue signal to modulate a 2 KHz tone fed to a Laserphoto facsimile receiver. The receiver uses a laser beam to expose dry silver paper (3M Type 7773) which is then heat developed. The density range of the resulting black and white separation is 0.15 to 1.60 and the spatial resolution is 100 lines per inch.

The separations are then pin-registered and each exposed in turn through a Wratten filter pack onto Polacolor 2 Type 108 film. The separations are illuminated by two 3200°K floodlamps mounted in bowl reflectors and run off a Variac to regulate the lamp voltage. The filter pack for each separation consists of a color filter $T^s(\lambda)$ sandwiched with a neutral density (ND) filter, chosen by trial and error so that equal separations give a visual neutral on the film. In other words, the combination of the 3200°K source and the separation filters reconstructs the daylight illuminant for which Polacolor 2 is balanced [52]. The red separation uses a W29 filter plus a 0.7 ND filter; the green, a W58 plus a 0.3 ND filter; and the blue, a W47B filter. The assumption that one separation exposes one dye-forming layer can be checked by substituting the transmittance functions $T^s(\lambda)$ of these printing filters, the spectrum $I(\lambda)$ of the 3200°K source, and the film spectral sensitivity functions $S_d(\lambda)$ into Equation 3.4-2. The normalized exposure matrix is

$$\begin{vmatrix} E_c^r/E_c^r & E_c^g/E_c^r & E_c^b/E_c^r \\ E_m^r/E_m^g & E_m^g/E_m^g & E_m^b/E_m^g \\ E_y^r/E_y^b & E_y^g/E_y^b & E_y^b/E_y^b \end{vmatrix} = \begin{vmatrix} 1.0 & 0.005 & 0 \\ 0.0006 & 1.0 & 0.013 \\ 0 & 0.006 & 1.0 \end{vmatrix} \qquad 5.4\text{-}1$$

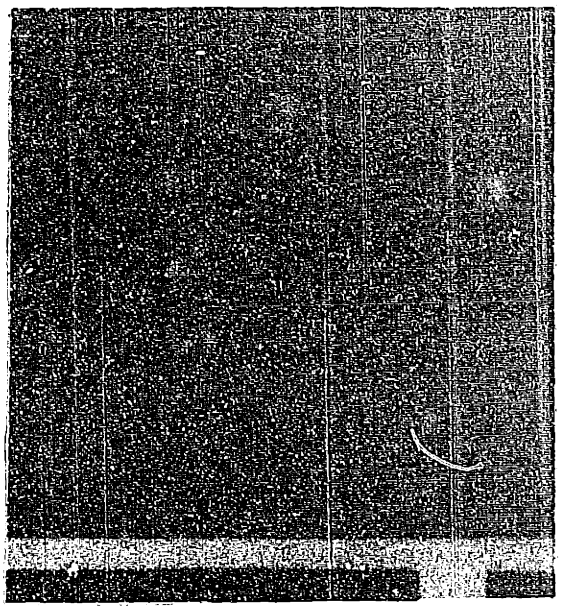

(a)

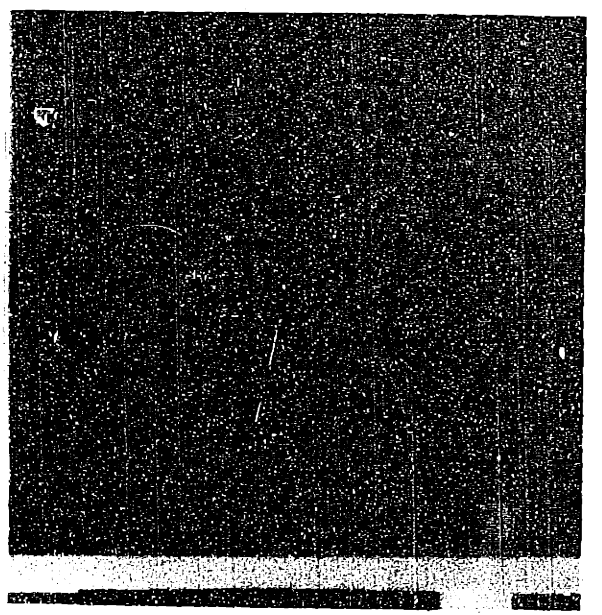

(b)

Figure 5-2. Chromaticity Gamut of the Color Reproduction System (a) on Polacolor 2 film
(b) copy on Kodak RC paper

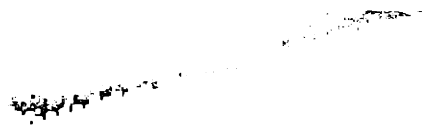

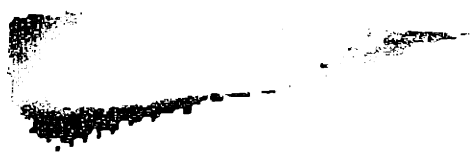

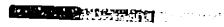

where E_d^s is the exposure given by separation s to dye d. According to this calculation, the assumption of the individual control of the dyes is justified.

Each separation is exposed twice at 1/15 second, f/4.7. The camera used is an MP-3 Prontor with a leaf shutter and a Land Pack Model 405 film holder. The prints are developed for 60 seconds at 73°±3°F and yield a density range of 0.25 to 1.60. This is the maximum dynamic range of the system. The dynamic range and spatial resolution of the system thus make its output equivalent to good quality newsprint.

The overall system can be tested by generating a test picture with a neutral step wedge and six color bars, scanning it, processing it according to the steps in Figure 5-1 (but without compression), and then combining the computed separations onto film to obtain a reproduction. Comparing it with the original gives a good indication of the quality of the system.

Another good figure (literally) of merit is a sample consisting of dye combinations that exercise the full gamut of the system. If they are laid out in the same relative positions as their chromaticities, we would have a figure similar to the painting by Louis Condax (see Plate 24 in [53]). Our version is shown in Figure 5-2(a). It takes the u-v chromaticity diagram and, for those chromaticities that are realizable with the dynamic range of the system, lays down dye amounts computed by the color correction algorithm that yield these chromaticities at their maximum luminance. The chromaticities outside the gamut are reproduced as a grey level. Figure 5-2(a) is the gamut on Polacolor 2. The experimental results in the next chapter are reproductions of Polacolor 2 prints made by the Polaroid Copy Service on Kodak RC paper. This cascades another color transformation with

the system that has been described here. As a reference point for gauging the effect this has on the color reproduction, Figure 5-2(b), the copy of Figure 5-2(a) on Kodak RC paper, is included for comparison. Its general effect is a shift in the color balance point toward the blue-green and a change in the tone scale characteristic.

Chapter 6

Experimental Results

6.1 Introduction

This research falls neatly into two parts: a theoretical analysis of color reproduction under the constraint of a compressed dynamic range and a practical part, its implementation on a digital system. They come together with an observer viewing selected pictures that have been processed by the system and making a decision on his or her preference from among a given number of alternatives. Herein lies the test of the success of any picture processing scheme. The final results involve the interaction of three things: first, the processing and in particular, the model on which it is based; second, the paradigm for subjective testing; and third, the choice of test materials. Two Polacolor 2 prints were selected as the test pictures: one is that of a house (Figure 6-2) with a large region of sky, some grassy areas, and a large number of dark colors and shadows. The other is the head shot of a girl (Figure 6-3) with lighter colors, including flesh tones whose correct rendition is an important test of any color reproduction system.

All the results in this chapter are based on the subjective evaluation of pictures produced by the system described in Chapter 5. The color pictures in this chapter are, however, are copies of the test pictures reproduced by Polaroid Copy Service on Kodak RC paper. This adds an extra step to the processing that was not considered in the original analysis. The transformation is constant for the series of HOUSE pictures and for the series of GIRL pictures, but this, in general, is insufficient to guarantee the invariance of the results obtained with the output of the system.

6.2 The Evaluation of the Model

The parameters of the color correction algorithm are given in Table A-2 of the Appendix. They were selected to reproduce exactly the six most saturated colors, generated by the system at its full dynamic range with combinations of minimum and maximum exposures E^S to the dye-forming layers. As a test, the color correction transforms were inverted and used to predict the color head values resulting from maximum and minimum exposures of the compressed dynamic range. In this case, the digital exposures E^S were limited to the interval [4,56], yielding a dynamic range of log(56/4) or 1.15, given that the gamma of the reproduction system is 1. Since one seldom encounters minimum densities larger than 0.25, D_{min} is made the same for both the full and compressed dynamic range systems so that compression is had by decreasing D_{max}. The agreement between the predicted and measured color head values for the six most saturated colors of the compressed system is very good: the root mean square error in density (log H) is 0.04. This is on the order of the resolution of the digital color head value at optical densities greater than 1.0. The largest deviations occurred for the green and blue color head values, as would be expected since these are the most sensitive channels. According to Table A-2, the gammas or 'gains' b_{ij} for the blue and green exposures are large, due to the considerable overlap of the absorption curves of the yellow and magenta dyes.

Optimizing color correction for the set of most saturated colors did not guarantee as good results for some other colors. In particular, the flesh tones in the GIRL picture were reproduced too yellow at first. Therefore, the transform for this region of the gamut (YR in Table A-2) was

modified by 'turning down the green gain' to obtain a better rendition of the skin colors, as determined by comparing the reproduction with the original scanned copy. The only other difficulty encountered was the sky color in the HOUSE picture: in the original copy, it is a bright saturated blue, outside the full dynamic range of the system. Applying the color correction transform for the blue-cyan BC region caused the blue exposure to saturate so that it was necessary to reduce it in order to obtain an acceptable if, strictly speaking, incorrect color.

6.3 Processing for a Compressed Dynamic Range

In meeting the constraint imposed by a compressed dynamic range, the output exposures $E_i \varepsilon [1,56]$ to the red, green, and blue emulsions, computed by the system at its full dynamic range, must be mapped onto the restricted output color solid, where $E_o \varepsilon [4,56]$. Three ways of performing this mapping were investigated.

The first method, shown by curve (a) in Figure 6-1, is a linear transform of the input density range onto the output density range,

$$\log E_o = k_1 \log E_i + \log E_{min} \qquad 6.3\text{-}1$$

where E_i and E_o are the exposures for the full and compressed dynamic ranges respectively and k_1 is the ratio of the output to the input dynamic ranges. E_{min} is the exposure that gives the maximum density D_{max} of the compressed system.

The second method is a linear mapping of the input exposure range onto the output exposure range,

$$E_o = k_2 E_i + E_{min} \qquad 6.3\text{-}2$$

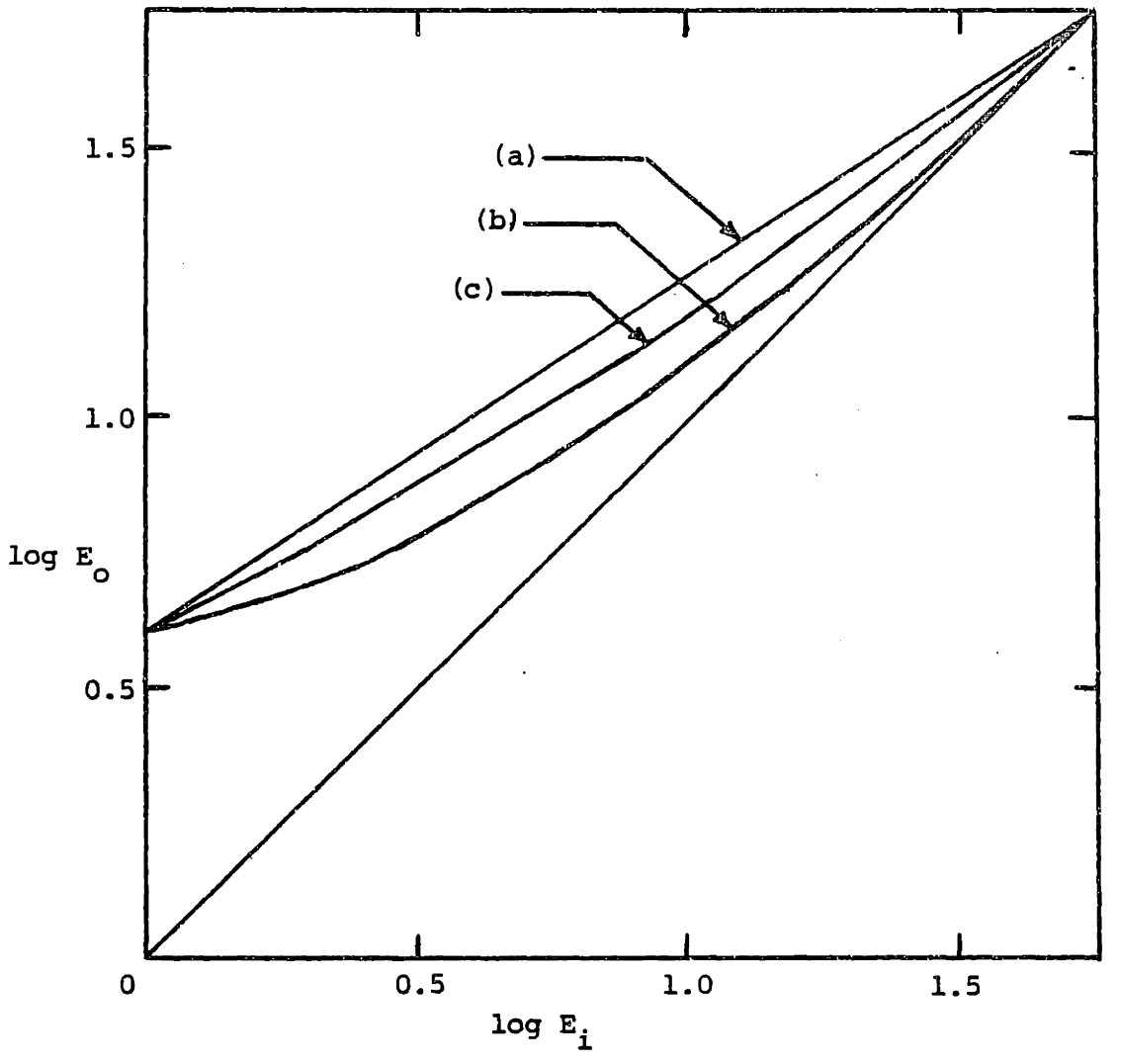

Figure 6-1. Tone Scale Transformations

(a) linear in log E

(b) linear in E

(c) linear in W*

where k_2 is the ratio of the output to the input exposure ranges. This transformation (curve (b) in Figure 6-1) confines the compression to the shadows while the midtones (and highlights) are reproduced with a gamma of nearly 1. Both of these tone scale transformations are inserted between the color correction transform and the tone scale linearizer in Figure 4-10 and are applied independently to the red E^r, green E^g, and blue E^b exposures.

The third method is compression preceding the color correction transform in the psychophysically more significant U*V*W* space. The lightness compression parameters (α,β in Equation 4.2-2) and the 'saturation' compression factor (γ in Equation 4.2-5) are determined after a search over the picture. The maximum and minimum output lightnesses W* are computed for the lightest and darkest neutrals, resulting from the maximum and minimum exposures respectively of the compressed system. Curve (c) in Figure 6-1 shows the neutral tone scale transformation with a linear mapping of the input lightness range onto the output lightness range. The other six colors required to specify the remaining vertices of the color solid of Figure 4-5 are had experimentally by combining maximum and minimum exposures on the separations so that the three dye-forming layers do not all receive the same exposure. Fitting planes to triplets of these points then gives the output color solid of the compressed system.

For the HOUSE picture, the lightness mapping was

$$W^*_{out} = 0.69\ W^*_{in} + 28.5 \qquad 6.3\text{-}3$$

for W* on the interval [1,100]. The search for the saturation compression factor returned γ's on the order of 0.2, due to the bright saturated blue of the sky in the original. Using this factor would have led to an

excessive desaturation of the picture, so that the γ applied was normalized with respect to what it would have been for the system at its full dynamic range. The normalized saturation compression factor actually used for processing the HOUSE picture was 0.80.

For the GIRL picture, the lightness mapping was

$$W^*_{out} = 0.79\ W^*_{in} + 19.8 \qquad 6.3\text{-}4$$

To obtain the saturation compression factor, a search was made over the shirt, chest, and face regions of the picture. The smallest γ returned was 1.0 so that no compression was required. At first, this seemed a surprising result, in view of the fact that the difference between the chromaticity (u,v) and the neutral point (u_o,v_o) declines with a smaller dynamic range. However, the lightness mapping in Equation 6.3-4 increased the lightnesses of the points in these areas so as to offset this decrease in the difference between u and u_o (or v and v_o) and thus give the same U* (or V*) as in the original. In other words, when D_{min} is held fixed but D_{max} decreased, the compressed U*V*W* color solid is not contained entirely within that of the system at its full dynamic range.

The results of these compression schemes are shown in Figures 6-2(b)-(d) and Figures 6-3(b)-(d) for the HOUSE and GIRL pictures respectively, along with the corresponding uncompressed pictures (Figures 6-2(a) and 6-3(a)) for comparison.

To increase visual contrast and color saturation, the picture compressed by a linear mapping over the exposure range (curve (b) in Figure 6-1) was filtered with the two-dimensional digital version of the second derivative (Laplacian). The impulse response of the filter is shown at the top of the next page.

0	$-\frac{1}{4}$	0
$-\frac{1}{4}$	2	$-\frac{1}{4}$
0	$-\frac{1}{4}$	0

The filtered versions of the HOUSE and GIRL pictures are shown in Figures 6-2(e)-(g) and 6-3(e)-(g) respectively. In picture (e) of these series, the filter was applied to the red, green, and blue exposures separately, prior to their compression; in (f), to the luminance component Y of the picture; and in (g), to the lightness component W*.

6.4 Subjective Evaluation of the Processed Pictures

For all pictures with a compressed dynamic range, D_{max} was checked with a densitometer to verify that the density range was 1.15 as predicted. The compressed versions of each test picture were then mounted side by side on a grey matte card and the uncompressed picture mounted on a separate card. Twenty subjects participated in the experiment: most were experienced in black and white image processing, but had relatively little or no background in color picture work. Each subject viewed the three compressed pictures under incandescent lamps and ranked them in order of preference. The subject was then shown the uncompressed picture and asked to rank the compressed pictures again, but this time in order of similarity to the unprocessed picture. The results were analyzed using the Friedman two-way analysis of variance by ranks test. This is a nonparametric test suitable when data from $k > 2$ related samples and N subjects are on an ordinal scale [54]. For both sets of pictures, there is a significant difference (at the 0.001 level) between the methods chosen for compressing the dynamic range,

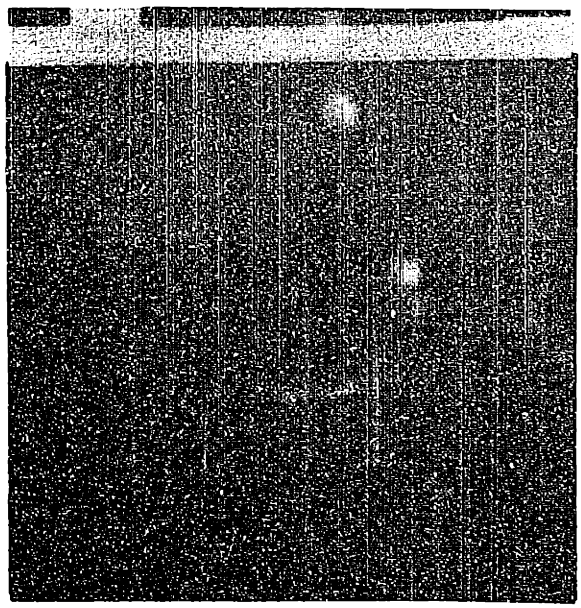

(a)

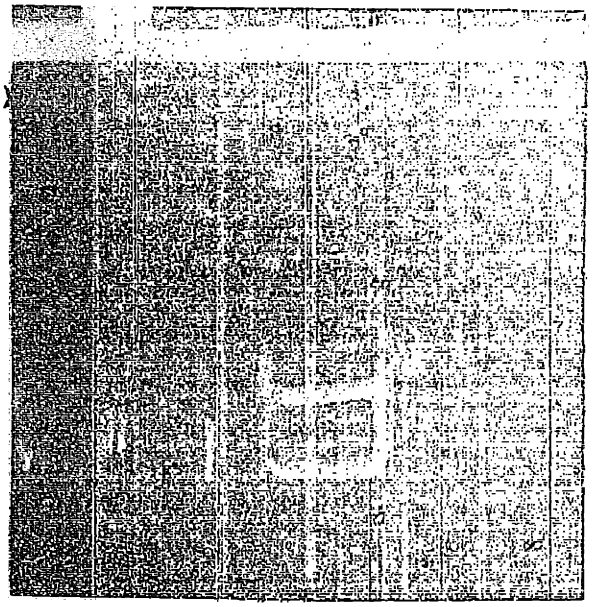

(b)

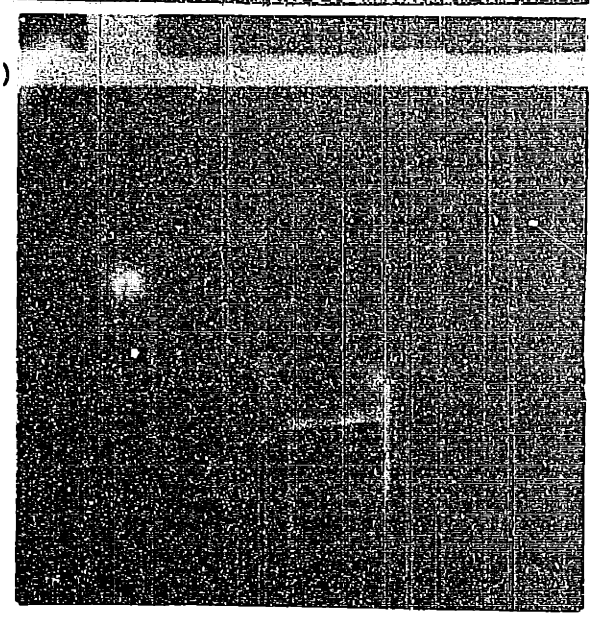

(c)

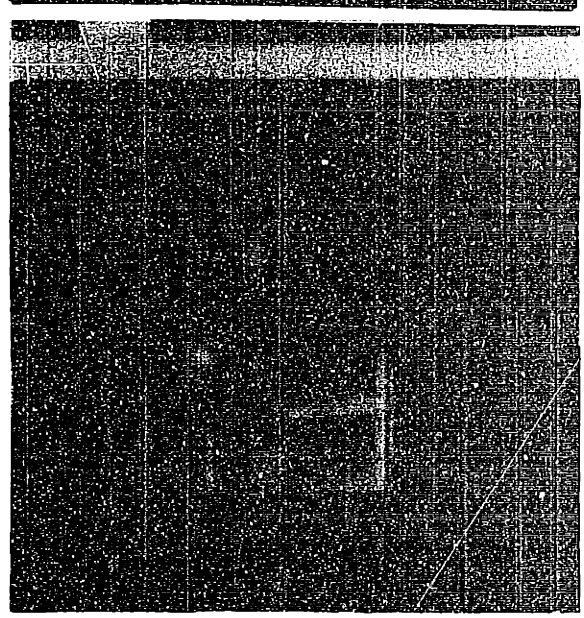

(d)

Figure 6-2. HOUSE Picture

(a) full dynamic range

(b) log E compression

(c) E compression

(d) U*V*W* compression

(e) exposures E^r, E^g, E^b of (c) filtered

(f) luminance Y of (c) filtered

(g) lightness W* of (c) filtered

(e)

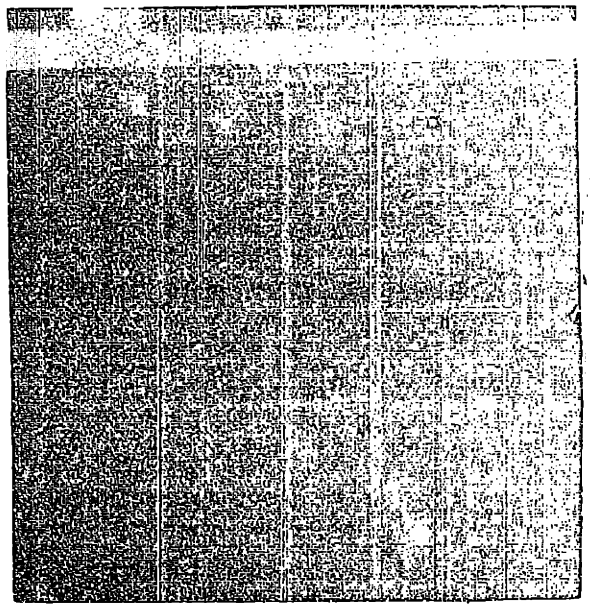

(f)

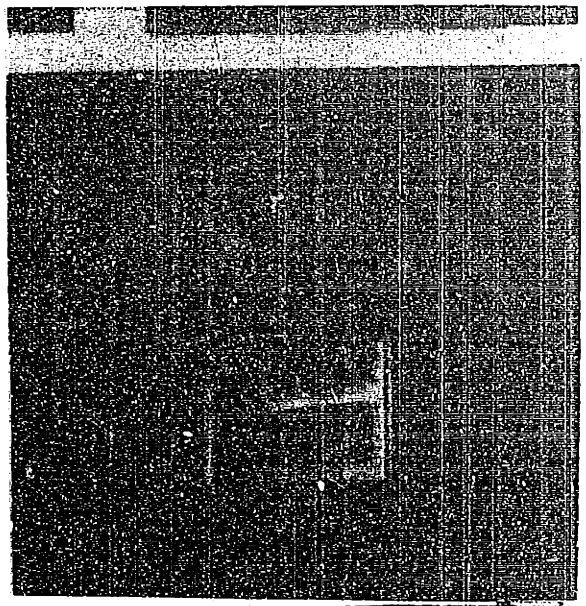

(g)

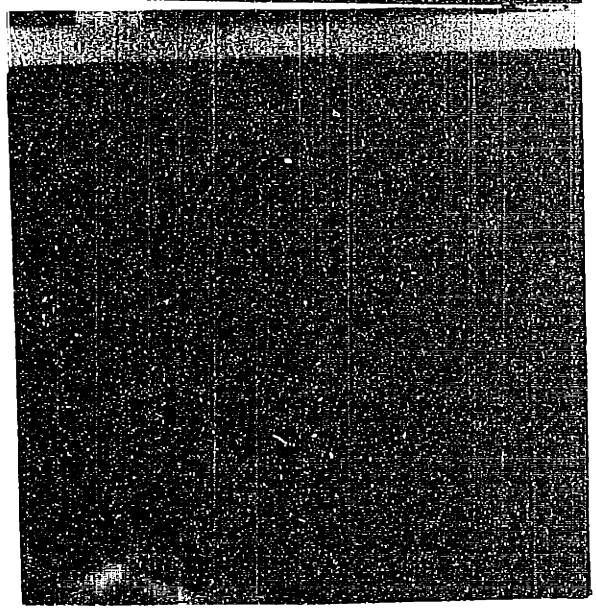

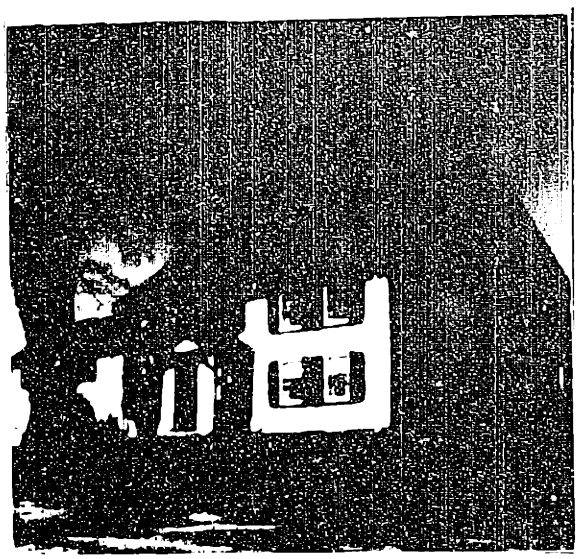

(a)

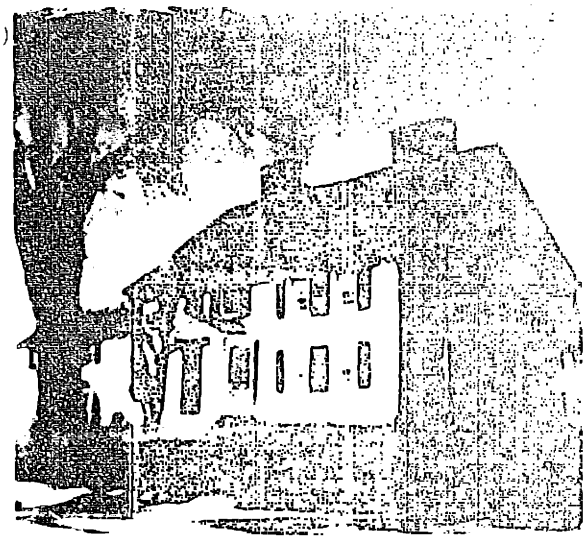

(b)

(c)

(d)

(د)

(ه)

(و)

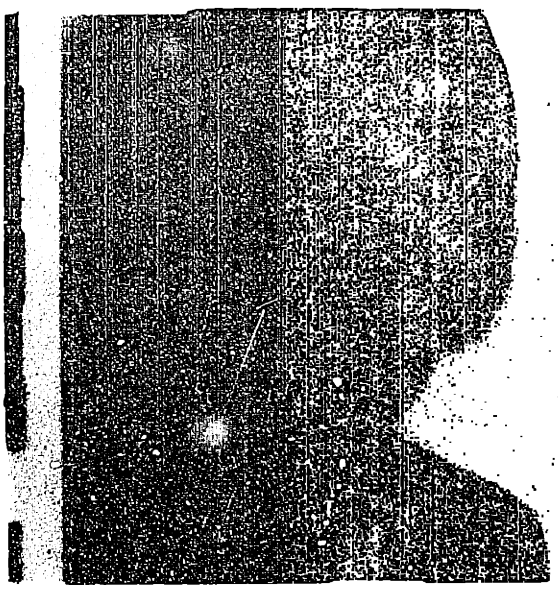

(a)

(b)

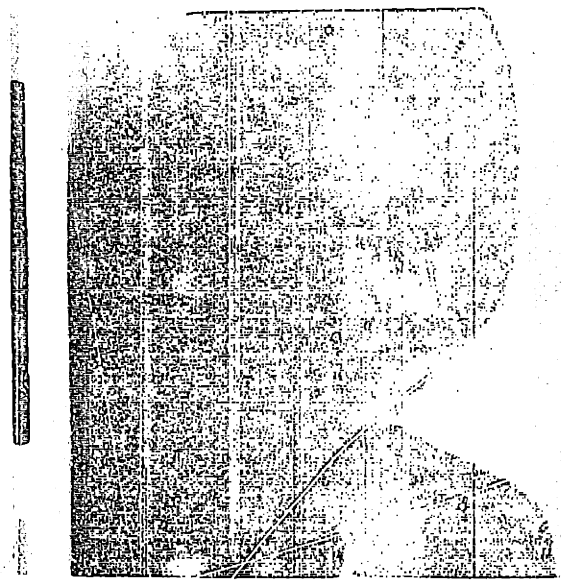

(c)

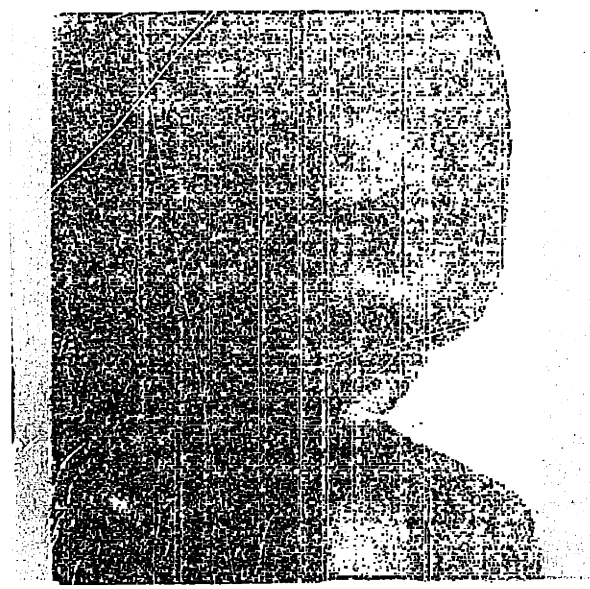

(d)

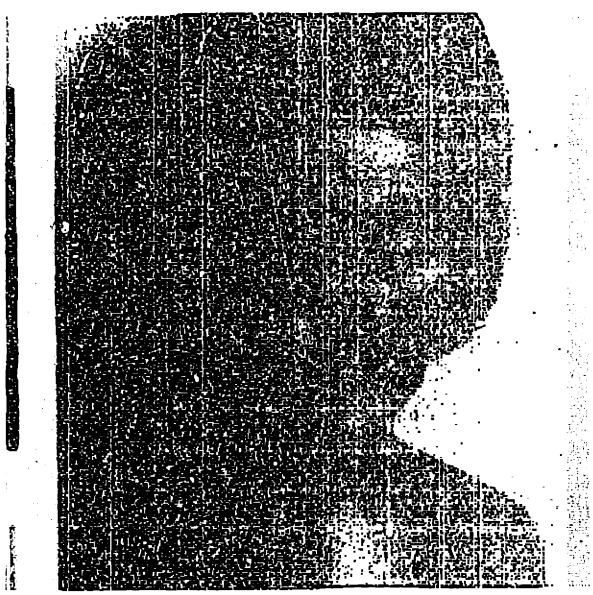

Figure 6-3. GIRL Picture

(a) full dynamic range

(b) log E compression

(c) E compression

(d) U*V*W* compression

(e) exposures E^r, E^g, E^b filtered

(f) luminance Y of (c) filtered

(g) lightness W* of (c) filtered

(e)

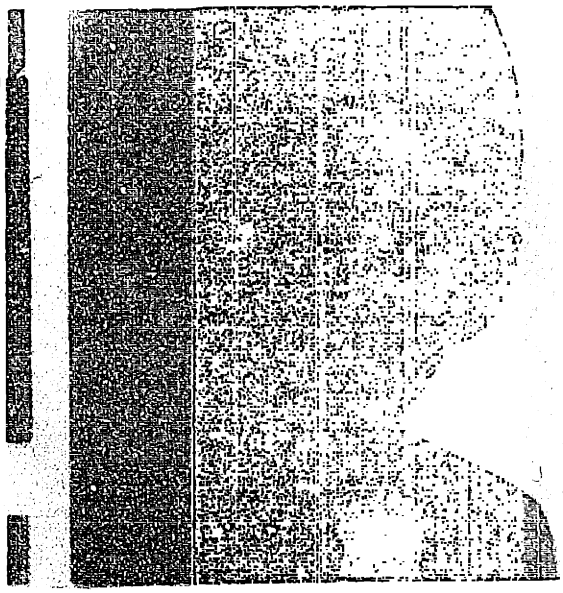

(f)

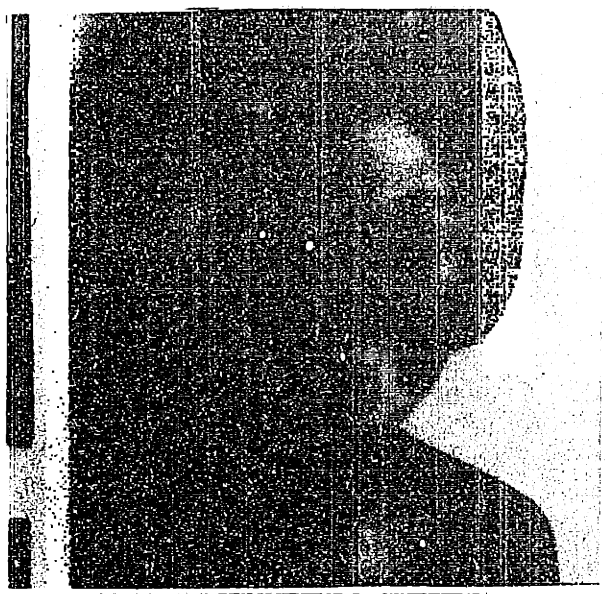

(g)

(a)

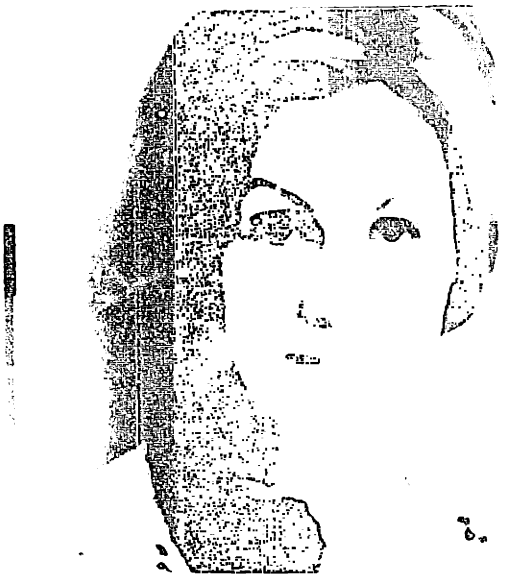

(b)

(c)

(d)

Figure 4-3. GIRL Picture

(a) Full dynamic range

(b) log E compression

(c) E compression

(d) U*V*W* compression

(e) expansion E^r, E^g, E^b filtered

(f) Luminance Y of (c) filtered

(g) Luminance W* of (c) filtered

(ب)

(ج)

(د)

with respect to the ordering both for preference and similarity to the unprocessed picture. In particular, the compression in E for the HOUSE picture and in log E for the GIRL picture gave the least preferred and least similar results. Eliminating these allows the use of the sign test [54] for testing the significance of the ranking of the two remaining pictures. For the GIRL picture, there was no significant difference as to which algorithm was preferred between compression in the log E domain and U*V*W* space, though the latter was judged to give results closest to the uncompressed picture (significant at the 0.01 level). For the HOUSE picture, the U*V*W* compressed picture was the one preferred (significant at the 0.05 level) though neither it nor the log E compressed picture were judged significantly closer to the uncompressed picture.

Linear compression in density (log E) gave good results for the HOUSE picture where it expanded the tone scale in the shadow region of the picture, increasing the visibility of shadow detail. On the other hand, it gave a 'washed-out' appearance to the GIRL picture. Linear compression in exposure (E) gave good results for the GIRL picture where the midtones and highlights are the important areas but was significantly poorer for the HOUSE picture, where it only succeeded in compressing the shadows more. For these two test pictures, compression in U*V*W* space showed the advantages of both the E and log E compression schemes, but without any of their disadvantages, and, besides giving good results for the GIRL picture, was the best compression scheme for the HOUSE picture. Its meeting its design criterion of hue invariance under compression is evident upon comparing the flesh tones and hair colors of the processed and unprocessed GIRL pictures and is presumably responsible for the U*V*W* compressed picture being judged most

similar to the processed one. It was not as clear with the HOUSE picture as the comparison of compressed with uncompressed pictures was a difficult task.

The filtered and compressed pictures are a clear improvement over the compressed but unfiltered picture. The saturation of small areas was increased and detail visibility much improved, almost to the point where some regions looked grainy. For the particular filter used, there is little difference between the exposure, luminance, and lightness filtered pictures, though filtering in the luminance domain appears to give slightly more pronounced results. As expected, the overall contrast appeared greater in the filtered pictures, though objective measurements with a densitometer verified that D_{max} is the same for both filtered and unfiltered pictures.

6.5 Topics for Future Research

Given the great deal of experience that has accumulated here and in other labs on monochrome picture enhancement via tone scale transformations and spatial filtering, it seems the appropriate time to extend the same notions to color pictures in a systematic way. This thesis has been a preliminary step in that direction. The optimum reproduction of color can be investigated along several 'dimensions'.

The sample space from which pictures are drawn for test processing should be increased and diversified in an attempt to reinforce the results of this study, based on two test pictures. The dynamic range constraints imposed on the reproduction of a given picture can take a number of forms, including an increase in D_{min}, a decrease in D_{max}, or both. It is

important to determine if the superiority of U*V*W* processing extends to other density range restrictions than the ones imposed in this study.

For reasons outlined in Chapters 2 and 4, the U*V*W* space was chosen as the most suitable for psychophysically-motivated color compression. It is not the sole possibility though and there are other combined lightness and chromaticness scales [19], such as the (L,a,b) space, the cube root color co-ordinate system [34], and the Adams chromatic value system [38] that have their adherents and may be superior choices as the domain in which to perform the compression.

Spatial filtering gives a definite improvement in color image quality though, with the test pictures in this study, it was not possible to say which is the optimum domain for filtering. An examination of the separations of the color picture obtained by filtering the three exposure signals showed quantization contours in the highlight regions. For other pictures than the ones used here, this effect may become severe enough to make filtering in the exposure domain unacceptable. When the luminance or lightness values are readily available, the computationally most efficient sharpening algorithm would filter one or the other of them.

The accuracy of the color correction algorithm for a given picture depended on the colors for which the parameters had been optimized. Rather than change the set of calibration colors from picture to picture, the dimensions of the color correction transform can be effectively increased by instituting more than six piecewise linear transforms, by adding luminance and saturation (or purity) to slope (hue) in the decision space for selecting the transform to apply to a given point. This method is an extrapolation of analogue (darkroom) masking techniques that have been

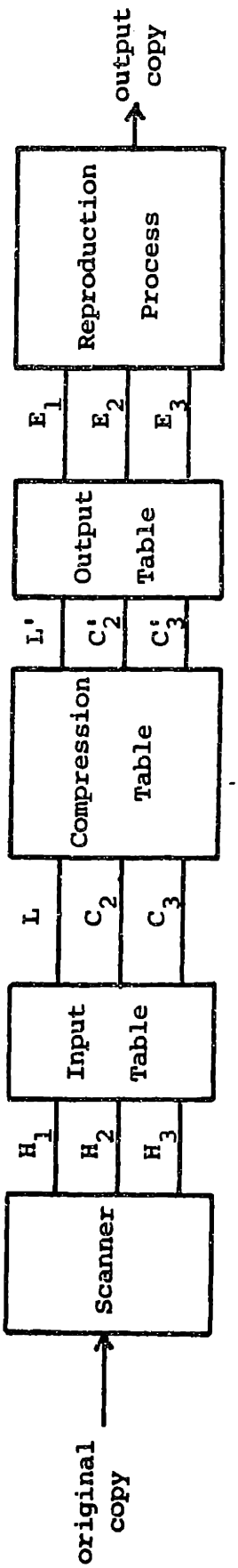

Figure 6-4. Color Correction and Compression by Table Look-up

given an extended life by the computational power of the analogue and digital computer. A uniquely digital approach to reproducing a given color would trade computation time off against memory and obtain color correction by table look-up (Figure 6-4). Color reproduction then becomes the cascading of two look-up tables. The first transforms the input scanned values (H_1,H_2,H_3) into an appropriate colorimetric space (L_1,C_1,C_2) for the colorants of the original copy. The second takes the color space co-ordinates and uses them to look up control signals (E_1,E_2,E_3) for the output process that yield the desired color point with the colorants used in the reproduction. In this way, the input and output colorants, whether they are dyes or inks, are decoupled and assumptions such as those that had to be made in Chapter 3 could be dispensed with entirely. In addition, another table could be implemented in the color space of the system to perform any mappings $(L,C_1,C_2) \rightarrow (L',C_1',C_2')$ that might be required by constraints imposed by the output color process, in other words, color compression. The disadvantages typically cited for color correction by table look-up is the large amount of storage that it requires: this could be mitigated by quantizing the color space so that reproduction errors are uniformly distributed over it. Alternatively, coding schemes such as Solomon's Luminance Scaled Chromaticity transform [33] could be used to make the most efficient use of the table space available.

6.6 Conclusions

An important problem in the color printing industry is the optimum reproduction of a good quality color picture on a medium with a compressed dynamic range. While the constraints are given in terms of physical variables, such as density or exposure, the results are evaluated in a

psychological color space. Colorimetry, with its extension to combined lightness and chroamticness scales, currently provides the best means of describing a complex visual stimulus, such as a color picture. The comparison was made between performing the compression from input to output in the density domain, matched to the physical process, and performing it in a domain matched to the observer. For two representative pictures, dynamic range compression in U*V*W* space gave results that were either closer to the original, unprocessed picture than reproductions obtained by compression in density or exposure, or else were preferred to them. Enhancement of a compressed picture was had economically by spatially filtering either the luminance or lightness .

In a color reproduction system, the requirements for the scanner spectral sensitivity functions for a closed form solution to the color correction (masking) problem and for colorimetric representation were shown to be conflicting. The problem of reconciling them was investigated for a given set of color head sensitivities, suitable for color correction, and a colorimetrically accurate system obtained by a combination of bi-linear and piecewise linear transformations on the color head values.

Appendix

Piecewise Linear Transforms

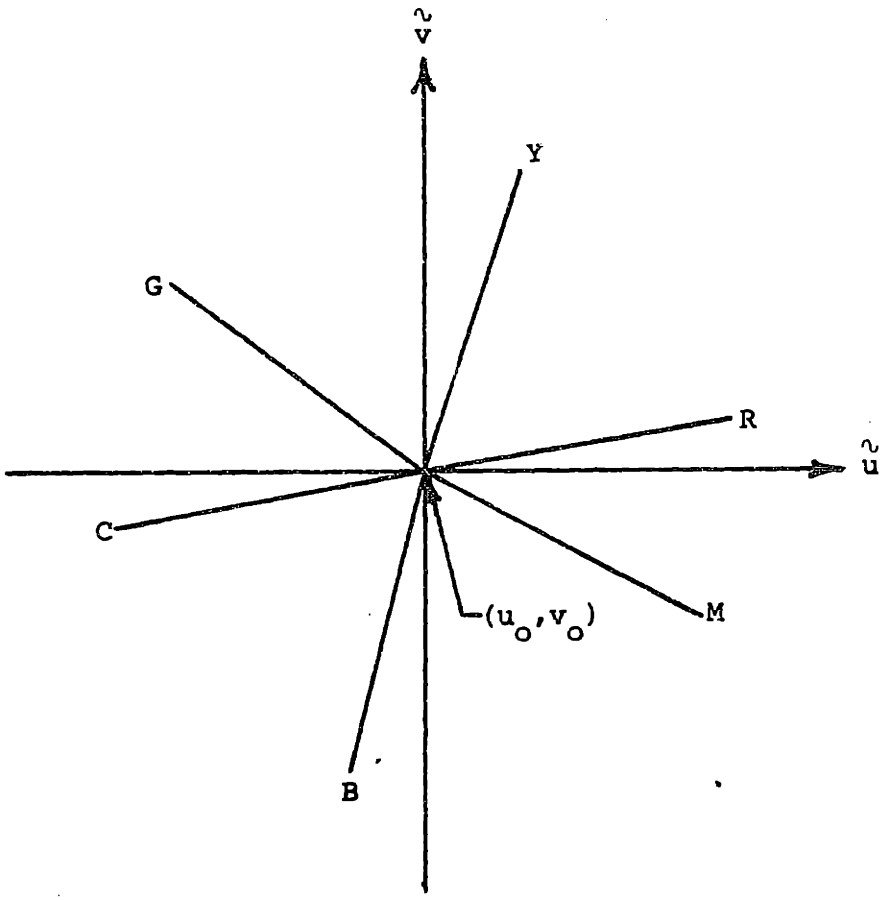

Figure A-1. Partitioning of the Plane of Chromaticity Estimates for the Hexagonal Affine Transforms (HAT).

$$\text{slope} = m = \frac{\tilde{v} - v_o}{\tilde{u} - u_o}$$

Table A-1. Hexagonal Affine Transform for Chromaticity Correction $\underline{T}_k$

k	Region	Slope	$\underline{T}_k$
1	YR	0.0645 < m < 2.7462	$\begin{bmatrix} 0.6930 & 0.3050 \\ 0.0369 & 0.9669 \end{bmatrix}$
2	RM	-0.3004 < m < 0.0645	$\begin{bmatrix} 0.7148 & -0.0338 \\ 0.0550 & 0.6864 \end{bmatrix}$
3	MB	1.0922<m,m <-0.3004	$\begin{bmatrix} 0.8179 & 0.3093 \\ 0.1171 & 0.8930 \end{bmatrix}$
4	BC	0.0735 < m < 1.0922	$\begin{bmatrix} 0.9246 & 0.2116 \\ 0.0693 & 0.9367 \end{bmatrix}$
5	CG	-0.4318 < m < 0.0735	$\begin{bmatrix} 0.9312 & 0.1220 \\ 0.0705 & 0.9198 \end{bmatrix}$
6	GY	2.7462<m,m <-0.4318	$\begin{bmatrix} 0.9671 & 0.2052 \\ 0.0835 & 0.9499 \end{bmatrix}$

Table A-2. Hexagonal Affine Transform for Color Correction $\underline{B}_k$

k	Region	Slope	$\underline{B}_k$
1	YR	$0.0771 < m < 1.9092$	$\begin{bmatrix} 1.1145 & -0.1071 & -0.0074 \\ -0.2436 & 1.5733 & -0.3296 \\ 0.2608 & -1.6841 & 2.4233 \end{bmatrix}$
2	RM	$-0.0723 < m < 0.0771$	$\begin{bmatrix} 1.1365 & -0.2492 & 0.1126 \\ -0.5215 & 3.3673 & -1.8458 \\ 0.3271 & -2.1123 & 2.7852 \end{bmatrix}$
3	MB	$1.1807 < m, m < -0.0723$	$\begin{bmatrix} 1.1129 & -0.3035 & 0.1906 \\ -0.3766 & 3.7007 & -2.3240 \\ 0.0365 & -2.7812 & 3.7447 \end{bmatrix}$
4	BC	$0.1191 < m < 1.1807$	$\begin{bmatrix} 1.5396 & -1.4506 & 0.9110 \\ -0.4228 & 3.8248 & -2.4019 \\ -0.2039 & -2.1349 & 3.3388 \end{bmatrix}$
5	CG	$-0.5166 < m < 0.1191$	$\begin{bmatrix} 1.5036 & -0.4685 & -0.0351 \\ -0.3442 & 1.6837 & -0.3396 \\ -0.2261 & -1.5306 & 2.7567 \end{bmatrix}$
6	GY	$1.9092 < m, m < -0.5166$	$\begin{bmatrix} 1.4388 & -0.5083 & 0.0695 \\ -0.3366 & 1.6883 & -0.3517 \\ 0.0164 & -1.3817 & 2.3653 \end{bmatrix}$

References

1. Bartleson, C.J., Color perception and color television. J.Soc.Mot. Pict.Tele.Eng., 77, 1 (1968)

2. Hunt, R.W.G., The Reproduction of Colour (Third Edition). New York. John Wiley & Sons, 1975.

3. Inter-Society Color Council. Proc. of Conf. on the Optimum Reproduction of Color, Williamsburg, VA. (M. Pearson, editor). Graphic Arts Research Center, Rochester Institute of Technology, 1971.

4. Jones, L.A. and Condit, H.R., Brightness scale of exterior scenes and the computation of correct photographic exposure. J.Opt.Soc.Am., 31, 651 (1941)

5. Rhodes, W.L., Limitations of the printing process. J.Phot.Sci., 9, 131 (1961)

6. Pearson, M., Review of Optimum Color Reproduction in the Graphic Arts. pp. 139-144 in [3].

7. Burnham, R.W., Hanes, R.M., and Bartleson, C.J., Color: A Guide to Basic Facts and Concepts. New York. John Wiley & Sons, 1963.

8. Ditchburn, R.W., Eye Movements and Visual Perception. Oxford. Clarendon Press, 1973.

9. MacAdam, D.L., Sources of Color Science. Cambridge. MIT Press, 1970.

10. Burch, R.M., Colour Printing and Colour Printers. New York. Baker & Taylor, 1910.

11. Wright, W.D., The Measurement of Colour (Third Edition). London. Hilger & Watts, 1964.

12. MacAdam, D.L., Color discrimination and the influence of color contrast on visual acuity. Revue d'Optique. 28, 161 (1949)

13. MacAdam, D.L., Projective transformations on ICI color specifications. J.Opt.Soc.Am., 27, 247 (1937)

14. Wyszecki, G., Proposal for a new color difference formula. J.Opt.Soc. Am., 53, 1318 (1963)

15. Cornwell-Clyne, A., Colour Cinematography, London. Chapman&Hall, 1951.

16. Land, E.H., Experiments in color vision. Sci.Am., 201, 84 (May 1959)

17. McCann, J.J., Human Color Perception. Color: Theory and Imaging Systems (R.A. Eynard, editor). Washington, Soc.Photo.Sci.Eng., 1973.

18. Friedman, J.S., History of Color Photography. Boston. American Photographic Publishing Co., 1944.

19. Wyszecki, G. and Stiles, W.S., Color Science: Concepts and Methods, Quantitiative Data and Formulas. New York. John Wiley & Sons, 1967.

20. Hardy, A.C. and Wurzburg, F.L., The theory of three-color reproduction. J.Opt.Soc.Am., 27, 227 (1937)

21. Umberger, J.Q., Color reproduction theory for subtractive color films. Photo.Sci.Eng., 7, 34 (1963)

22. Neblette, C.B., Photography: Its Materials and Processes (Sixth Edition). Princeton, NJ. D. Van Nostrand Co. Inc., 1962.

23. Ohta, N., Color gamut obtainable by the combination of subtractive color dyes III Hypothetical four dye system. Phot.Sci.Eng., 20, 149 (1976)

24. Hanson, W.T. and Horton, C.A., Subtractive color reproduction interimage effects. J.Opt.Soc.Am., 42, 663 (1952)

25. Williams, F.C. and Clapper, F.R., Multiple internal reflections in photographic color prints. J.Opt.Soc.Am., 43, 595 (1953)

26. Mees, C.E.K., The Theory of the Photographic Process. New York. Macmillan Co., 1966.

27. Oppenheim, A.V. and Schafer, R.W., Digital Signal Processing. Englewood Cliffs, NJ. Prentice-Hall Inc., 1975.

28. Miller, C.W., The matrix algebra and color reproduction. J.Opt.Soc. Am., 31, 477 (1941)

29. Yule, J.A.C., The theory of subtractive color photography I Conditions for perfect color rendering. J.Opt.Soc.Am., 28, 419 (1938)

30. Yule, J.A.C., Principles of Color Reproduction. New York. John Wiley & Sons, 1967.

31. Heyl, J.K., A Digital Correction for the Cross Absorption of Photographic Dyes. MSc Thesis, Department of Computer Science, University of Utah, 1974.

32. Brewer, W.L., Hanson, W.T., and Horton, C.A., Subtractive color reproduction. The approximate reproduction of selected colors. J.Opt. Soc.Am., 39, 924 (1949)

33. Solomon, R.D., Color Coding for a Facsimile System. Ph.D. Thesis. Department of Electrical Engineering, Massachusetts Institute of Technology, 1975.

34. Wallis, R.H., Film Recording of Digital Color Images. USCIPI Report 570. Image Processing Institute, University of Southern California, May 1975.

35. Gutteridge, C., A method of computing the mask characteristics required for accurate color reproduction in photomechanical processes. Phot.Sci.Eng., 16, 214 (1972)

36. MacAdam, D.L., Subtractive color mixture and color reproduction. J. Opt.Soc.Am., 28, 466 (1938)

37. Evans, R.M., Visual processes and color photography. J.Opt.Soc.Am., 33, 579 (1943)

38. Pobboravsky, I., Pearson, M., and Yule, J.A.C., The relationships between photomechanical reproduction and the original copy. pp. 159 -190 in [3].

39. Neuegebaeur, H.E.J., Quality factor for filters whose spectral transmittances are different from color mixture curves and its application to color photography. J.Opt.Soc.Am., 46, 821 (1956)

40. Park, S.K. and Huck, F.O., A Spectral Reflectance Estimation Technique using Multispectral Data from the Viking Lander Camera. NASA TN D-8292, 1976.

41. Evans, R.M., Accuracy in color photography and color television. pp. 38-59 in [3].

42. Rosenfeld, A., Picture Processing by Computer. New York. Academic Press, 1969.

43. Schreiber, W.F., Wirephoto quality improvement by unsharp masking. Pattern Recognition, 2, 117 (1970)

44. Gilkes, A.M., Photograph Enhancement by Adaptive Digital Unsharp Masking. SM Thesis. Department of Electrical Engineering, Massachusetts Institute of Technology, 1974.

45. Kanisza, G., Alcune Osservazione sull'effetto Musatti. Arch.Piscologia Neuroglia Psichiatria, 15, 265 (1954)

46. Walraven, J., Spatial characteristics of chromatic induction; segregation of lateral effects from straylight artifacts. Vis.Res., 13, 1739 (1973)

47. Yund, E.W. and Armington, J.C., Color and brightness contrast effects as a function of spatial variables. Vis.Res., 15, 917 (1975)

48. van der Horst, G.J.C. and Bouman, M.A., On searching for 'Mach Band type' phenomena in colour vision. Vis.Res., 7, 1027 (1967)

49. Green, D.G. and Fast, M.B., On the appearance of Mach Bands in gradients of varying color. Vis.Res., 11, 1147 (1971)

50. Stockham, T.G., Image Processing in the context of a visual model. Proc. IEEE, 60, 828 (1972)

51. Solomon, R.D., The Design of a Color Head and Color Mask Correction System for a Facsimile Transmitter. Internal Report. Cognitive Information Processing Group, Research Laboratory of Electronics, Massachusetts Institute of Technology, March 1975.

52. Polaroid Corporation, Polacolor 2 Technical Data Guide. Publication No. 75-6. Cambridge, MA.

53. Optical Society of America, Committee on Colorimetry, The Science of Color. New York. Thomas Y. Crowell Co., 1953.

54. Siegel, S., Nonparametric Statistics for the Behavioral Sciences. New York. McGraw-Hill Co. Inc., 1956.